Characterising indoor and ambient particulate matter in Kwazamokuhle, Mpumalanga

MM Qhekwana

orcid.org 0000-0003-2312-8093

Dissertation accepted in fulfilment of the requirements for the degree *Masters of Science in Geography and Environmental Management* at the North-West University

Supervisor:	Dr RP Burger
Co-supervisor:	Prof SJ Piketh
Assistant supervisor:	Dr JA Adesina

Graduation October 2019

24362042

ABSTRACT

KwaZamokuhle is typical of the townships home to a large portion of South Africans. If the air quality here can be understood, it may help researchers find better solutions to poor air quality including particulate matter (PM), one of South Africa's biggest environmental issues. This study focused on the characterisation of indoor/outdoor (I/O) PM_4 concentrations at two Reconstruction and Development Program (RDP) houses, one which practiced solid fuel burning and the second solely reliant on electricity. The study further established the I/O relationship of PM_4 in the representative dwellings in the community and lastly identified sources of PM_4. KwaZamokuhle often has little wind, resulting in smoke from coal stoves remaining trapped by the inversion layer overlying the community, especially during winter. Therefore, although ambient air quality standards are exceeded most days of the year, the exceedances are greatest during the coldest part of winter (June–August). The health risk to the local community from poor air quality from household coal and wood use is thus greatest during the winter. The morning and evening pollution concentration peaks are associated with domestic cooking and space-heating with solid fuels. Respirable particulate matter (PM_4) was found to be especially high indoors and could be attributed to the morning and evening peak pollution concentrations. The 24-hr National Ambient Air Quality Standard (NAAQS) for $PM_{2.5}$ (40 μg m^{-3}) showed exceedances of up to 30% in the morning and 60 % in the evening. The 24-hr PM_{10} limit (75 μg m^{-3}) was exceeded by a factor of 10. It was found that during periods of the day where no indoor solid fuel burning was practiced, there is still a noticeable increase in PM_4 levels inside the dwellings of both fuel-burning and electricity-based households. This finding suggests the infiltration of PM into the dwellings. Source apportionment results showed that during winter, the dominant sources in the coarse fractions were residential coal burning (38 %) and soil dust (28 %). Suspended ambient dust made up the largest contribution to the PM loading when accounting for all sources associated with crustal material in the coarse fraction (42.5 %). During the summer, road and wind-blown dust (43 %), motor vehicle emissions (26 %) and coal combustion (15 %) contributed most to the detected aerosol loading. Domestic coal combustion particulates accounted for 52 % of the fine fraction during the winter in KwaZamokuhle. Emissions from petrol motor vehicles (~11 %) and secondary aerosols (7 %) (sulfate and nitrate) and re-suspended and wind-blown dust (8 %) were also important sources of PM in the township. During the summer motor vehicle emissions (34 %) had the highest contribution to the fine fraction. Road and wind-blown dust (16 %) and secondary aerosols (13 %) contributed almost equal amounts. A large contribution for an as yet unaccounted-for source or sources was present in the fine fraction of the collected PM mass (21 %).

Key terms: Indoor/outdoor, infiltration, domestic solid fuel burning, low-income settlement

PREFACE

The research presented in this document is the author's authentic work and has not formerly been submitted at the North West University or any other tertiary institution. The author was responsible for the data collection, analysis and interpretation of the results. The data collection was conducted during winter (26 July–17 August) and summer (02–28 November) 2017, respectively. The document was compiled in 2018 by the author.

Format of the dissertation

Chapter 1: Introduction

The chapter introduces both the core concepts relevant to particulate matter (PM) pollution in low-income settlements, as well as the human health impacts associated with indoor and outdoor exposure. The justification for conducting the study is outlined, followed by a statement of the aim and objectives of the study.

Chapter 2: Literature Review

The characteristics and sources of PM are explored in this part of the document, taking cognisance of references and important literature on the subject of I/O PM relationships. Relevant literature relating to related health impacts is reviewed in the chapter.

Chapter 3: Materials and Methods

A description of the study site is provided and the project design is articulated in this part of the dissertation. Relevant data collection methods and analysis techniques are discussed towards the fulfilment of the objectives outlined in Chapter 1.

Chapter 4: Results and Discussion

The results for the research are presented in this chapter. The graphs and tables showing the statistical importance of the data collected are also given here.

Chapter 5: Summary and Conclusions

The key findings of the study are presented in the chapter, followed by conclusions derived from the discussions and data represented. The limitations and assumptions pertaining to such a study are also outlined here.

Conference presentations and articles

Conference presentations and articles derived from the study:

- Marvin M. Qhekwana, Thapelo A. F. Letsholo. Roelof P. Burger. Joseph A. Adesina, and Stuart J. Piketh. Characterizing indoor PM_4 loading of two contrasting houses in Kwazamokuhle, Mpumalanga. *National Association for Clean Air Conference 28 October –01 November 2018.*

Acknowledgements

Gratitude is given to Almighty God for his guidance and unwavering favour during the compilation of this dissertation. When the road seemed bleak, all I had to do was kneel and look to the Heavens and from there my path would become clear. I am also thankful to the various people that were part of this part of my academic career. An African proverb states “it takes a village to raise a child”, and this is absolutely true in my case. I am sincerely grateful to Dr Roelof Burger for your guidance during this journey. It was never easy but through it all I admire how calm you remained even in the most frantic moments. You helped me keep my head on my shoulders during periods of despair. I would like to express humble gratitude to Prof. Stuart J. Piketh for the endless opportunities that he has offered me during my tenure as a Master’s student. I am absolutely humbled to have had a supervisor such as yourself, and I will continue to remember all the lessons you taught me. Thank you Joseph for always being there to assist with challenges faced during collection of data and the process of putting this document together. To all my colleagues, I am deeply humbled by the sincere generosity you displayed each day. Your selflessness and continuous help of others has been remarkable during my time with all of you. Special thanks to Prof. Harold Annnegarn, Henno Havenga and Brigitte Language for assistance with language and data analysis. I would also like to express deep gratitude to Mr. Thapelo Letsholo for his counsel through this tough but fruitful journey. I would further like to acknowledge ESKOM (*RT & D)* for funding and commissioning the research and proving opportunities to better understand the air pollution problem in low-income settlements. Thank you to the National Research foundation (NRF) for their financial support which assisted in the completion of my studies. Special thanks go to my mother Mrs. Matshiliso Susanna Qhekwana and my father Mr. Makwanyane Andrew Qhekwana for their unconditional love and support. Sincere gratitude to Thatoyaone and Makgamane you guys were great motivation in this journey.

ABBREVIATIONS

AT	Air Temperature
AQMP	Air Quality Management Plan
CMB	Chemical Mass Balance Model
DEA	Department of Environmental Affairs
DEAT	Department of Environmental Affairs and Tourism
EC	Elemental Carbon
ECMWF	European Centre for Medium-Range Weather Forecasts
EF	Enrichment Factors
GHG	Greenhouse Gases
HPA	Highveld Priority Area
IAQ	Indoor Air Quality
I/O	Indoor/Outdoor
ITCZ	Inter-Tropical Convergence Zone
MSLP	Mean Sea Level Pressure
NAAQS	National Ambient Air Quality Standards
NEMA	National Environmental Management Act
NEM: AQA	National Environmental Management: Air Quality (Act No.39 of 2004)
NSFB	Non-Solid Fuel Burning
OC	Organic Carbon
PBL	Planetary Boundary Layer
PCA	Principal Component Analysis
PM	Particulate Matter
PMF	Positive Matrix Factorization
RDP	Reconstruction and Development Programme
RH	Relative Humidity

RSA	Republic of South Africa
SFB	Solid Fuel Burning
T2M	temperature at 2 m
TSP	Total Suspended Particulate Matter
US-EPA	United States Environmental Protection Agency
WHO	World Health Organisation
WD-XRF	Wavelength Dispersive X-Ray Fluorescence
WHO	World Health Organisation
WS	Wind Speed

TABLE OF CONTENTS

LIST OF TABLES

LIST OF FIGURES

CHAPTER 1 INTRODUCTION

The main aim and objectives of the research are outlined in the chapter and a brief background on air pollution and particulate matter in low-income communities are presented.

1.1 Introduction

Particulate matter (PM) in ambient and indoor air impacts on people's quality of life by causing diseases that lead to premature death (Wright *et al.,* 2011; World Health Organisation (WHO), 2013; Cohen *et al.,* 2017). Approximately five million human deaths across the globe are linked to illnesses related to increased personal exposure of indoor and outdoor air pollution (Wright *et al.,* 2011; Jimoda, 2012; Cohen *et al*., 2017). Vulnerable communities in developing nations carry the greatest burden of disease risk from poor air quality (Bruce *et al.,* 2000). Infants, the elderly, women, and people who are sick or disabled are regarded as being especially vulnerable to disease from poor air quality (Bruce *et al.,* 2000; Bruce *et al.,* 2002). This is particularly true in the South African context given the country's air pollution levels (Mduli *et al.,* 2005). Populations, and in particular, vulnerable groups, in low-income settlements in South Arica experience high concentrations of ambient and indoor PM (Mdluli *et al*., 2005), and KwaZamokuhle located in the Mpumalanga Province of South Africa is no exception. This is despite Section 24 of The Constitution of the Republic of South Africa (1996), states that "everyone has the right to an environment that is not harmful to people's health and well-being". Thus, the current state of air quality in such areas is in stark contrast to this constitutional right (RSA, 1996; Feris, 2010; Scorgie, 2012).

Different sources of PM exist in South Africa's settlements and these range from biomass burning, domestic solid fuel combustion, indiscriminate waste-burning, motor-vehicle emissions and dust entrainment from vehicles traveling on unpaved roads (Annegarn *et al.,* 1998; Engelbrecht *et al.,* 2000; Engelbrecht *et al.,* 2001; Engelbrecht *et al.,* 2002; Mdluli *et al.,* 2005; Worobeic *et al.,* 2011). Studies have found indoor concentrations to be a factor of four times higher than the ambient levels due to domestic solid fuel burning (Wernecke *et al.,* 2016). The combustion of the solid fuels in homes has been identified as a major source of PM in the ambient and indoor

environment of low-income settlements like KwaZamokuhle (Annegarn *et al.,* 1998; Engelbrecht *et al.,* 2000; Engelbrecht *et al.,* 2001; Engelbrecht *et al.,* 2002; Mdluli *et al.,* 2005; Worobeic *et al.,* 2011).

Although 75% of low-income areas in South Africa have access to electricity, inhabitants of the low-income settlements still rely on non-renewable energy carriers exclusively for space-heating and food preparation (Nkomo, 2005; Statistics South Africa (StatsSA), ,2012). The cost of electricity is expensive for poor households that have no income or solely rely on government social grants (Alastair and Mhlanga, 2013). Supply of electricity is often not consistent in rural areas where power-cuts occur often (Balmer, 2007; Alastair and Mhlanga, 2013). Solid fuels are being used as a primary energy carrier in the poorest communities in rural areas and low-income areas for daily activities (Balmer, 2007; Mdluli *et al.,* 2005; Masekoameng, 2014). Solid fuels such as coal, wood, animal dung and agricultural crop residue are used for space-heating during winter, boiling water and meal preparation (Nkomo, 2005; Masekoameng, 2014). On the other hand, electricity as an energy carrier is generally used for lighting, charging cellular phone batteries, entertainment and refrigeration (Nkomo, 2005, Masekoameng, 2014).

Accessibility to coal in most urban areas is easy due to the proximity of coal transportation routes, mines, and stockyards (Friedl *et al.,* 2008). Wood tends to be used in more rural settings. Coal and wood are the domestic solid fuels which are commonly used in urban areas of the Highveld (Friedl *et al*., 2008) situated in the high-lying interior of the country including the Gauteng and Mpumalanga provinces. In contrast to the urban areas, the combination of wood and animal dung is typically used in the lowest-earning rural households constituting the poorest households in South Africa (Friedl *et al*., 2008, StatsSA, 2012).

Solid fuel burning tends to take place inside old and poorly-designed stoves that have cracks which release pollutants indoors (Traynor *et al*., 1987; Bruce *et al*., 2000; Balmer, 2007). Furthermore, Mdluli *et al.* (2005) found that most houses that use solid fuels are poorly ventilated and inhabitants are exposed to high levels of PM. Households that do not open windows and doors periodically display higher personal exposure to PM (Mdluli *et al.,* 2005). Mdluli *et al.,* (2005) highlighted the fundamental importance of managing the indoor air just as much as that in the outdoors (Mdluli *et al.,* 2005).

Townships in South Africa accommodate low-income communities (Harrison, 1992; Wilkinson, 1998; Balmer, 2007; Pernegger and Godehart, 2007). The spatial planning of low-income settlements makes it possible for residents to travel to work without spending too much money on transport (Harrison,1992; Wilkinson, 1998; Pernegger and Godehart, 2007). Industries and factories where people are employed are usually located adjacent to low-income residential areas (Matooane *et al.,* 2004; Masekoameng, 2014). However, pollution emanating from industries negatively impacts on the air quality of these residential areas (Piketh *et al.,* 2016). The general state of ambient air in and around low-income areas is also poor due to solid fuel and waste-burning practiced in the settlements (Friedl *et al*., 2008; Piketh *et al.,* 2016). This is further worsened by biomass burning and dust entrainment from paved and unpaved roads (Friedl *et al*., 2008; Piketh *et al.,* 2016).

The use of non-renewable energy carriers in preference to electricity in low-income households was noted above. Besides pragmatic reasons including cost of electricity and insecurity of supply some residents have cultural preferences that require their food to be prepared using the traditional methods which rely on solid fuel burning. An important consideration in the choice of solid fuels is that they provide a dual function, namely simultaneously providing space-heating while the cooking is being done (Nkomo, 2005; Nkosi, 2017). Alastair and Mhlanga (2013) revealed that most residents use alternative sources of energy due to the high running costs and inadequate/unreliable supply of electricity in low-income areas.

Slow economic growth and unemployment over the past decade have made air quality management difficult in South Africa (Barnes *et al.,* 2009; RSA, 2012; Alastair and Mhlanga, 2013;). Ambient PM concentrations are regulated by standards prescribed by the South African Department of Environmental Affairs (DEA)(RSA, 2012), see Table 1-1 for regulatory standards.

Table 1-1: South African National Ambient Air Quality Standards for PM (RSA, 2009; RSA, 2012)

Pollutant	Averaging Period	Concentration (µg m^{-3})	Permitted exceedances
PM_{10}	24 hours	75	4
	1 year	40	0
$PM_{2.5}$	24 hours	40	4
	1 year	20	0

A major challenge for authorities is the control of emissions from non-regulated emitters such as low-income settlements (RSA, 2012). From an emissions calculation point of view, it can be established that scheduled industries contribute a large fraction of PM to the ambient air on an annual basis (Spiegel and Maystre, 1998; Balakrishnan *et al.,* 2011). However, the biggest risk of exposure to communities is not from listed industries, but rather from domestic combustion of solid fuels, uncontrolled waste-burning and other daily activities that occur in low-income settlements (Piketh and Burger, 2013; Naidoo, 2014). Following this reasoning, it can be argued that the health symptoms from poor air quality that manifest in low-income communities located around industrialised areas emanate not so much from the surrounding industry, but rather from sources in the settlement itself (Bruce *et al.,* 2000; Balmer, 2007). Jimoda (2012) states that communities that live in such areas suffer from respiratory complications related to the ambient particulate pollution. However, the susceptibility of the communities to respiratory complications is not limited to ambient exposure, as indoor concentrations have a significant if not a greater impact on health (Jimoda, 2012; Piketh *et al.,* 2016). Tuberculosis, asthma, eye irritation and carbon monoxide poisoning are some of the adverse health impacts that arise from the domestic solid fuel burning (Balmer, 2007; Ni *et al.,* 2012; Naidoo *et al.,* 2013). Elevated concentrations of indoor PM are commonly measured during periods of meal preparation and space-heating (Javed *et al.,* 2015). The elevated concentrations of fine PM trigger chronic respiratory illnesses such as tuberculosis (TB), asthma, pneumonia, and lung cytokinesis, which are primary causes of mortality in South African communities (WHO, 2007; WHO, 2010; Wright *et al.,* 2011). However, it has been observed by Wright *et al.,* (2011) that affected low-income community members have limited knowledge about the health impacts associated with the use of solid fuels and poor air quality.

The ambient air in South Africa is managed and regulated by the National Environmental Management Air Quality Act, 2004 (Act No.39 of 2004) (RSA, 2005). The regulation is different from the previous Atmospheric Pollution Prevention Act (APPA) of 1965 (APPA, 1965); this preceding legislation focused exclusively on mitigation of air pollution solely from a point source perspective (RSA, 2009). This resulted in ambient concentrations at receptor sites not being considered when deciding on the granting of emission licenses to industry and other major sources. In contrast, the current Air Quality Management Act (No. 39 of 2004) is based on the status of air pollution in the ambient environment. With the new legislation it is recognised as important to measure, monitor and report criteria pollutants in the ambient air (RSA, 2009; RSA, 2011). This better informs what mitigation strategies can be implemented at sources and receptors to effectively manage air quality holistically (RSA, 2012). Three levels of government, namely national, provincial and local, control ambient air quality by stipulating restrictions or emission standards on contributing sources in a specific airshed (RSA, 1998). An important finding stipulates that the regulation of both point and non-point sources is fundamental towards the improvement of ambient concentrations of pollutants (Piketh and Burger, 2013).

1.2 The motivation for the research

The National Environmental Management Act (NEMA) (Act No 107 of 1998) was adopted to protect everyone's right "to have an environment that is not harmful to their health and well-being and to protect the environment from degradation through sustainable development" (RSA, 1998). The National Environmental Management: Air Quality Act (NEM: AQA) (Act No.39 of 2004) was adopted under the NEMA framework (RSA, 2005). The management and control of air pollution in South Africa remains a complex matter as a result of inadequate data and statistics (RSA, 2012). With the adoption of NEM; AQA in 2004, it was expected that better air quality management would prevail in reducing environmental degradation and health impacts. In 2014, an Air Quality Amendment Act was promulgated to specify the penalties for unauthorised industrial emissions. This also provided an enhanced pollution prevention strategy for assessing, monitoring and reporting of emissions. Although there is legislation in place, an ongoing challenge is the availability of data and the correct measurement of emissions. Large industries are commonly referred to as the primary polluters; hence there is a presumption that if these industries reduce their total annual emissions, air

quality will improve. However, this strategy fails to include other sources that are not monitored but also contribute to atmospheric loading of coarse and fine PM. The total atmospheric loading of PM is associated with a diverse set of sources. In the context of the South African Highveld Priority Area (HPA) defined further in Chapter 2, these sources include agricultural activities; domestic fuel burning; opencast mining; power generation; metallurgy industries; refuse-burning; windblown dust and motor vehicle emissions (Scorgie *et al.,* 2012). For the implementation of an effective strategy to reduce ambient PM levels, it is important to understand the contribution of each source listed above to poor air quality (Scorgie *et al.,* 2012). Research aim and objectives

The primary aim of this research was to understand the relationship between indoor and outdoor respirable PM (PM_4) in KwaZamokuhle and further understand the influence that meteorological conditions have on PM concentrations.

To achieve the aim, three objectives were defined as outlined below:

I. Understand the temporal variation of PM_4 concentrations and meteorological conditions in KwaZamokuhle.
II. Explore the relationship between indoor and outdoor PM_4 levels for KwaZamokuhle households.
III. Identify sources of PM_4 in KwaZamokuhle.

1.3 Research focus

The research in this dissertation focused on understanding the relationship of indoor I/O PM_4 in KwaZamokuhle. Measurements of PM_4 concentrations were taken over a few days during summer and winter 2017. Solid fuel combustion is a widespread practice in KwaZamokuhle as indicated by the census conducted in 2011 (StatsSA, 2012). The solid fuel burning occurs inside old, poorly designed stoves that are cracked and release pollutants into the indoor environment (Balmer, 2007). Furthermore, houses tend to be poorly ventilated (Mdluli *et al.,* 2005). This makes it important for researchers to understand and expand the existing body of knowledge on what the difference is between indoor and outdoor concentrations of PM measured concurrently. The combustion not only influences the indoor and outdoor environment but also impacts negatively on human health. Despite being one of the greatest contributors to aerosol

loading, domestic solid fuel use is not regulated through any specific legislation or standard. Combined with the fact of the pollution being generated by millions of households, this makes it one of the most difficult types of emission to manage. An estimation of the contribution of solid fuel burning to ambient PM loading is also important.

.

CHAPTER 2 LITERATURE REVIEW

Chapter 2 reflects on important concepts that need to be understood for the study of the I/O particulate matter (PM) pollution. Concepts such as infiltration, I/O ratio's, health impacts linked to exposure and characteristics of PM are represented. The chapter further looks into source profiles and various receptor methods used to determine the sources of particulate matter.

2.1 Characteristics of particulate matter

Particulate matter (PM) in the atmosphere can be found in two forms namely, liquid or solid, and in various size fractions (Seinfeld, 1986; Kampa and Castanas, 2008). The smaller size fractions are able to pass through the human body's natural defences such as hair follicles in the nose, eventually penetrating into the upper respiratory system (Kamapa and Castanas, 2008). Particles and aerosols contribute to the composition of the earth's atmosphere (Pilinis *et al.,* 1995; Seinfeld and Pandis, 2016). The PM in the atmosphere originates from two source types, specifically, anthropogenic and natural processes (Tyson and Preston-Whyte, 2000; Seinfeld and Pandis, 2016). Marine salt, dust and volcanoes are examples of natural sources (Yatkin and Bayram. 2008). Domestic solid-fuel burning, mining, coal-fired power plants, agricultural activities, transport, metal smelters and petrochemical industries are examples of the anthropogenic sources of PM (Yatkin and Bayram, 2008). The particles have varying physical properties and can be characterised according to shape, size and chemical composition (Seinfeld and Pandis, 2016). These characteristics influence dispersion, transport and the existence of the different particles (Seinfeld and Pandis, 2016). Figure 2-1 shows particle size distribution in the atmosphere which ranges from nucleation/ultrafine (0.01 µm–0.1 µm), accumulation (0.1 µm–1 µm) and coarse mode (≥ 2–3 µm) (Seinfeld, 1986; Reidmiller *et al.,* 2006; Seinfeld and Pandis, 2016).

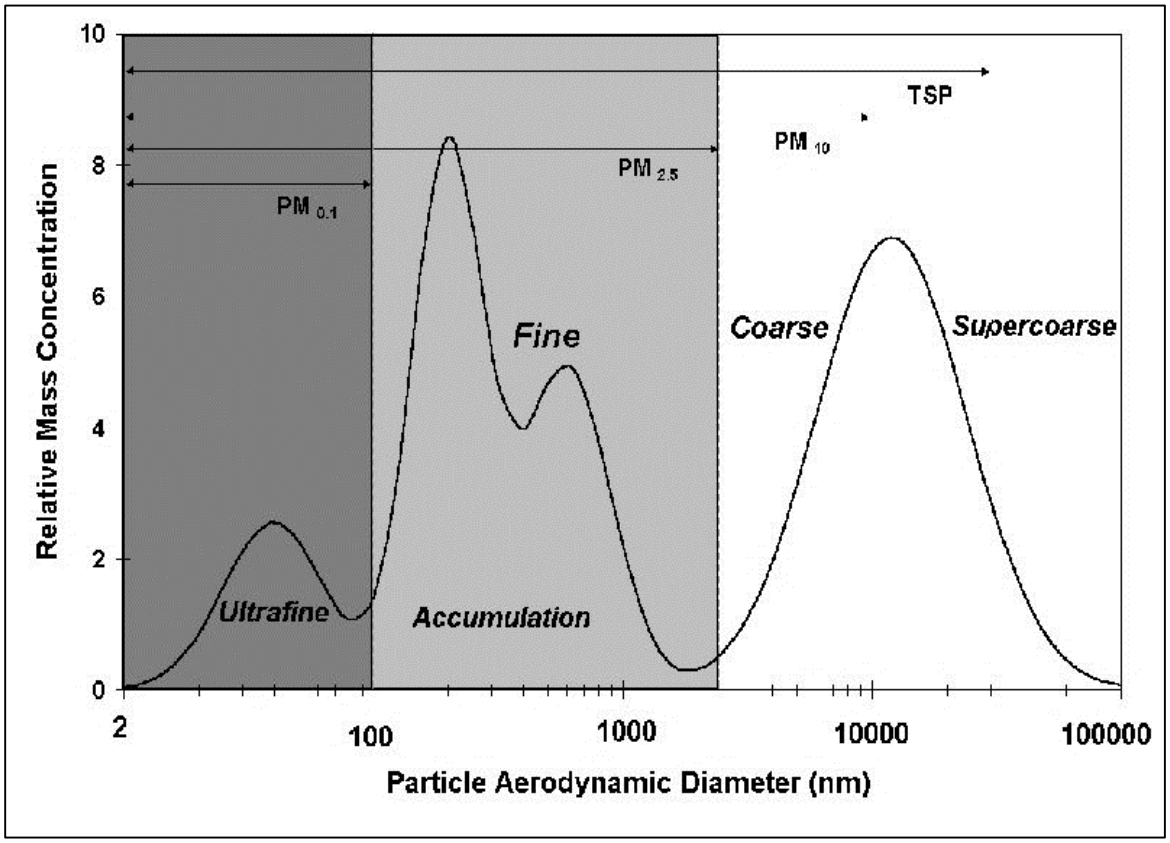

Figure 2-1: Illustration depicting the particle size distribution in the air (Chow, 1995).

The size of particles in the atmosphere has an influence on the duration they remain suspended (Chow, 1995). Larger particles have a short residence time and fine particles remain suspended for longer periods in the atmosphere (Chow, 1995; Aluko and Noll, 2006; Walton, 2006). The longer residence time of a fine particle makes it possible for the particle to travel great distances (> 300 km) (Chow, 1995; Aluko and Noll, 2006; Walton, 2006). In fact, fine particles have the potential to remain suspended for several weeks to years. In contrast, larger/coarse particles stay in the atmosphere for short periods i.e. a few hours or days (Chow, 1995; Walton, 2006). Friedlander (1970) recognized that the concentration of particles in a given space and time is influenced by either size or chemical composition. The particles are considered as toxins when they comprise of harmful elements, such as lead (Pb) and sulphates (SO_4^{2-}) (Harrison and Yin, 2000; Kelly and Fussell, 2012; Tutic *et al.,* 2015; Manahan, 2017). Stanek *et al.* (2011) similarly noted that the chemical composition of particles is complex and presents greater health and environmental risk than the gravimetric characteristic. The chemical

composition can be established from the particle's surface or internal structure (Kelly and Fussell, 2012). Soluble compounds such as SO_4^{2-} (sulphates), NO_3^-(nitrates) and NH_4^+ (ammonium) are found in the $PM_{2.5}$ size fraction (Chow, 1995; Watson *et al.,* 1995; Watson *et al.,* 1997; Dominici *et al.,* 2015). This further extends to insoluble elemental carbon (EC) and organic carbon (OC) (Harrison and Yin, 2000). Sources can be apportioned through the unique particle chemicals emitted (Chow, 1995; Watson *et al.,* 1997). The United States Environmental Protection Agency (US-EPA) database has an extensive source profile inventory that can be used to identify different sources (Watson, 2001; US-EPA, 2014;). Gravimetric sampling and analysis are the methods commonly used to determine the concentration and total amount of suspended particles.

2.2 Health impacts related to particulate matter exposure

The health impacts associated with varying size fractions of PM and the level to which they can penetrate the lungs are depicted in Figure 2-2. PM_{10} causes decreased lung function and intensifies acute inflammation of the lungs, tuberculosis (TB), asthma and pneumonia (Laratta and van Eeden, 2016; Hamanaka and Mutlu, 2018). Prolonged exposure to high concentrations of PM in industrial areas exacerbates the risk of cancerous illnesses (lung cancer) and arteriosclerosis (Pope *et al.,* 1995; Hamanaka and Mutlu, 2018). Short exposure periods to rapid peaks in PM triggers pre-existing respiratory and pulmonary conditions, such as abrupt changes in heart rate, asthma and bronchitis (Pope *et al.,* 1995; Hamanaka and Mutlu, 2018). Pope *et al.,* (1995) also realised that some particles deposited in the lower respiratory region undergo a chemical transformation and are oxidised to create secondary particles. These secondary particles damage blood vessels and membranes and are detrimental to cell growth (Pope *et al.,* 1995; Davidson *et al.,* 2005; Anderson *et al.,* 2012). Health studies have focused generally on the impact that the size of particulate matter has on health, however, more recently emphasis has been put into trying to understand the impacts of the particle chemistry (Kim *et al.,* 2015). The chemical composition of PM has been found to have a greater impact on health as particles undergo chemical transformation when mixed with liquids in the body. Kim *et al.,* (2015) reported that

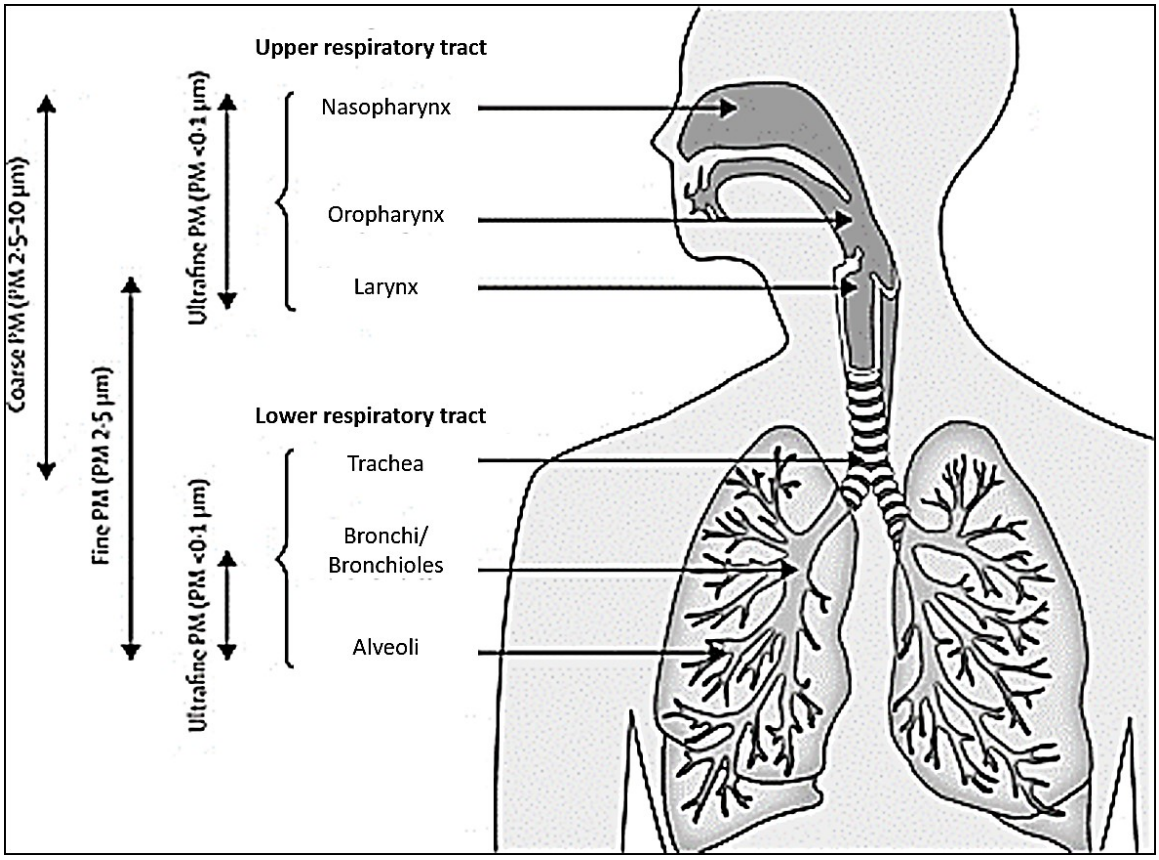

Figure 2-2: Diagram showing different parts of the human respiratory system and the level to which fine particulate matter (PM) penetrates the lungs (RSA, 2008; Kaonga and Ebenso, 2011).

Community members from low-income settlements report more health complications related to air pollution than people from wealthier residential areas (Govender *et al.,* 2011; Jimoda, 2012; Kelly and Fussell, 2015). Research conducted in low-income communities where high levels of air pollutants have been measured report more hospitalisations than other areas with lower pollutant concentrations (Fung *et al.,* 2007; Terblanche, 2009; Jimoda, 2012; Künzli, 2012; Kelly and Fussell, 2015; Tian *et al.,* 2018). Cases of hospitalisation increased from a rate of 0.5% to 5% for an increase of approximately 9.5 µg m^{-3} in outdoor PM_{10} (Anderson *et al.,* 2012; Kelly and Fussell, 2015). The rate was determined for ambient PM_{10} concentrations in industrialized areas that ranged 30–60 µg m^{-3} (Anderson *et al.,* 2012; Kelly and Fussell, 2015). The dilemma with low-income communities is that a large portion of pollution comes from PM-releasing activities (waste and solid fuel burning) within the settlements and at the same

time the most vulnerable people in society reside in these communities (Friedl *et al.,* 2008; Govender, 2011; Motsoene; 2014). Obtaining a broader understanding of the impacts of PM and showing the incidence of exposure in low-income communities of South Africa is one of the integral parts towards improving resident's quality of life.

2.3 Environmental impacts of particulate matter

Not only does natural or anthropogenic PM pose a threat to health (Anderson *et al.,* 2012; Kelly and Fussell, 2015), but anthropogenic PM also has a detrimental impact on the natural environment too (Tai *et al.,* 2010). The impacts manifest in global climate change where increased scattering and absorption cause fluctuations in average global temperatures (Tai *et al.,* 2010). Chen *et al.* (2018) observed that anthropogenic emissions of fine PM into the atmosphere cause an increase in the amount of greenhouse gases (GHG). The diverse chemical properties of PM result in the warming of the atmosphere, impacting on the net radiation budget of the planet (Lydia, 2010; Atique *et al.,* 2014; Chen *et al.,* 2018). Of high importance, particulate matter can comprise compounds such as the GHG CO_2 which when emitted into the atmosphere have a warming effect that alters the planets total radiative energy budget (Kirkinen *et al.,* 2007; Seinfeld and Pandis, 2016). The direct physical impacts of PM also influence climate through absorption and scattering of short-wave energy; this also results in reflecting of incoming solar radiation back into space (Lydia, 2010; Atique *et al.,* 2014). The indirect impacts of the presence of PM involves the alteration of cloud properties, such as provision of condensation nuclei for cloud formation and through changing cloud life-time (Lydia, 2010). Elevated concentrations of PM in the atmosphere also have a great impact on visibility, with one such example in South Africa being the Cape Town Brown Haze during the early 2000s (Wicking-Baird *et al.,* 1997; Zunckel *et al.,* 2004; Walton, 2006; Hwang and Hopke, 2007). Poor visibility can lead to fatal accidents and an increase in human deaths. The components of radiative forcing associated with increase of anthropogenic aerosols in the atmosphere are illustrated in Figure 2-3 below.

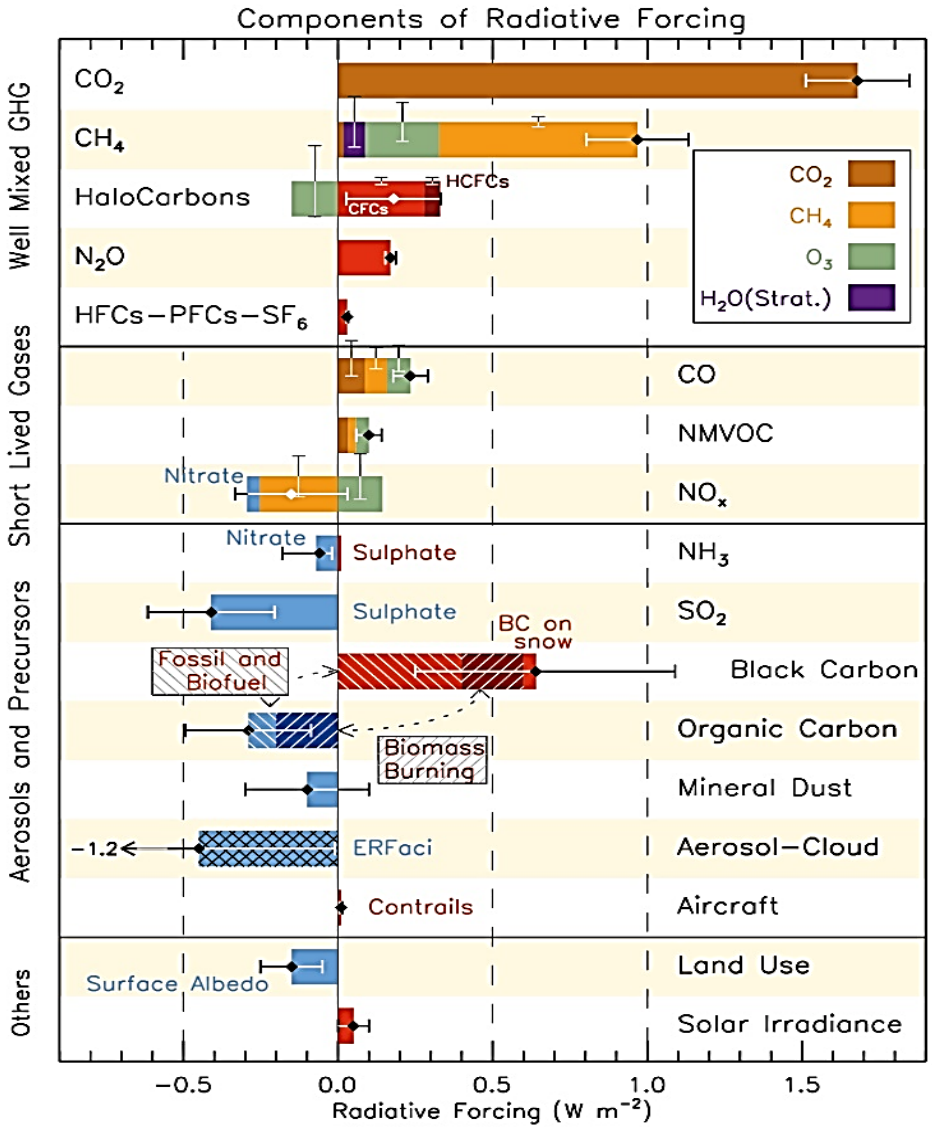

Figure 2-3: Components of radiative forcing (Myhre *et al.,* 2013).

2.4 Indoor/Outdoor (I/O) relationship of PM

Yocom (1982) and Moraskwa *et al.,* (2001) made the assertion that it is important to understand the relationship between indoor and outdoor PM and how they vary in space and time. Adgate *et al.,* (2002) reported that outdoor concentrations of PM are generally lower than those found in the indoor environment. The spatial and temporal variability of ambient PM is governed by meteorological conditions, synoptic circulation and atmospheric stability (Gatebe *et al.,* 1999; Milner *et al.,* 2005; Mkoma and Mjemah,

2011; Zeng and Yang 2017). Indoor concentrations of PM rely mainly on the strength of the indoor source, infiltration, resuspension and ventilation methods of a dwelling (Milner *et al.,* 2005; Chen and Zhao, 2011; Lv *et al.,* 2017). Milner *et al.* (2005) suggests that PM originating from outdoor sources in cases where no indoor sources exist have been found to be dependent on numerous factors: household ventilation habits, airtightness or leakage of the house, physical characteristics of PM (resuspension, deposition, chemical processes) and meteorological conditions prevailing around the house (dispersion, temperature, relative humidity) (Milner *et al.,* 2005; Lv *et al.,* 2017).

I/O PM ratio

The build-up of outdoor concentrations of PM can be influenced by the stability of the atmosphere, subsequently influencing I/O ratios (Chaloulakou *et al.,* 2003; Riain *et al.,* 2003; Chen and Zhao, 2011). The prevalence of stable atmospheric conditions in the evening results in low dispersion of pollutants and is favorable for elevated concentrations of PM within low-income areas (Chen and Zhao, 2011). Low-level sources found in and around communities emit PM below the stable layer and the pollutants are trapped for extended periods of time which has an impact on the I/O ratios. A diagram showing how outdoor particles typically enter the indoor environment of a residential dwelling is represented in Figure 2-4.

The relationship between indoor and outdoor PM concentrations is expressed through the I/O ratio which is commonly denoted as, Equation 2-1:

$$I/O\ ratio = \frac{C_{in}}{C_{out}} \qquad \text{Equation 2-1}$$

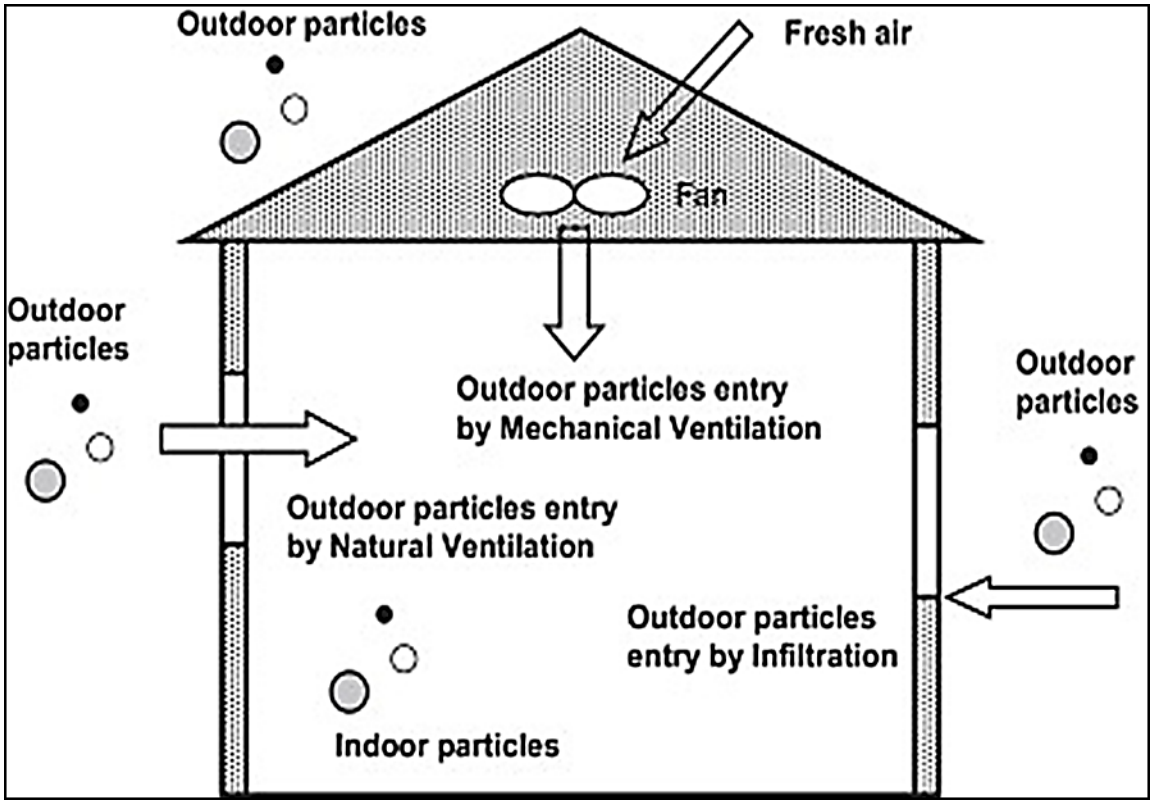

Figure 2-4: Typical pathways of particulate matter (PM) from the outdoor penetrating the indoor environment (Chen and Zhao, 2011).

Particulate matter concentrations have been observed to be higher during inversions, periods of low wind speeds and in the late evenings to early mornings (Chaloulakou *et al.,* 2003; Chen and Zhao, 2011). Indoor and outdoor ratios have been observed to be higher during the evening due to higher air exchange rates and lower wind speeds (Ni Riain *et al.,* 2003; Chen and Zhao, 2011). During the evening, indoor concentrations are higher than those in the outdoors (Ni Riain *et al.,* 2003). Outdoor concentrations of PM are largely influenced by atmospheric parameters and consequently influence indoor concentrations (Milner *et al.,* 2005; Mkoma and Mjemah, 2011). Firstly, the dispersion and dilution of PM around a house influences the concentrations around the building. Secondly, the behavior of occupants of a house and air exchange rates of the building influences the concentrations found indoors (Milner *et al.,* 2005; Guo *et al.,* 2010).

Infiltration coefficient of PM

Infiltration of PM into the house is due to the penetration of air from outside into the interior of the building (Chaloulakou *et al*., 2003; Lv *et al*., 2005; Milner *et al*., 2005;). The infiltration occurs due to the passage of air from the outside into the building through doors or cracks in the walls/windows or roof (Milner *et al.,* 2005). Liddament (1996) termed the flow/loss of air from the indoor to the outdoor environment as "exfiltration". The reduction of air infiltration into a building's interior presents many benefits including energy-saving and greatly reduces the impact of outdoor sources of air pollution inside the house (Liddament, 1996; Chaloulakou *et al*., 2003). According to Liddament (1996), an airtight building provides more comfort to occupants and ventilation can be achieved through the intentional opening of windows and doors when desired. Stephen (2000) noted that the largest database of air leakage rates was conducted in the United Kingdom by Building Research Establishmen (BRE.). The study covered 471 houses and set out to better understand air exchange rates and the correlation between airtightness and ventilation (Dimitroulopoulou *et al*., 2005).

The extent to which outdoor air pollution affects the indoor environment is represented by the infiltration coefficient (F_{in}). A linear regression model is used to get the relationship between indoor and outdoor PM and is also referred to as the RCS (Random component superposition model), expressed as follows:

$$C_{in} = F_{in}C_{out} + C_s \qquad \text{Equation 2-2}$$

Where C_{in} is the indoor particles concentration (μg m^{-3}), C_{out} the outdoor particles concentration (μg.m^{-3}), C_s the indoor source strength (μg.m^{-3}) and $F_{in}$the infiltration coefficient. This suggests that sources can be attributed to the indoor and outdoor environment as a function of infiltration.

Bivariate correlation analysis of Indoor/Outdoor PM

The correlation between two known components is established using a bivariate correlation investigation. The strength of the relationship is established by the (r) value representative of the Pearson correlation coefficient. The expression can be denoted as follows:

$$r = \frac{\sum(X-\bar{X})(Y-\bar{Y})}{\sqrt{(X-\bar{X})^2(Y-\bar{Y})^2}}$$ Equation 2-3

Where X and Y represent variables, and $\bar{X}$ and $\bar{Y}$ represent the means of the variables. In this document, the Pearson coefficient (r) is used to express the correlation between indoor and outdoor particles and other meteorological factors.

2.5 Sources of particulate matter in KwaZamokuhle

There are a diverse set of sources responsible for PM pollution in KwaZamokuhle (Held,1996; van den Berg, 2015; Wernecke *et al.,* 2018). These sources range from agricultural activities to domestic (solid fuel and waste-burning), industry and power generation. Other contributors include aeolian dust particles and open cast coal mining. The sections below describe the sources in more detail.

Agricultural activity and wind-blown dust

Typical particle emissions from agriculture are released from crop burning, livestock, odour from manure and fertilizers, chemical spraying of crops and eroded wind-blown dust (National Research Council (NRC), 2003; Voiland, 2010). The dust comprises a mixture of particles including pollen and seeds from crops (Lodhi *et al.,* 2009; Voiland, 2010). Chemicals used for spraying crops also form a constituent of PM from agriculture (Arslan and Aybek, 2012; Qi *et al.,* 2015). When herbicides and pesticides are applied during temperature inversions, their area of impact can be far greater than estimated (Fritz *et al.,* 2008; Alewu and Nosiri, 2011; Arslan and Aybek, 2012). This makes the control and mitigation of emissions from this sector quite challenging (Qi *et al.,* 2015). The roads between agricultural lands are gravel and are also a significant source of dust (Kuhns *et al*., 2005). Vehicles traveling on the unpaved roads produce dust entrainment and an increase in particulates in the atmosphere (Etymezian *et al*., 2003; Luhana *et al.,* 2004; Kuhns *et al*., 2005; Fritz *et al.,* 2008; Arslan and Aybek, 2012). The extent of entrainment is influenced by the volume and speed of traffic on the gravel roads (Etyemezian *et al.,* 2003; Kuhns *et al.,* 2005).

Agricultural PM emissions (dust and ammonium) tend to be seasonal and come from a large surface area (US-EPA, 1995). The highest particulate loading is generally recorded in the dry winter months, and the rainy summer seasons show lower concentrations

(Lodhi *et al.*, 2009; Arkouli *et al.,* 2010, Qi *et al.,* 2015). Meteorological conditions have control over emissions from agricultural crop and biomass burning and ultimately ambient air quality (Arslan and Aybek, 2012; Arunrat *et al.*, 2018*).* During thermal inversions, the potential for pollutants to disperse is reduced as they are trapped under stable conditions (Held *et al.*, 1996; Lydia, 2010; Qi *et al*., 2015). The latter finding indicates that biomass- and crop-burning should occur at mid-day and at the start of the dry season when the sub-tropical high pressure is dominant (Chen *et al.,* 2018).

P*ower-generation through coal.*

Electricity in South Africa (up to 90%) is predominantly generated by coal-fired power stations (Winkler, 2005; StatsSA, 2012; Pretorius *et al.,* 2015). These facilities contribute the largest portion of particulate loading on an annual basis in the ambient environment (Pretorius *et al*., 2015). The facilities emit pollutants that range from PM, SO_2, NO, NO_2, CO, CO_2 and trace elements of mercury (Pretorius *et al.,* 2015; Contini *et al.,* 2016). Tall stacks allow emissions to be released well above the stable surface layer (Muthige, 2014). However, emissions may still occur from wind-blown dust from coal stockpile yards and ash dumps (Muthige, 2014). Pollution abatement technology such as Bag Filters and Electrostatic Precipitators (ESP's) are installed at the power stations to reduce emissions and the environmental footprint of operations (Zhou *et al.,* 2005).

Indiscriminate waste-burning

Waste-burning is a major problem in South African low-income settlements and contributes to the increase in ambient PM (Nuwarinda, *2007;* Naidoo *et al,* 2013*;* Piketh *et al.,* 2016). These areas are densely-populated and a high volume of waste is generated (Pauw, 2008; Naidoo *et al.,* 2013). The local municipality in which a community resides is responsible for the routine collection of waste, usually on a weekly basis (Nkosi, 2015; Saucy *et al.,* 2018). Be that as it may, the amount of refuse generated exceeds the collection efficiency of municipalities (Naidoo *et al.,* 2013). This triggers the burning of waste in low-income settlements as community members see it as a best-fit strategy for reduction (DEA, 2013; Nkosi, 2015).

The accumulation of waste is an invitation to rodent infestation; hence residents keep the waste to a minimum by burning it. The combustion of the waste, however, comes

with health implications (Annegarn *et al.,* 1998; Rushton, 2003; Medina, 2010). The refuse is burned indiscriminately, without separation of wastes unsuitable for burning. This results in the release of harmful chemicals and fine PM. The waste contains anything from plastic to cloth, paper, rubber, aerosol cans and incombustible materials (Rushton, 2003; Medina, 2010; RSA, 2013). It is set alight and the flaming period is usually very brief, leaving the remaining residue to smoulder for hours at low temperatures (Annegarn *et al.,* 1998; Medina, 2010). The smouldering residual waste contributes to particulate loading and contains hazardous chemical compounds, such a polycyclic aromatic hydrocarbon Li *et al.,* 2012; Wang *et al.,* 2012).

Aeolian dust particles

Piketh *et al*., (1999) expressed that Aeolian dust is the major contributor to the total aerosol loading annually. Dust is defined as particles that have a diameter smaller than 1000 µm, usually suspended in the atmosphere or deposited on a surface (Haller, 1999; Kok, 2011; Moja and Mnisi, 2013). Meteorological factors and seasons influence the amount of suspended dust in the ambient air (Giri *et al.,* 2008). During dry and windy seasons, more dust is entrained and suspended in the atmosphere, while the opposite is true for periods when there is rain (Piketh *et al.,* 1999). Over the plateau, Aeolian dust is at a maximum in the dry South African winter, with percentage contributions to the detected loading varying between 64% and 73%. During summer, Aeolian contributions range between 20% and 40% over the interior. This can be noted when there are turbulent winds, when dust particles in the air naturally increase (Giri *et al.,* 2008). Vegetation on a terrain also has an impact on the amount of topsoil available to be eroded and transported. Maher *et al.,* (2010) reflects that the influence of dust on air quality and the climate needs further study and quantification.

Opencast coal mining

The mining of coal is a prominent activity in the Highveld region of South Africa where there is an abundance of coal and hence where majority of the country's coal-fired power stations are located. The mining operations are carried out in opencast mines using intensive extraction methods that initiate dust entrainment (Thompson and Visser, 2001). Activities that contribute to PM include blasting, a common practice used to mine coal and loosen overburden in opencast mines. Heavy diesel-operated equipment and

haul trucks also travel on unpaved roads to transport ore from blasting zones to screening areas and stockpiles (Thompson and Visser, 2001). Mine tailings also contribute to PM loadings, even long after the mine has shut down.

Thompson and Visser (2001) noted that “mechanical disintegration” of material is the most problematic feature that causes dust associated with opencast coal mining. Thompson and Visser (2001) put together an emission inventory of open dust sources and further went on to study the environmental implications related to dust. The core basis of the emission inventory was to enable assumptions of ambient PM concentrations and identification of problematic areas through the creation of a dispersion model for sources over a specific time period. The US-EPA42 guidelines were used as reference for analysis, and it was found by Amponsah-Dacosta (2015) that mine haul roads accounted for up to 93.3 % of the overall emissions from mine operations. The second-highest contributor to PM loading was linked to topsoil handling, see Figure 2-5.

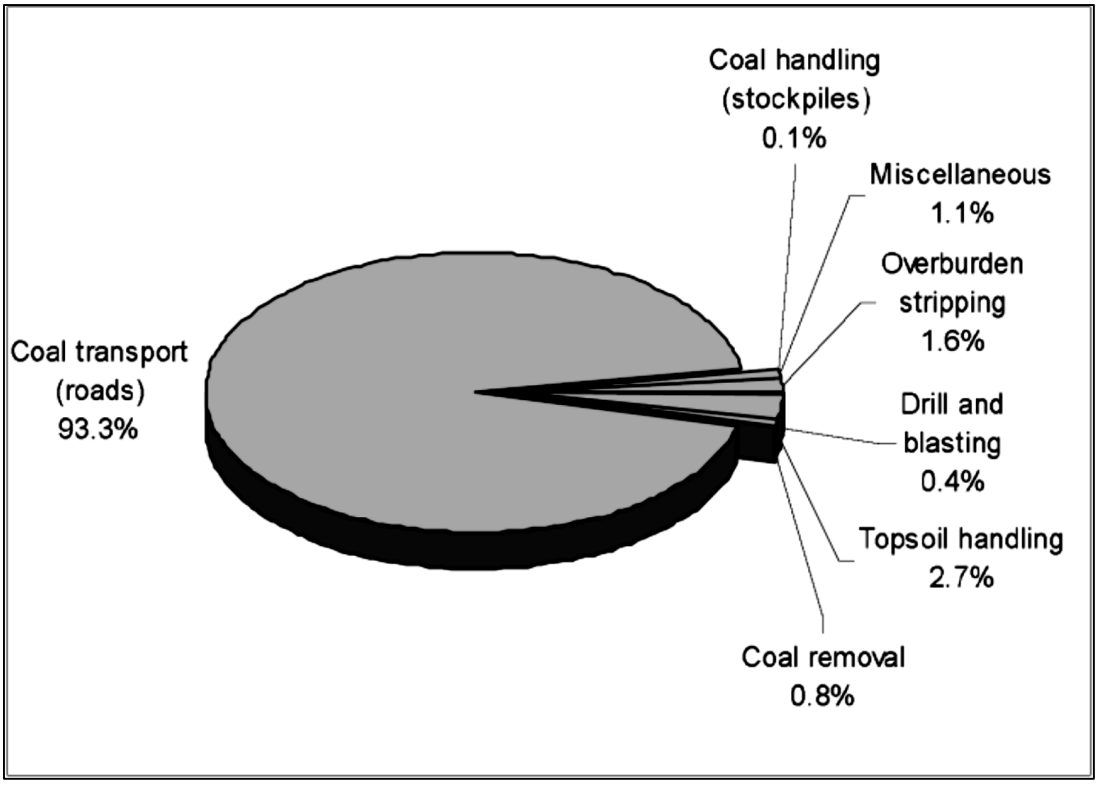

Figure 2-5: Percentage contributions to over-all dust emissions from representative South African opencast coal mine operations (Visser and Thompson, 2001).

Transport

KwaZamokuhle is situated between Middleburg and Ermelo alongside the N11 which carries heavy traffic volumes. There is a high proportion of diesel-powered vehicles along the route contributing significant amounts of PM to the ambient air. Trace elements emitted from diesel-powered vehicles contain high concentrations of black carbon (BC), magnesium (Mg), silicon (Si) and iron (Fe) particles (Maricq *et al.,* 2002; Kim *et al.,* 2003; Begum *et al.,* 2004; Begum *et al.,* 2007). Vehicular emissions are regarded as one of the most prevalent pollution sources in an urban setting. Vehicular emissions include nitrogen oxide (NO_x), carbon monoxide (CO), PM_{10} and volatile organic compounds (VOC's), and in some cases benzene (C_6H_6). A diverse set of activities that take place in a vehicle contribute to the emissions released. These include the start-up of an engine, revving of the vehicle (tailpipe emissions), refuelling, braking and evaporation from the engine (Kim *et al.,* 2003). The toxic gas carbon monoxide results from partial combustion of the fuel and the carbon is not fully oxidized to form carbon dioxide (CO_2). The reaction of nitrogen and oxygen under high pressure and temperature in the engine leads to the formation of nitrogen oxide (NO_x) (Kim *et al.,* 2003), which contributes to smog and acid deposition. Diesel engines, brake and clutch linings wear of vehicles are responsible for sulphur dioxide (SO_2) emissions (Begum *et al.,* 2007) and acidic deposition. A number of factors influence the emissions produced by different vehicles and these include, driving speed, type of fuel used, age and emission control technology so the emissions rate differs from vehicle to vehicle.

Domestic solid fuel burning

Studies have identified domestic burning of solid fuels such as coal and wood as potentially being the largest source to PM that people are exposed to on a daily basis (Desai *et al.,* 2004; Balakrishnan *et al.,* 2011; Naidoo *et al.,* 2013; Makonese *et al.,* 2017). Low-income areas generally rely on a mixture of fuels to meet energy requirements and these fuels range from coal, wood, paraffin, liquid petroleum gas (LPG), crop residue, animal dung and other waste material to a lesser extent (Makonese *et al.,* 2017; Francioli, 2018). Although electricity is available in most low-income areas, supply is not consistent and the cost per unit is expensive for residents who are largely unemployed or depend on social grants (Ismail and Khembo, 2015; Francioli, 2018). Besides the difficulty in affording of electricity, cultural preferences for cooking of certain

dishes influences solid fuel use in some households (Nkosi *et al.,* 2017; Makonese *et al.,* 2017). A further motivating factor which encourages residents to continue using coal and wood is the dual function it offers during winter whereby residents can simultaneously cook and space-heat (Balakrishnan *et al.,* 2011; Makonese *et al.,* 2017).

Domestic solid fuel burning often takes place in old and poorly-designed cast iron stoves and braziers. These appliances are situated inside the home and householders inhale high concentrations of the emitted pollutants. Low-income settlements are densely populated and the use of solid fuels by most residents has a significant influence on PM concentrations observed in such areas (Naidoo *et al.,* 2013). Household income, availability of electricity and presence of informal households are some contributing factors to high levels in townships. A number of factors have been identified as drivers of fuel choice, namely: household income per month (the higher the income, the lower the dependence of solid fuel); proximity to coal merchant or mine (ease of access promotes use of coal); local availability of trees as a source of fuel; average/minimum winter temperatures (the colder the temperature, the greater the need for solid fuel use); housing construction and insulation type (Balmer, 2007). The signature pattern from household emissions has been identified as diurnal and seasonal and this is attributable to household energy use. The peaks in energy use and emission release are in the early morning and early evening which are generally periods when meal preparation and space-heating are undertaken. Increased burning of fuel and emissions is also seen in the height of winter this is expected due to the demand for space-heating during the coldest winter months (Pauw, 2008).

2.6 Particulate matter source characteristics

Assigning PM species to a precise source can be achieved due to the uniqueness of chemical characteristics of PMs emitted. The chemical composition of PM from each source type is summarised in Table 2-1. Abundances of Si, Al, K, Ca and Fe are associated with crustal or geological material. The overall abundance of K is approximately 15–30 times that of K^+. The relative abundances of Fe, K, Ca and Al are comparable across source profiles although Si is typically present in abundances of 14% in unpaved versus 20% in paved road dust. Organic carbon (OC) abundances in natural soil samples are in the range 5 – 15%, but are most abundant in agricultural and paved

road dust. Elemental carbon (EC) abundances vary greatly in crustal material and are often insignificant in natural soil samples. Road transport (motor-vehicles) contributes to OC and EC abundances seen in paved road dust samples. Motor-vehicles before the early 2000s contributed significantly to lead (Pb) abundances; however, the contribution has reduced significantly following the removal of Pb from fuel in South Africa. In general, abundances of SO_4^{2-}, NO_3^-, NH_4^+, are low, falling in the range of 0–0.3% for gravimetric samples. Na and Cl are also low, making up less than 0.5% of PM samples on average. Elemental and organic carbon are the most abundant species in PM from motor vehicle tail-pipe exhausts, contributing over 95% of the total mass. However, Pb and Br abundances are low and highly variable. Zn is found in most vehicle exhaust profiles, although having a low abundance (0.05% or less) (Watson *et al.,* 2001).

Fine fraction particulate profiles undertaken by Watson *et al*., (1997) for residential wood and coal combustion and forest fires showed average organic carbon abundances to range from approximately 50% in residential wood combustion and forest fire profiles to approximately 70% in the residential coal combustion profiles. Elemental carbon profiles averaged 3%, 12% and 26% in forest fires, residential wood combustion and residential coal combustion profiles respectively. The OC/total carbon ratio are greatest in the forest fire profile with a ratio of 0.94. Similar ratios have been observed for residential wood and coal combustion profiles, with 0.81 and 0.73 recorded respectively (Watson *et al.,* 2004). Calloway *et al.,* (1989) found K^+/K ratios of 0.80 to 0.90 in burning profiles compared to the low ratios measured in geological material. SO_4^{2-}, NO_3^-, and Si abundances in residential coal combustion are 2–4 times higher than those in residential wood combustion and forest fire profile. Highly variable NH_4^+ abundances have been measured, with an average of 1.4% in residential coal combustion and 0.1% in the residential wood combustion and forest fire profiles respectively (Watson *et al.,* 2004).

Profiles for coal-fired electricity generation vary considerably from residential coal combustion, regardless of the similarity of the fuels. Owing to the different emission abatement technologies used. SO_4^{2-} has very high abundances in the particle phase of while SO_2 can be hundreds to thousands of times higher than the particle mass. Crustal elements such as Si, Ca and Fe in the coal-fired power generation profiles are present at 30–50% of the equivalent amounts found in the geological material. Aluminium is found at comparable or higher levels in the power generation profile compared to the crustal

material. Other elements such as P, K, Ti, Cr, Mn, Sr, Zr, and Ba have less than 1% abundances. Selenium has also been detected at abundances of 0.2–0.4% in coal-fired power station emissions where scrubbers were not installed, where there are scrubbers (Watson *et al*., 1997).

Abundances of SO_4^{2-}, NO_3^-, and NH_4^+ of particles directly emitted cannot account for the concentration of the species measured in the atmosphere as ambient concentrations contain both primary and secondary particles. SO_2, NH_4^+, and NO_x are the precursors for sulphuric acid, ammonium bisulphate, ammonium sulphate, and ammonium nitrate particles (Seinfeld, 1986; Watson *et al.,* 1994). Several volatile organic compounds (VOCs) may also change into particles due to photochemical transformation (Grosjean and Seinfeld, 1989). Many of the particles from fertilizers, particularly those containing ammonium nitrate, are volatile and transfer mass between the gas and particle phase to maintain a chemical equilibrium (Stelson and Seinfeld, 1982). This instability has consequences for ambient gas and particle concentrations in the atmosphere.

Table 2-1: Chemical species in various emission sources (Watson *et al*., 2004).

Source	Particle size	Chemical Abundances in % Mass			
		< 0.1%	0.1 to 1%	1 to 10%	> 10%
Paved Road Dust	Coarse	CR, SR, Pb, Zr	SO_4^{2-}, Na^+, K^+, P, S, Cl, Mn, Zn, Ba, Ti	EC, Al, K, Ca, Fe	OC, Si
Unpaved Road Dust	Coarse	NO_3^-, NH_4^+, K^+, P, S, Cl, Ti	SO_4^{2-}, Na^+, K^+, P, S, Cl, Mn, Ba, Ti	OC, Al, K, Ca, Fe	Si
Construction	Coarse	Cr, Mn, Zn, Sr, Ba	SO_4^{2-}, K^+, S, Ti	OC, Al, K, Ca, Fe	Si
Agricultural Soil	Coarse	NO_3^-, NH_4^+, Cr, Zn, Sr	SO_4^{2-}, Na^+, K^+, S, Cl, Mn, Ba, Ti	Oc, Al, K, Ca, Fe	Si
Natural Soil	Coarse	Cr, Mn, Sr, Zn, Ba	Cl^-, Na^+, EC, P,S, Cl, Ti	Oc, Al, Mg, K, Ca, Fe	Si
Motor Vehicle	Fine	Cr, Ni, Y	NH_4^+, Si, Cl, Al, Si, P, Ca, Mn, Fe, Zn, Br, Pb	Cl^-, NO_3^-, SO_4^2, NH_4^+, S	OC, EC
Vegetative Burning	Fine	Ca, Mn, Fe, Zn, Br, Rb, Pb	NO^-, SO_4^2, NH_4^+, S, N^+	Cl^-, K^+, Cl, K	OC, EC
Residential Oil Combustion	Fine	K^+, OC, Cl, Ti, Cr, Co, Ga, Se	NH_4^+, Na^+, Zn, Fe, Si	V, OC, EC, Ni	S, SO_4^2
Incinerator	Fine	V, Mn, Cu, Ag, Sn	K^+, Al, Ti, Zn, Hg	NO_3^-, Na^+, EC, Si, S, Ca, Fe, Br, La, Pb	SO_4^2, NH_4^+, CO, Cl
Coal-fired boiler	Fine	Cl, Cr, Mn, Ga, As, Se, Br, Rb, Zr	NH_4^+, P, K, Ti, V, Ni, Zn, Sr, Ba, Pb	SO_4^2, OC, EC, Al, S, Ca, Fe	Si
Marine	Fine and Coarse	Ti, V, Ni, Sr, Zr, Pd, Ag, Sn, Sb, Pb	Al, Si, K, Ca, Fe, Cu, Zn, Ba, La	SO_4^2, NO_3^-, S, OC, EC	Cl^-, Na^+, Na, Cl

2.7 Synoptic circulation pollution dispersion over southern Africa

The prevailing atmospheric circulation over southern Africa is referred to as the "descending limb of the Hadley high pressure cell" (Tyson *et al.,* 1996a; Piketh *et al.,* 1999; Nguyen *et al.,* 2013). It dominates the tropospheric region with periodic subtropical anticyclones at atmospheric heights of 800 hPa (Tyson *et al.,* 1996a; Piketh *et al.,* 1999; Nguyen *et al.,* 2013). Sinking air in the tropospheric region is heated and dried, and a stable temperature inversion layer is created (Tyson *et al.,* 1996b; Piketh *et al.,* 1999).

The transportation of pollutants across the sub-continent is determined by numerous stable layers between which air parcels get trapped during tropospheric convection (Tyson *et al.,* 1996a; Garstang *et al.,* 1996). During periods of surface inversions, the stable layers that exist over the interior terrain prevent the vertical mixing of horizontal spreading of pollutants leading to higher concentrations at release points of emissions (Cosjin and Tyson 1996; Zunckel *et al.,* 2000; Freiman and Piketh, 2003; Nguyen *et al.,* 2013; Seinfeld and Pandis, 2016).

Over the Highveld region of South Africa, stable anti-cyclonic conditions provide suitable environments for the development of surface inversions (Held *et al*., 1990 Tyson *et al.,* 1996a; Lydia, 2010). PM released below the boundary layer remains stagnant resulting in high levels of PM concentrations. Surface inversions generally occur during the evening at heights of 90–200 m above the ground (Parker *et al.,* 1993; Held *et al.,* 1996; Lydia, 2010). The surface inversions occur mostly in winter and have the potential to be as low as 90 m above the earth's surface (Lydia, 2010).

CHAPTER 3 MATERIALS AND METHODS

This chapter provides an outline of the sampling protocol followed to acquire data for this study and the methods used to interpret the data. A detailed description of the research equipment used and quality procedures that were followed for the collection of good quality and reliable data-sets is provided. All calculations and statistical methods conducted in the data processing are explained in this chapter. The materials and methods are conceptualised to fulfil the research aim and objectives outlined in Chapter 1.

3.1 Study site description

This research was conducted in KwaZamokuhle, a low-income settlement in the Mpumalanga Province, South Africa and forming part of the Highveld Priority Area (HPA). The HPA, declared a priority area by the Minister of Environmental Affairs on the 23rd of November 2007 (Department of Environmental Affairs and Tourism (DEAT), 2011), spans across two provinces, namely, Mpumalanga and Gauteng. In all, the HPA covers an area of approximately 31 106km^2 and includes one metropolitan city, three district municipalities and nine local municipalities (DEAT, 2006). The HPA is infamous for high levels of criteria pollutants in the atmosphere which can be attributed to industrial, commercial and domestic sources (Held *et al.,* 1996; DEAT, 2006; Masekoameng, 2014). In this study, the primary focus is on respirable PM (PM_4). Known sources of PM in the HPA include agricultural activity, dust entrainment, waste-burning, petrochemical industries, smelters, power-generation, open-cast mining and domestic solid fuel burning (Scorgie *et al.,* 2012).

The topography of the HPA is relatively flat, forming part of the elevated inland plateau with gentle slopes that are situated at elevations between 1400 m and 1800 m above sea level (Lydia, 2010; RSA, 2011). The lowest areas lie to the north-west (Delmas Local Municipality) and the highest elevation is found in the south-eastern region (Pixley ka Seme Local Municipality) (Lydia, 2010; RSA, 2011). Ekurhuleni hosts the largest portion of its population and this can be attributed to it being a Metropolitan Municipality.

While the HPA falls in the Grassland Biome (Mucina and Rutherford, 2006) it has anthropogenic activities taking place in most areas (RSA, 2013). The activities include commercialised and subsistence farming of crops, livestock and forestation (RSA, 2013). Mining of coal and other minerals is also extensively practiced. The coal mined in the area is supplied to local power stations, is exported and used by residential households (RSA, 2013). Urban and rural settlements also form a large constituent of the anthropogenic land-use in the HPA.

KwaZamokuhle

KwaZamokuhle is a low-income settlement situated 26.1338°S, 29.7339°E, in the Mpumalanga Province adjacent to the small town of Hendrina, Figure 3-1. The town of Hendrina is Commercial centres in the broader vicinity of Hendrina are Middleburg situated 48 km to the north-north-east and Ermelo located 50 km to the south-west (SW). The N11 national road route passes through Hendrina, 2.5 km south-east of the and is a major transport route for light and heavy vehicles. KwaZamokuhle is located in the Nkangala District and Steve Tshwete Local Municipality. The settlement has a population of approximately 20427 people from 5874 households. Since the settlement falls in the HPA, the air quality can be expected to be poor. Three coal-fired power stations are located in the proximity of the settlement, 18.3 km north-west of Hendrina, 22.5 km north-north-east of Arnot and 27.3 km West North West (WNW) of Komati.

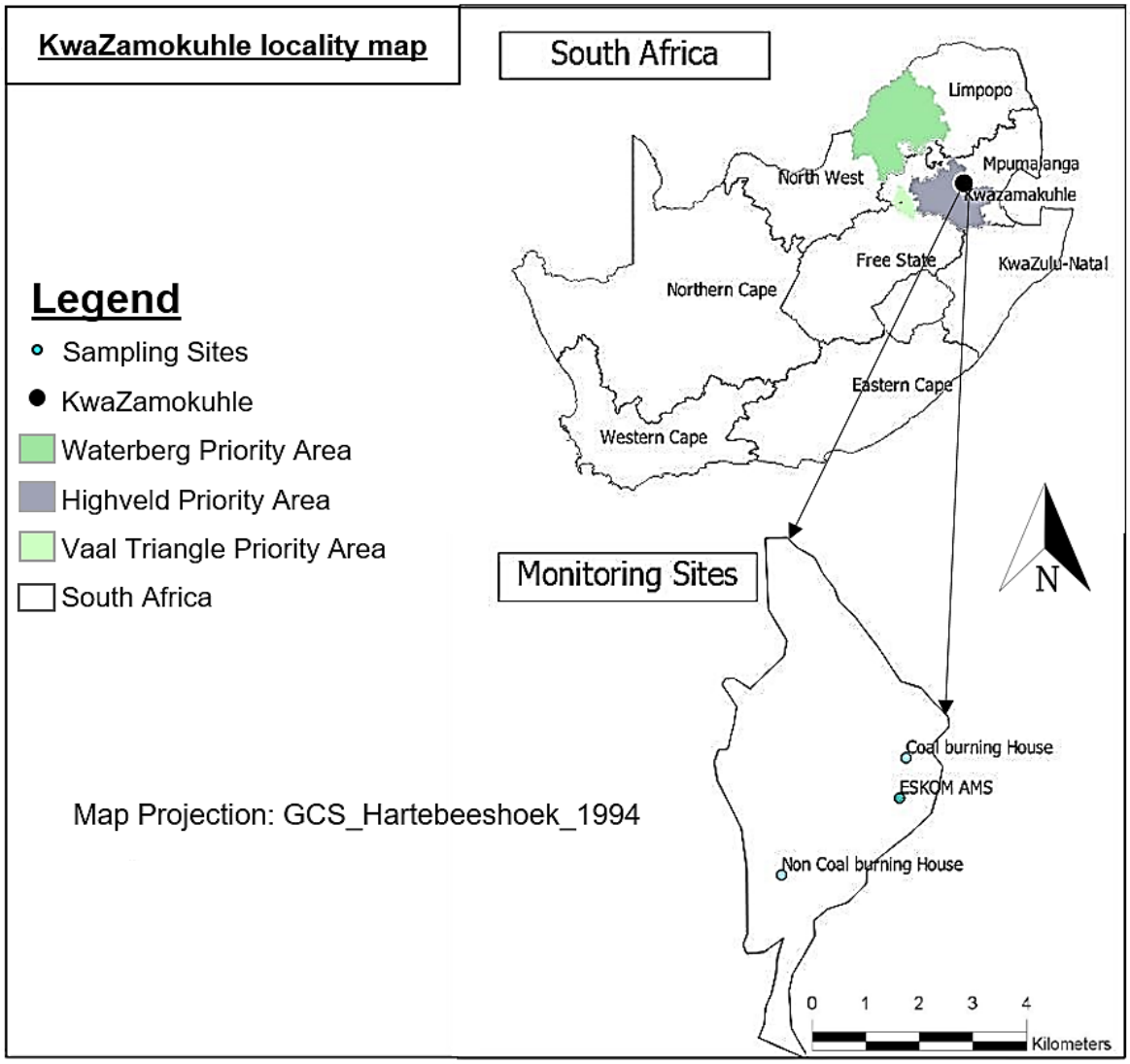

Figure 3-1: Spatial distribution of the sampling sites within KwaZamokuhle, and the locality of the study area in South Africa.

Meteorological conditions of the HPA

Climatic conditions in the HPA are temperate and winters are typically cold and dry with little to no rainfall. Warmer temperatures are experienced in the summer with rainfall in the form of thundershowers (Held *et al.,* 1990). The dry winters are a result of the prevailing subtropical high-pressure system while the summer rainfall is attributed to the low-pressure trough which develops over the central interior (Held *et al*., 1990). The distribution of rainfall in the area is such that the high-lying areas in the east receive approximately 900 mm, and the low-lying western parts receive around 650 mm

annually. Rainfall season is falls between October and March during the summer period. Surface winds that most frequently dominate the HPA are north to north-easterly and these can be attributed to the anti-cyclonic circulation (Tyson and Preston-Whyte, 2002), Figure 3-2. The second-most prevalent winds are easterly winds. Annual wind speeds vary between 2 m s^{-1} and 4 m s^{-1} on average, with a maximum of 6 m s^{-1} between August and September (Tyson and Preston-Whyte, 2002).

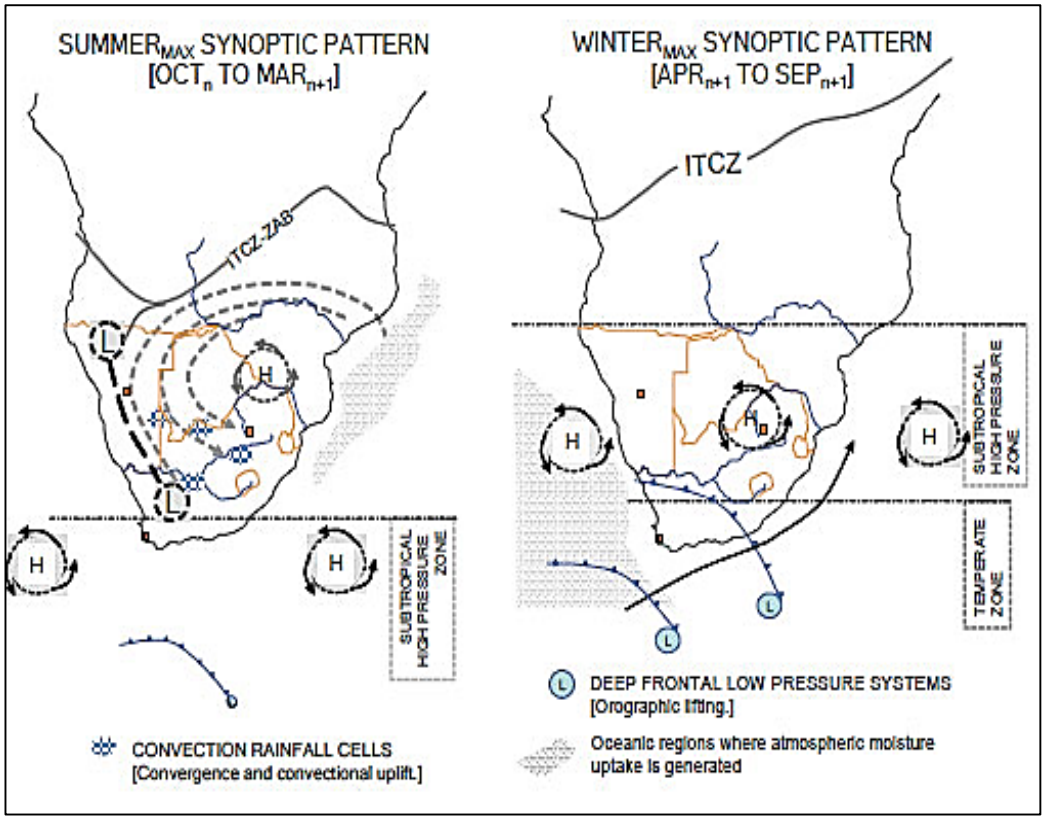

Figure 3-2: Annual winter and summer synoptic conditions over the sub-continent of Africa This circulation is important for the dispersion and transport of pollutants over the HPA (van Wyk, 2011).

Dispersion potential of pollutants in the atmosphere

The deposition, dispersion and transportation of atmospheric pollutants is determined by the meteorology and topography of an area (Tyson and Preston-Whyte, 2002). The atmosphere has the capability of diluting or remove pollutants released from any source and this ability is referred to as the “dispersion potential” (Tyson and Preston-Whyte, 2002). Pollutants and their potential to cause health problems are largely determined by

the source and also the ability of the atmosphere to dilute and disperse the air pollutant (Tyson and Preston-Whyte, 2002).

Dispersion in the atmosphere is driven by two factors, namely, the average wind flow that transports the pollutants up and downwind, and, the turbulent wind speed changes that disperse the pollutants in different directions (Tyson and Preston-Whyte, 2002). In the boundary layer of the earth's atmosphere (nearest to the surface), the amount of turbulence will determine the degree to which air pollutants are dispersed (Tyson and Preston-Whyte, 2002).

Air moves in a vertical or horizontal orientation in the atmosphere (Tyson and Preston-Whyte, 2002). The vertical movement of air occurs as a result of the thermal transmittance from the surface traveling upwards mixing to heights of about 5000 m (Tyson and Preston-Whyte, 2002). The atmosphere's stability and depth of the surface boundary layer are important in the determination of the vertical profile (Tyson and Preston-Whyte, 2002). Horizontal dispersion of pollutants in the boundary layer, on the other hand, is a result of wind speed and topography. While wind speed will determine the rate which pollutants are dispersed, diluted and transported down-wind (Tyson and Preston-Whyte, 2002), topography will influence the magnitude of turbulence experienced in the atmosphere (Tyson and Preston-Whyte, 2002). Pollutants follow the direction of horizontal wind flow, and since wind direction is highly variable, so too is the direction in which pollutants move (Tyson and Preston-Whyte, 2000). It can be seen that the concentration of pollutants at any given point is reliant on a number of factors, particularly atmospheric stability, mixing depths and topography (Tyson and Preston-Whyte, 2002). Meteorological conditions are the fundamental features that are responsible for pollution dispersion and subsequent removal from atmosphere, therefore important for the determination of the dispersion potential of an area (Tyson and Preston-Whyte, 2002). The meteorological parameters include temperature, rainfall, wind speed/direction and humidity (Tyson and Preston-Whyte, 2002).

The horizontal transport of pollutants and air circulation over the Highveld

The level of pollution in the air is determined by the micro-climate of an area; this includes the horizontal and vertical wind flow respectively. Daily and average pollution concentrations are influenced by atmospheric stability, and the horizontal wind-flow

determines the rate at which pollutants are transported and dispersed across the terrain (Tyson and Preston–Whyte, 2000). In the HPA, horizontal flow is responsible for the transport and dispersion of atmospheric pollutants. Horizontal transport is persistent on a local and meso-scale and influences the removal of air pollutants. Recirculation, on the other hand, maintains elevated concentrations of pollution in the area. The southern part of Africa is associated with a diverse set of meteorological conditions which have a direct bearing on emissions, transport and radiative forcing of aerosols (Garstang *et al.,* 1996; Andreae *et al.,* 2001; Ichoku *et al.,* 2003; Schulz *et al.,* 2006). Vertical mixing of pollutants is inhibited by prevailing anti-cyclonic conditions, stable-layers and inversions over the subcontinent (Tyson and Von Gogh, 1976; Tyson *et al.,* 1996a; Freiman and Tyson, 2000; Piketh and Walton, 2004).

3.2 Study Design

The characterisation of respirable PM (PM_4) was accounted for by implementing various methodological approaches, as represented in the conceptual flow diagram, Figure 3-3.

The main experimental procedures included in the study were those of continuous monitoring and gravimetric sampling. The continuous monitoring was conducted in both the indoor (I) and outdoor (O) environment, while continuous monitoring and gravimetric sampling were conducted within the indoor environment. The continuous monitoring was implemented to identify subtle changes in particulate loading and meteorology over time and to ascertain if there are specific periods of increased exposure in the indoor and outdoor environment.

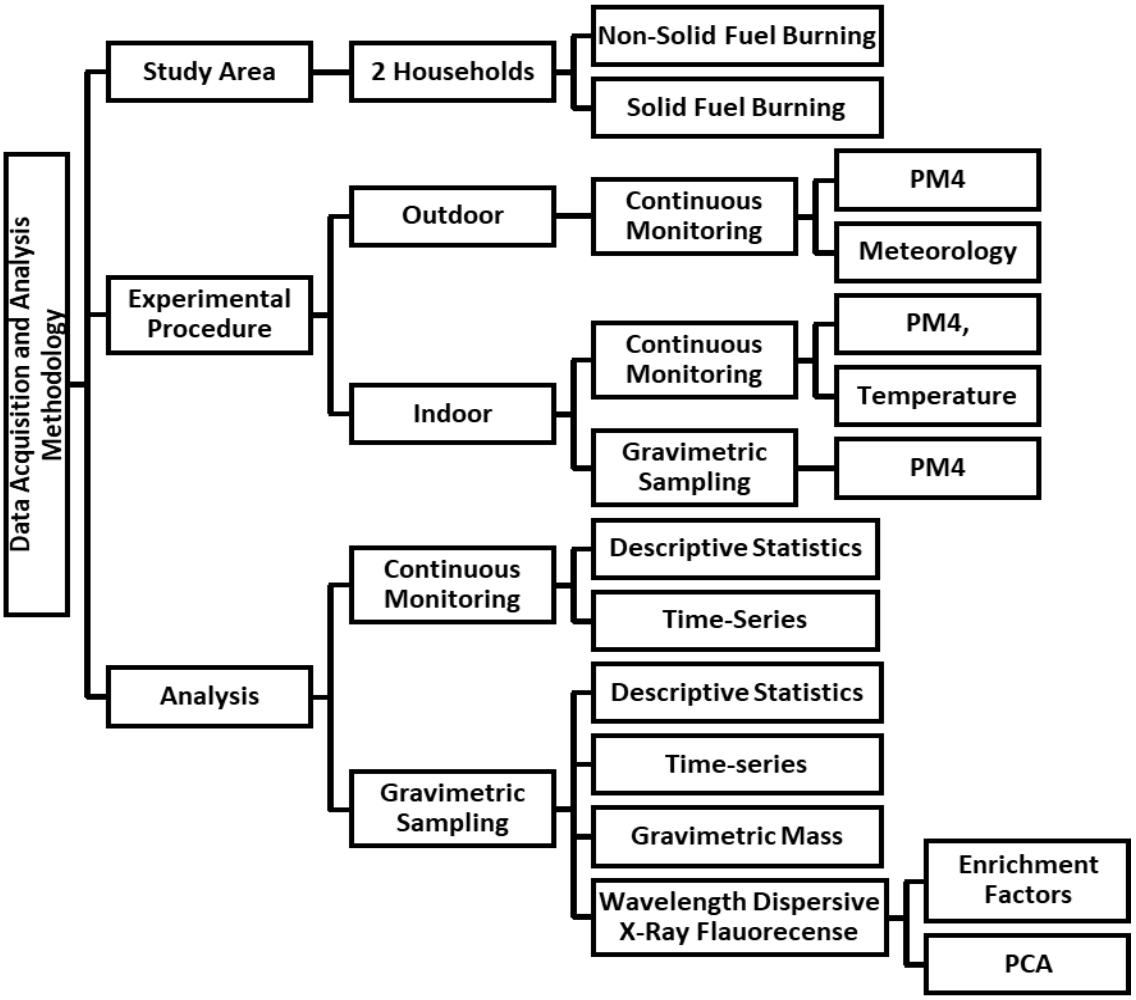

Figure 3-3. Conceptual flow diagram outlining the data acquisition and analyses methodology utilised in the study.

This study was conducted during winter and summer 2017 for the periods outlined in Table 3-1 below. Samples were collected from two households in KwaZamokuhle settlement. The houses where samples were collected had representative characteristics and demographics of a typical household in a low-income settlement, see Table 3-2 for classification. The selected houses were formed part of the Reconstruction and Development Programme (RDP) and as such were given to residents by the South African government. The household energy use for the two houses differed, with one house exclusively using electricity as the energy carrier and the other where a mixture of electricity and coal was used.

Table 3-1: Duration of sample collection for summer and winter 2017 in KwaZamokuhle.

Season	Start date	Stop date
Winter	17 July 2017	09 August 2017
Summer	01 November 2017	28 November 2017

Household descriptions

The study made use of two standard RDP houses which meant that these houses had no additional extensions built onto the initial structure; thus the houses were similar in size and dimension. The two households are further classified into solid fuel burning (SFB) and non-solid fuel burning (NSFB). The household classification is summarised in Table 3-2.

Table 3-2: Classification of a non-solid fuel burning (NSFB) household and a solid fuel burning (SFB) household where samples were collected in KwaZamokuhle during summer and winter 2017.

House No.	House type	Insulation	Occupants	Energy carriers	PM sources	Classification
H01	Formal RDP	Ceiling, plastered walls	4	Electricity	Next to an unpaved road	NSFB
H02	Formal RDP	No ceiling walls not plastered.	3	Electricity, coal, wood.	Domestic solid-fuel-burning, waste-burning	SFB

Non-solid fuel burning (NSFB) household

The NSFB house was situated next to an unpaved road, which could impact significantly on the PM loading in and around the house. The house was noted to consist of two bedrooms, a bathroom and an open-plan kitchen and living room area. These areas had access to window ventilation Figure 3-4. The front door access to the house was situated in the living room, while there was a back-exit door in the kitchen. The two bedrooms were situated on the north-facing side that receives most direct sunlight. The house had some insulation as it had plastered walls and a ceiling. Four occupants were

found to be staying in the house at the time of sampling. These residents made use of electricity as their main energy carrier.

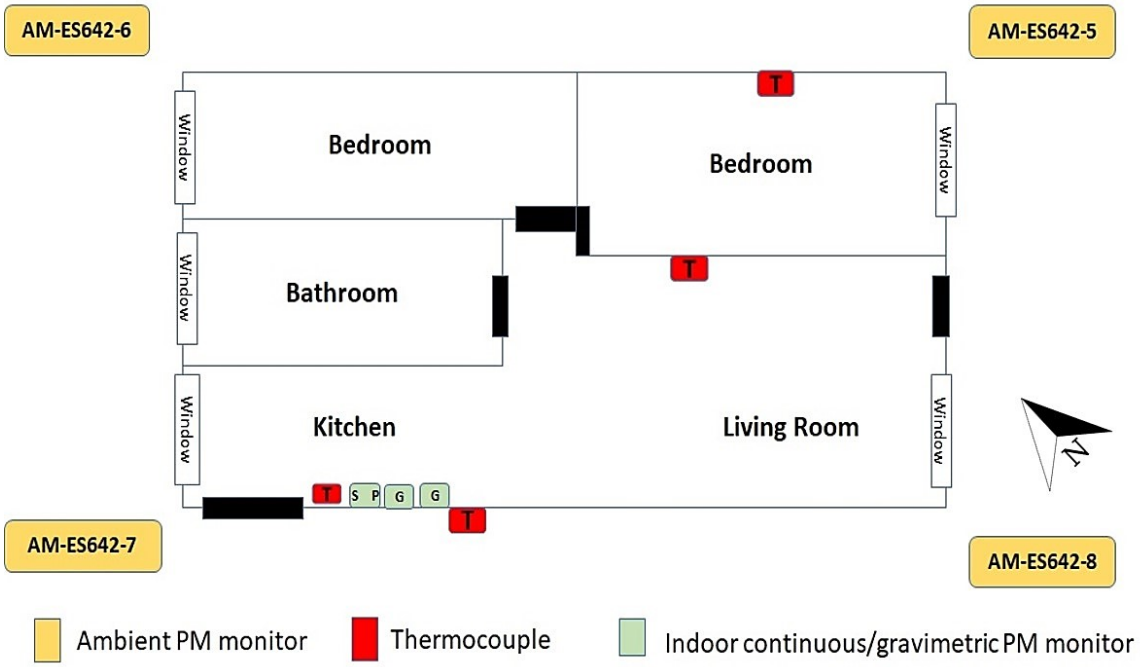

Figure 3-4: Schematic drawing of the non-solid fuel burning (NSFB) household including the placement of instruments in the indoor- and outdoor environments.

Solid fuel burning (SFB) household

The SFB household was not situated next to an unpaved road; however, it was close to waste-burning activities that could contribute to increased particulate loadings. The house was noted to be divided into three distinctive areas, namely, a single bedroom, kitchen and living room (Figure 3-5). The front entrance of the house was situated in the living room while the back exit was in the kitchen. Both these areas also were noted to be north-facing. It was also found that the house was not insulated lacking both ceilings and plastered walls. There were three occupants residing in the house during the time of sampling. The residents made use of electricity, coal, and wood as their main energy carriers.

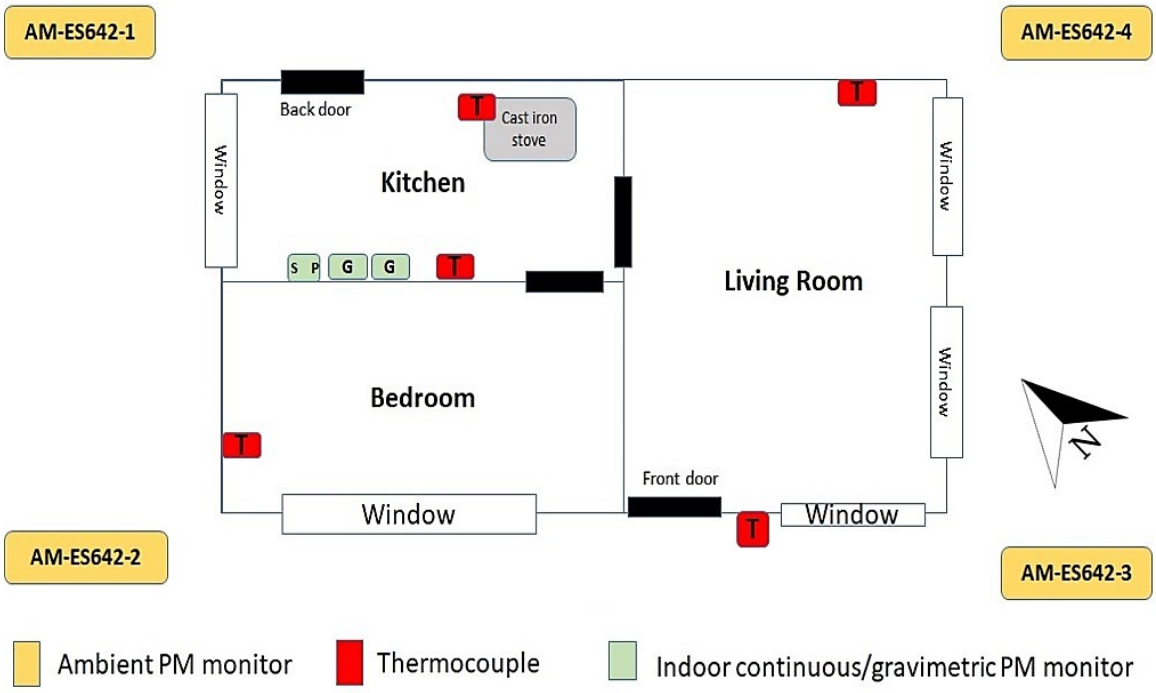

Figure 3-5: Schematic drawing of the solid fuel burning (SFB) household including the placement of instruments in the indoor- and outdoor environments.

The experimental procedure followed to collect and analyse the data is discussed in detail in Section 3.5.

3.3 Meteorological conditions

The KwaZamokuhle project was conducted during the summer and late winter season of 2017. The synoptic scale circulation and the subsequent diurnal variation in temperature, planetary boundary layer (PBL) height and wind speed (WS), has a major impact on the atmospheric dispersion of pollutants over the study area. The variation in climatic conditions also affects the behaviour of pollutants in the atmosphere.

South-Africa's location in the mid-latitudes, and beneath the descending leg of the Hadley cell, means it is affected by both tropical easterly disturbances in the summer and more moderate westerly disturbances during the winter, however, South-Africa's circulation is mainly dominated by a semi-permanent continental high-pressure system. The continental high-pressure system has a strong inter-seasonal variation that is

impacted by the seasonal north-south, south-north movement of Inter Tropical Convergence Zone (ITCZ). During summer months this high-pressure system is displaced south-wards and the central interior of the country experiences warm – tropical conditions with convective rainfall as the dominant source of precipitation. These convective processes are associated with the upward movement of warm air (convection) and result in an unstable PBL, ideal for the dispersion of pollutants.

During the winter the opposite occurs as the ITCZ moves north-wards with the onset of winter and the continental high-pressure system starts dominating the central interior circulation of South-Africa. The weather during winter months over central South-Africa is characteristically calm and mild. The predominant descending air column creates a stable PBL layer with very little mixing. Air, and pollutants, is subsequently trapped inside this stable layer and conditions for the dispersion of pollutants are not ideal. The difference in summer and winter temperature is also noticeable – varying from extreme warm daytime temperatures during the summer months, to cold evening and mild day time temperatures in the winter.

The meteorology section reports on the climatic conditions over the study area for the summer and winter measurement campaigns. Data is used from the European Centre for Medium-Range Weather Forecasts (ECMWF) ERA-Interim reanalysis with a spatial resolution of 0.75°×0.75° is used in this study. Three variables that have an impact on air pollution and dispersion are discussed here, this is mean sea level pressure (MSLP), Geopotential at 500 hPa (ZG500), PBL height and temperature at 2 m (T2M). Both MSLP and ZG500 represents the dominant airflow over the subcontinent and is used to indicate the presence of low and high-pressure systems, while the PBL height represents the layer of the troposphere in which mixing occurs, from a stable PBL in the winter to unstable conditions in the summer.

3.3.1. Mean winter synoptic conditions

The KwaZamokuhle winter campaign was conducted 2017/07/26 – 2017/08/16, towards the end of the winter season. The mean climatic conditions during this time are characteristically cold in the morning and evenings, while mid-day conditions are milder. The mean circulation and associated surface temperature are illustrated in Figure 3-6 and clearly indicates this diurnal variation in temperature during the period, the time

series plot (Figure 3-7) and the box and whisker plot (Figure 3-8) clearly shows the variation between evening and noon conditions with a mean difference of almost 15 degrees between 00h00 and 12h00 noon temperatures in the model data. Early mornings and evenings are characteristically cold, while mid-day temperatures are mild to warm. During winter the dominant continental high-pressure system plays a major part in preventing dispersion of pollutants via the descending column of air associated with it. This also effects the surface temperature and as discussed later the PBL height.

The atmospheric circulation and temperature further play a major role in the boundary layer's meteorological properties and diurnal variation, as illustrated in Figure 3-9. During the winter the dominant continental high-pressure systems prevent the major PBL variations observed in summer months, but an average 3000 m difference can still be observed as illustrated in Figure 3-10 and Figure 3-11.

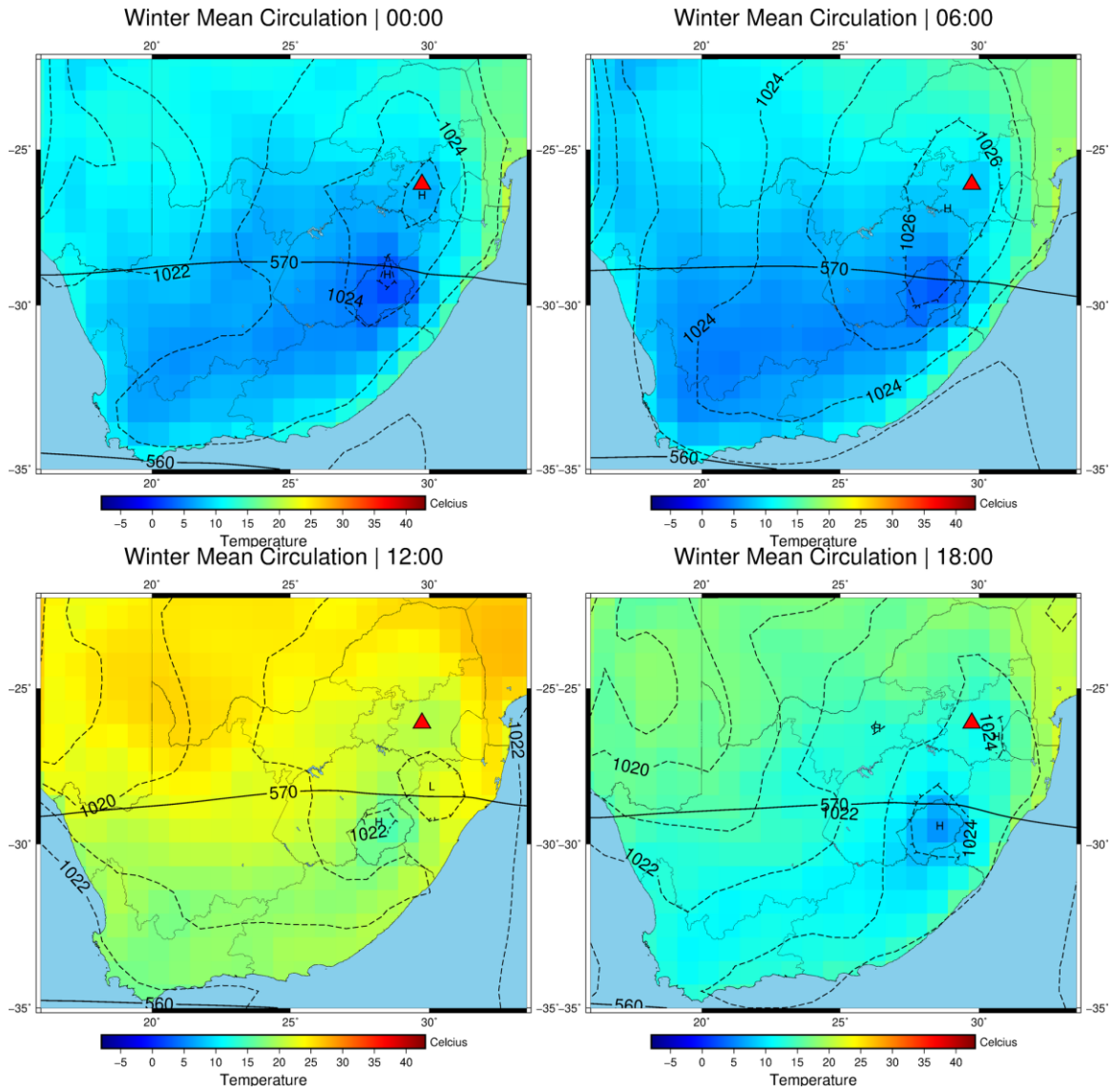

Figure 3-6. The mean winter circulation pattern for KwaZamokuhle (indicated here with the red triangle) as seen above shows the diurnal variation in temperature as well as the dominant circulation patterns during the campaign period.

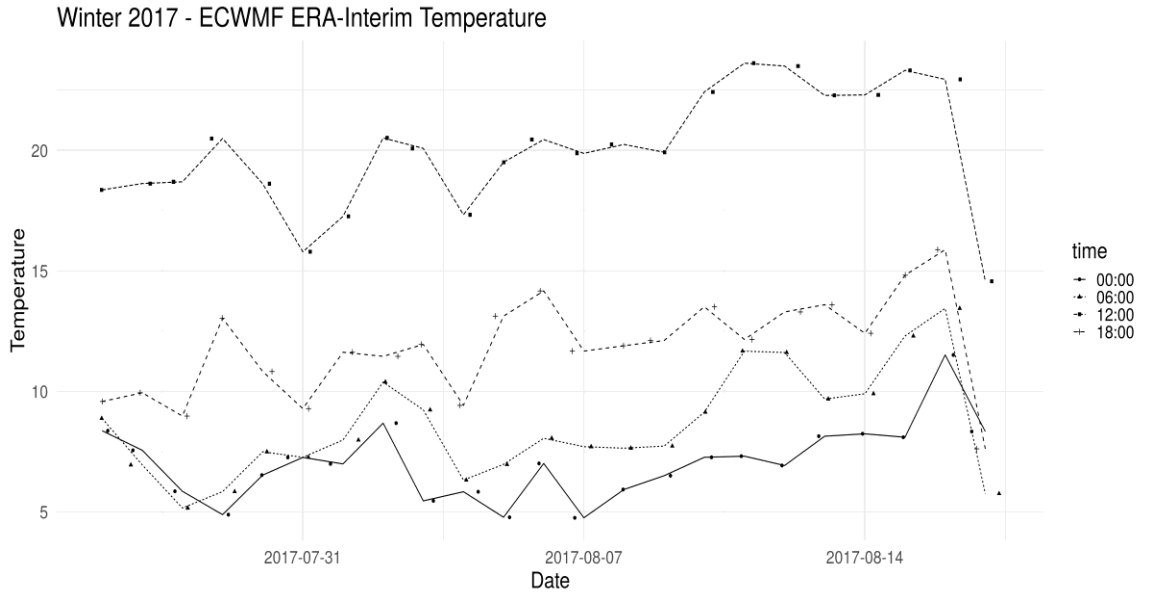

Figure 3-7. The above time series analysis indicates the surface temperature as a function of time from the ECWMF Era-Interim data.

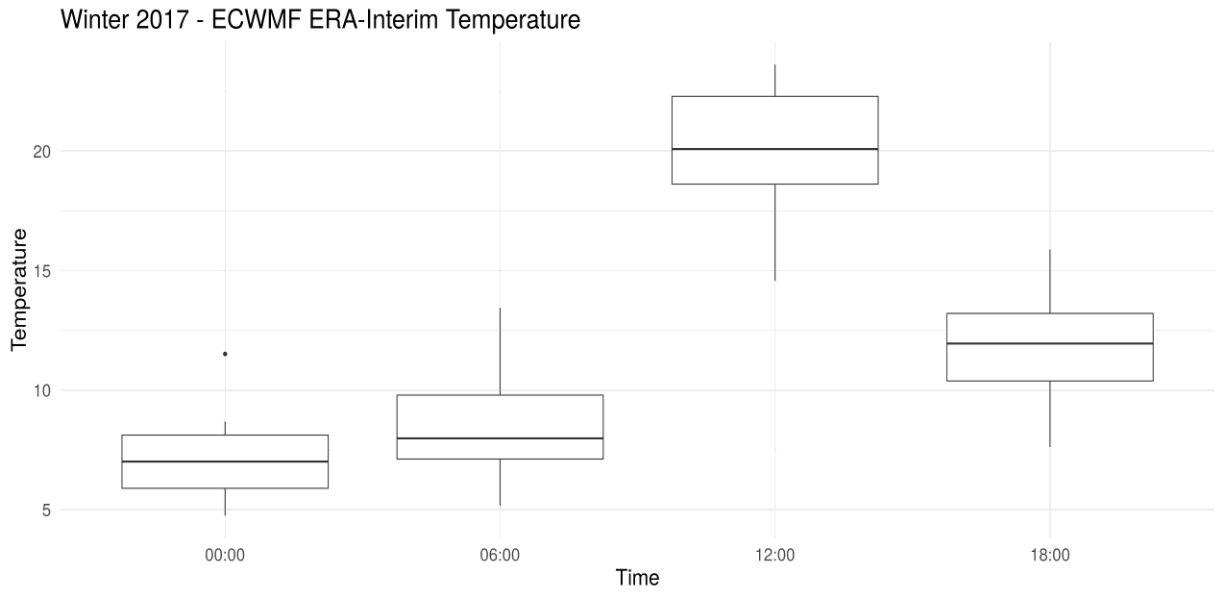

Figure 3-8. The box and whisker plot shows the difference between modelled surface temperature during midnight, morning, noon and late afternoon. The variation between the time steps are significant with mean 12:00 temperature and mean 00:00 differing by almost 11 degrees Celsius.

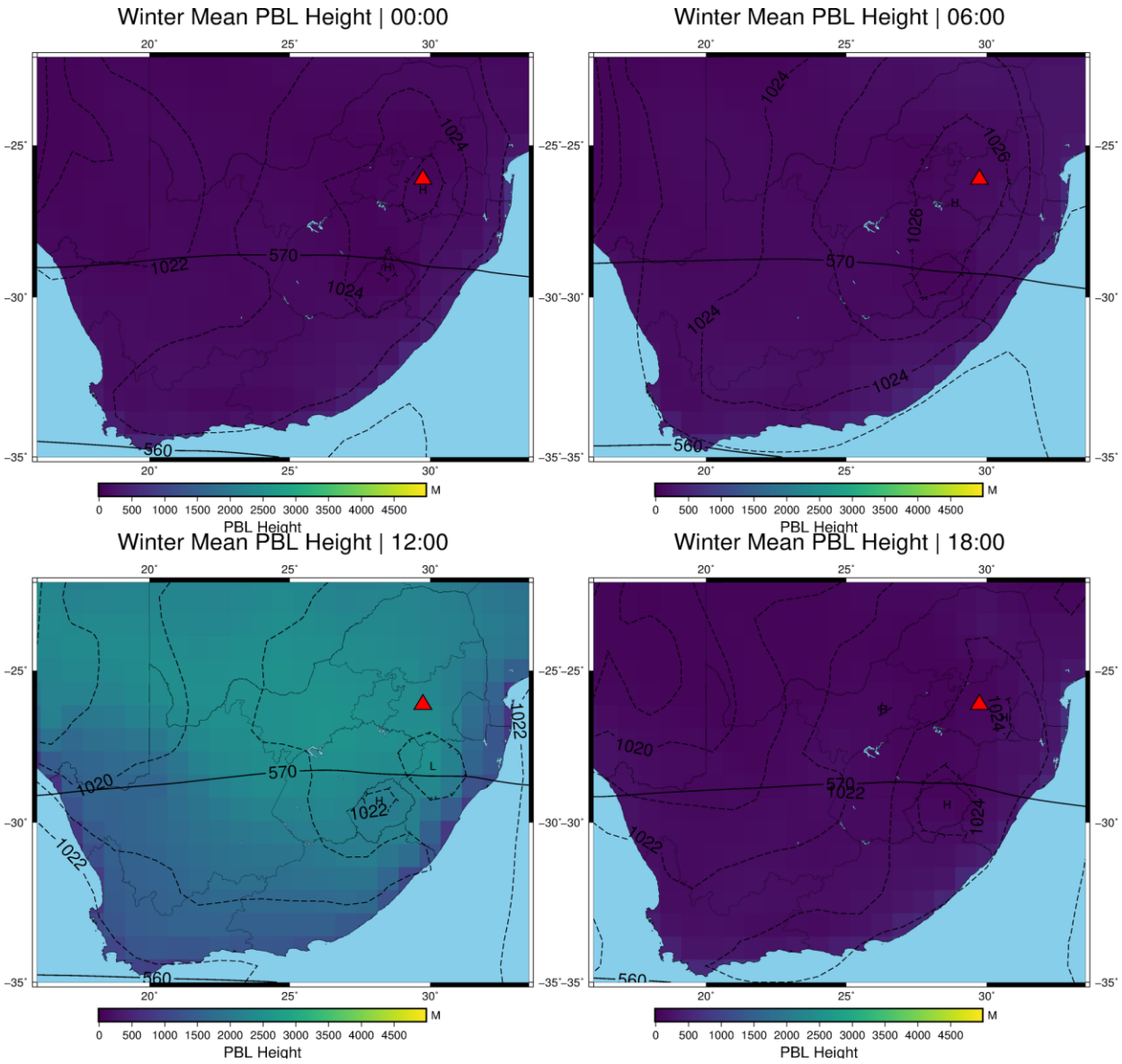

Figure 3-9. The PBL is also greatly influenced by the continental high-pressure system and its seasonal movement. During winter, as indicated above, the PBL is significantly lower during all times of the day. This then acts as a stable layer in the atmosphere, effectively "trapping" pollution close to the surface. As the sun rises and the earth's surface warms up the PBL rises and subsequently allows for mixing and dispersion of pollutants to take place.

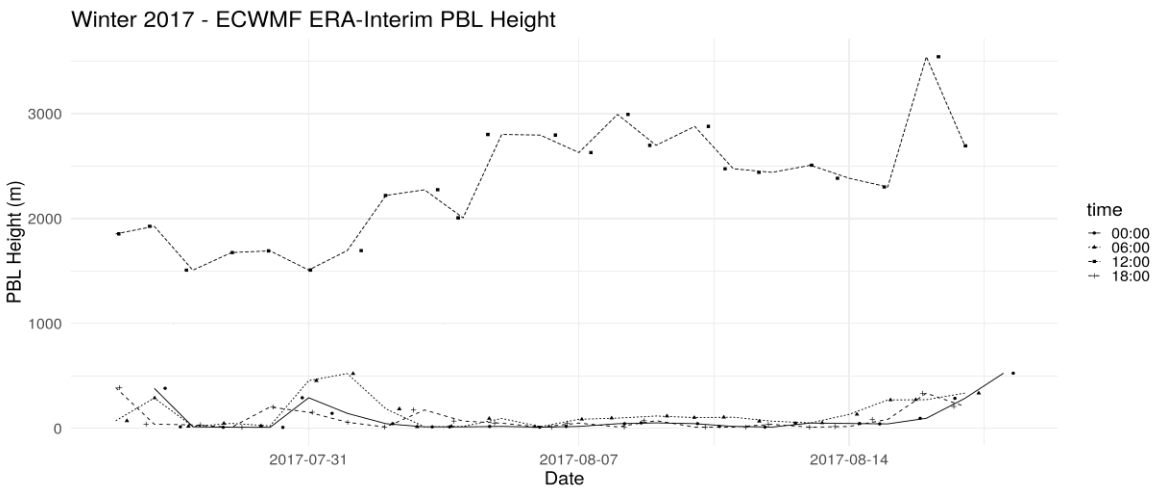

Figure 3-10. The variation in PBL height is clearly seen here with as much as a 3000m difference modelled between 6hr/24hr. This is mainly a result of the earth surface heating up during the day and convective processes lifting the PBL.

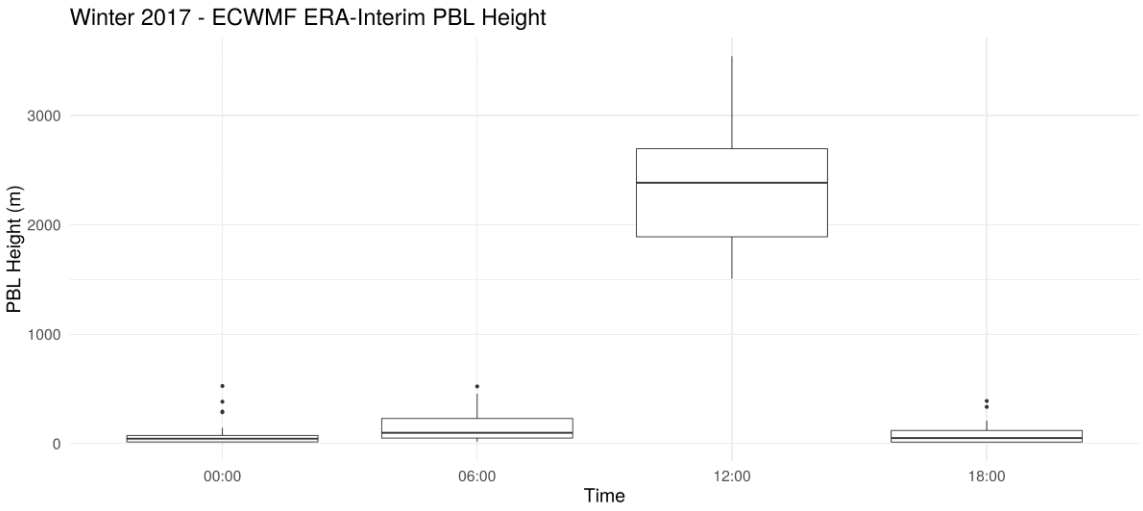

Figure 3-11. The statistical variation in the PBL height discussed in the previous time series is further illustrated in the above box and whisker plot. The diurnal variation is seen here is significant in its effect on air dispersion.

3.3.2. Mean summer synoptic conditions

Summer circulation is also impacted by the dominant and semi-permanent continental high-pressure system over South-Africa, but as the summer intensifies the systems are displaced and the circulation of South-Africa becomes more tropical by nature. During

this period rainfall is predominantly convective in nature and the surface temperatures increase. This also means that the PBL shows greater variability and air is usually dispersed more effectively over the subcontinent. Figure 3-12 indicates the mean synoptic and surface temperature conditions for the summer measurement campaign conducted from 2017/11/01 – 2017/11/28. The mean conditions show the easterly wave and low circulation prominent over the north-western part of the country while the continental high-pressure system is still observed over Mpumalanga and eastern South-Africa. The diurnal variation in temperature as indicated in Figure 3-13 shows interesting changes in the daily temperature's which could be the result of frontal systems moving over the study area during this time.

Examining the PBL (Figure 3-15) shows how the variation in temperature effects the PBL height too. The PBL is at its highest in the model during noon and subsequently moves with the diurnal cycle downwards as the sun sets. The time-series analysis of the PBL which can be seen in Figure 3-16 clearly shows the volatility of summer PBL height levels compared to stable winter levels. The morning and noon heights are significantly different from winter conditions, this allows for air to mix more effectively and also reduce the overall concentration of boundary layer pollution.

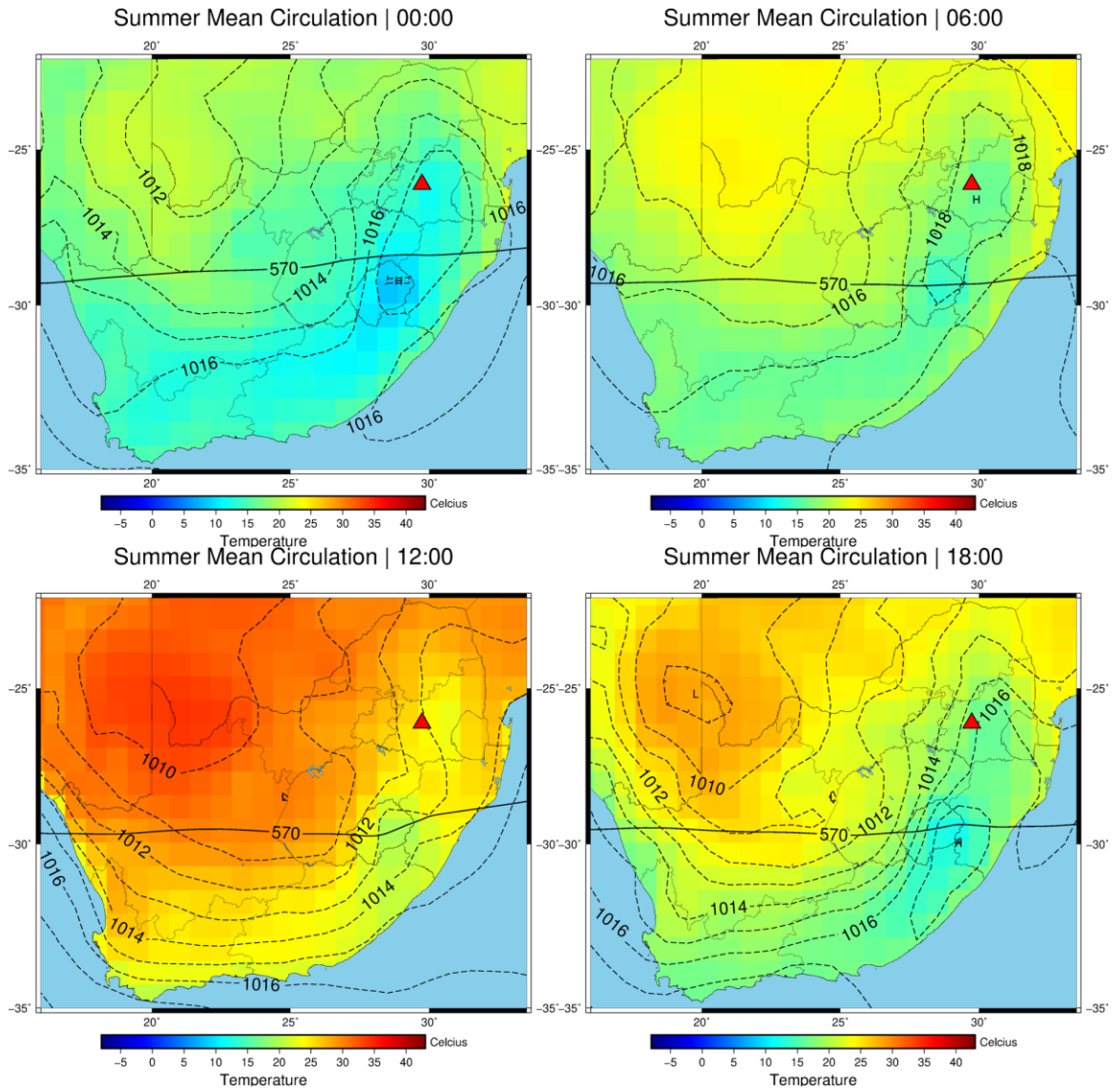

Figure 3-12. The summer circulation and surface temperature from the modelled data is significantly different from the winter campaign conditions. Temperatures across all time steps are higher and noon temperatures over KwaZamokuhle (indicated with the red triangle) is over 25 degrees Celsius during mid-day. The temperature plays a major role in the PBL height, stable layers and air pollution dispersion.

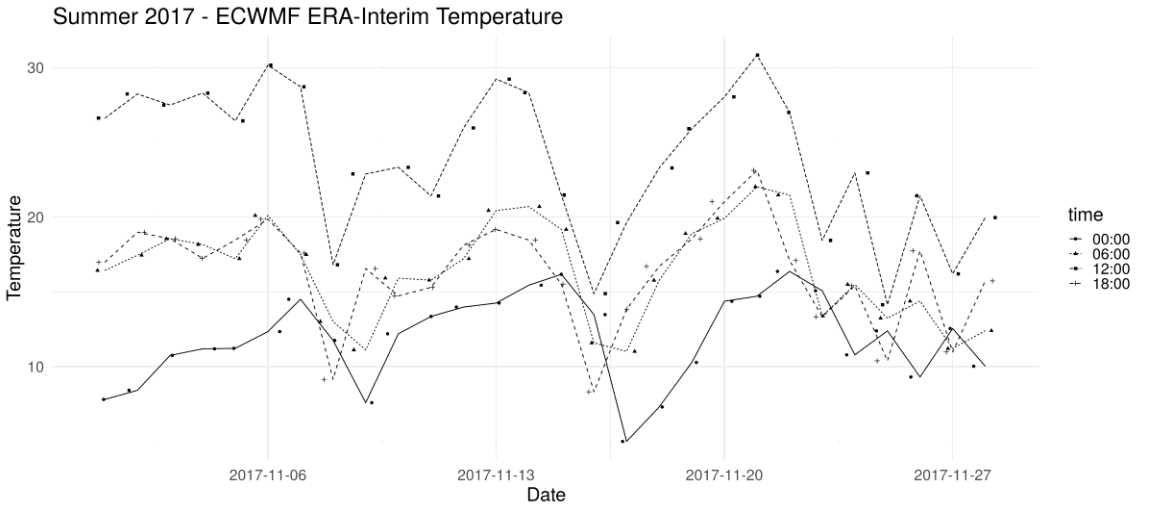

Figure 3-13. The modelled temperature variation across 6hr/24hr period over KwaZamokuhle show major differences during the campaign possibly as a result of the frontal system moving through the area.

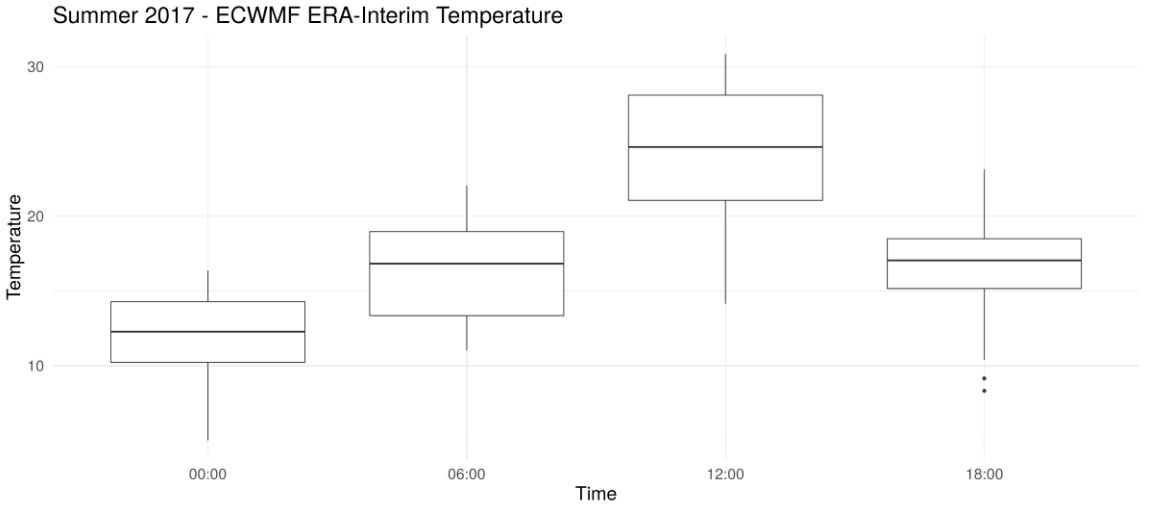

Figure 3-14. The box and whisker diagram shows that temperatures across all time steps are significantly warmer during the summer campaign. The effect of this variation can be seen in the next figure indicating the PBL height. Surface temperature and convection play a major role in the lifting and sinking of the PBL.

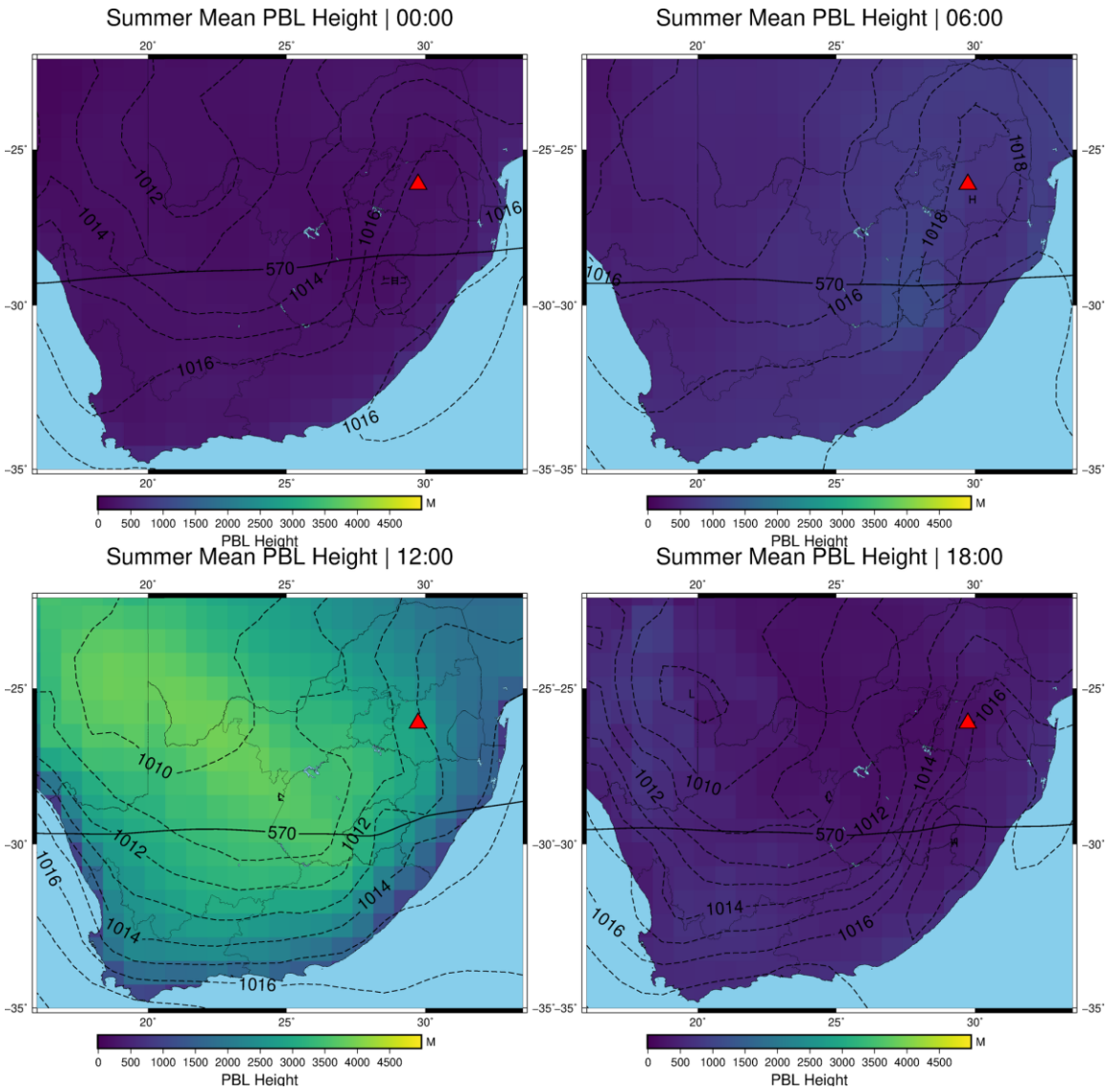

Figure 3-15. The PBL height varies significantly during summer months as a result of surface heating and atmospheric heating. In contrast with winter months, air is dispersed more effectively during this time. At its maximum (12:00 noon) the PBL rises to 5000m. Morning PBL height is also significantly different from winter conditions with at a mean height just above 1000m. This allows for air pollutants to already start dispersing early mornings.

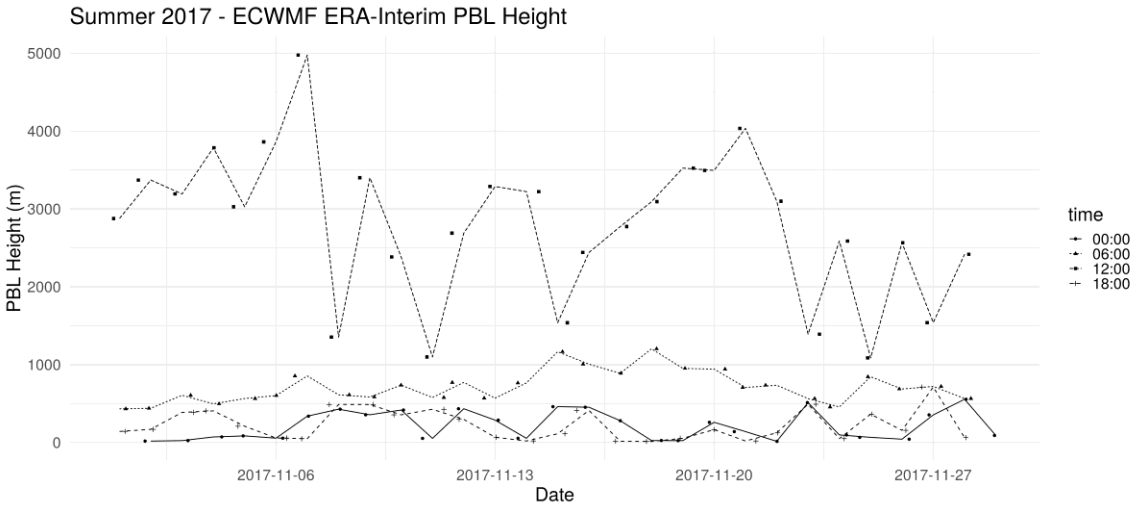

Figure 3-16. The time series indicates the variation in height of the PBL over KwaZamokuhle for the summer measurement campaign. Due to the displacement of the continental high-pressure system, surface heating and convective process the PBL height varies a lot more than the relatively stable winter conditions. This also has an impact on pollution as air is dispersed more effectively.

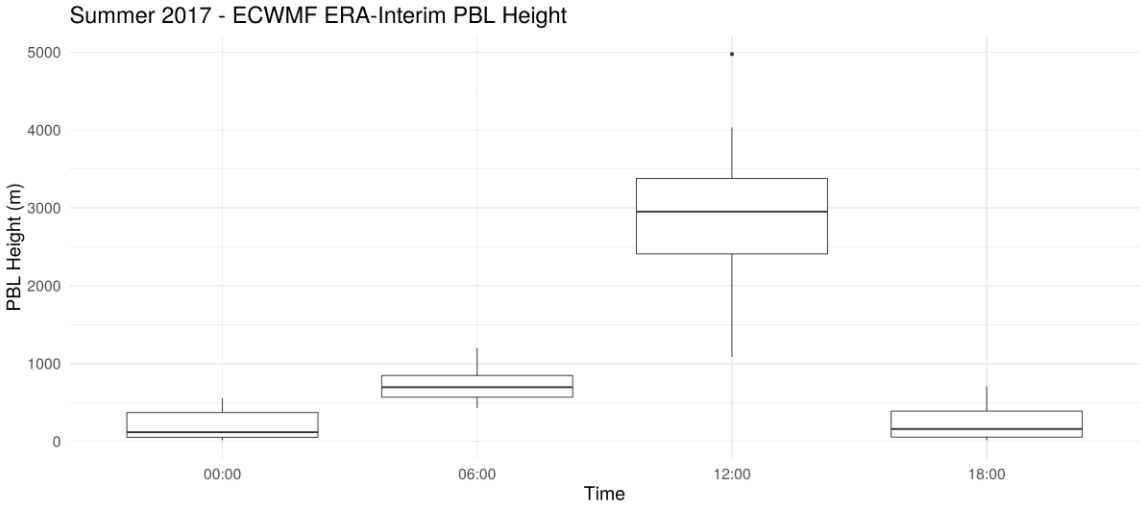

Figure 3-17. In the box and whisker plot the variation in PBL height at each modelled time step is clearly indicated. As expected 12:00 noon is when the PBL is at its highest and air pollutants are dispersed the most effectively, in contrast midnight the PBL is at its lowest and also the most stable effectively trapping air in this stable layer.

3.3.3. Meteorological characterisation at NSFB and SFB

Ambient air quality is dependent on the meteorological conditions that are prevalent when pollutants are been received by the receptors from the emission sources. Especially in solid fuel burning environments, meteorology is very crucial affecting both the rate and direction of dispersion of the pollutants. This section takes a cursory look at the meteorological conditions experienced at NSFB and SFB during both winter and summer.

3.3.4. Non-solid fuel burning house (NSFB)

House NSFB local meteorological conditions during the winter is similar to that seen in the modelled data, the mean temperature of 11.71 degrees Celsius indicate that cold conditions prevail during this time of the year and only get warmer during noon, during winter the relative humidity (RH) is also lower in the mean as due to dry conditions prevailing (see Table 3-3). The wind direction is prominently North-East, however, it has to be noted that there was an error in the instrumentation as seen in Figure 3-18 a. The local conditions during summer time show markable different meteorological conditions most notably in the temperature where a maximum of 31 degrees Celsius was observed (see Table 3-3). The diurnal variation in RH and temperature is clearly observed in Figure 3-19, wind speed and direction throughout both seasonal are similar with a predominantly North, North-Eastern origin.

Table 3-3. Descriptive statistics for the meteorological conditions (wind speed, wind direction, temperature, and relative humidity) recorded at NSFB during winter and summer, 2017.

Variable	Min	1st Q	Median	Mean	3rd Q	Max
Winter (26 July to 17 August)						
WS (m/s)	0	1	2	2	3	10
WD (deg)	4	13	18	23	26	101
Temp (degC)	-1	6	11	12	19	24
RH (%)	14	27	50	53	73	100
Summer (1 November to 28 November)						
WS (m/s)	0	2	3	3	4	9
WD (deg)	3	17	24	29	36	94
Temp (degC)	5	14	17	18	24	30
RH (%)	8.32	37	60	58	81	100

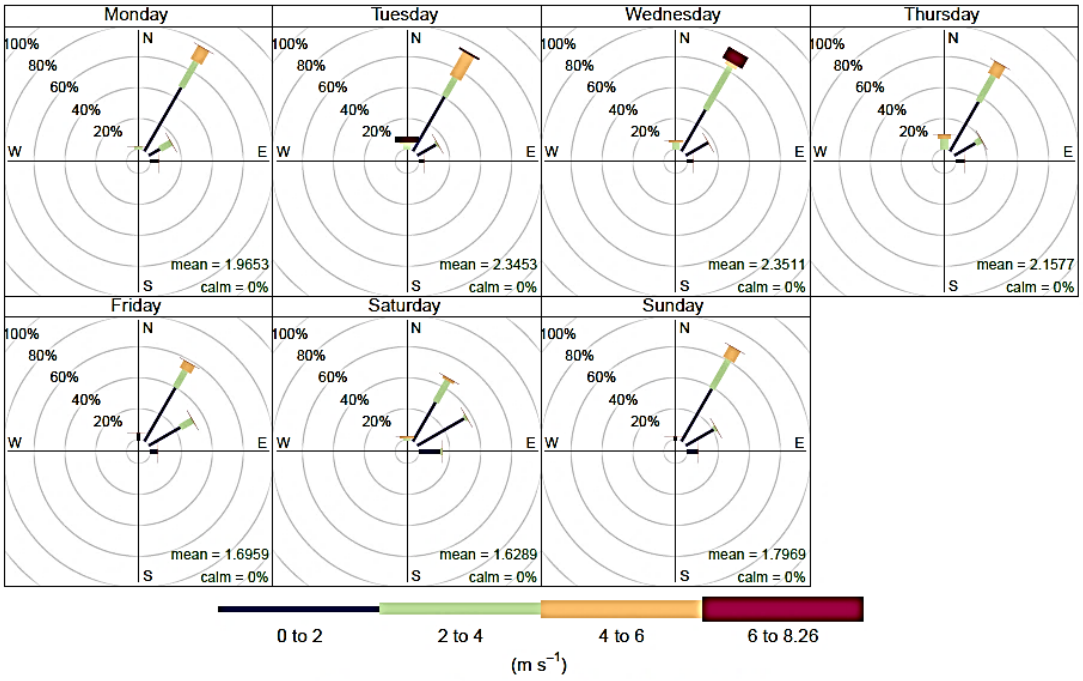

a.)

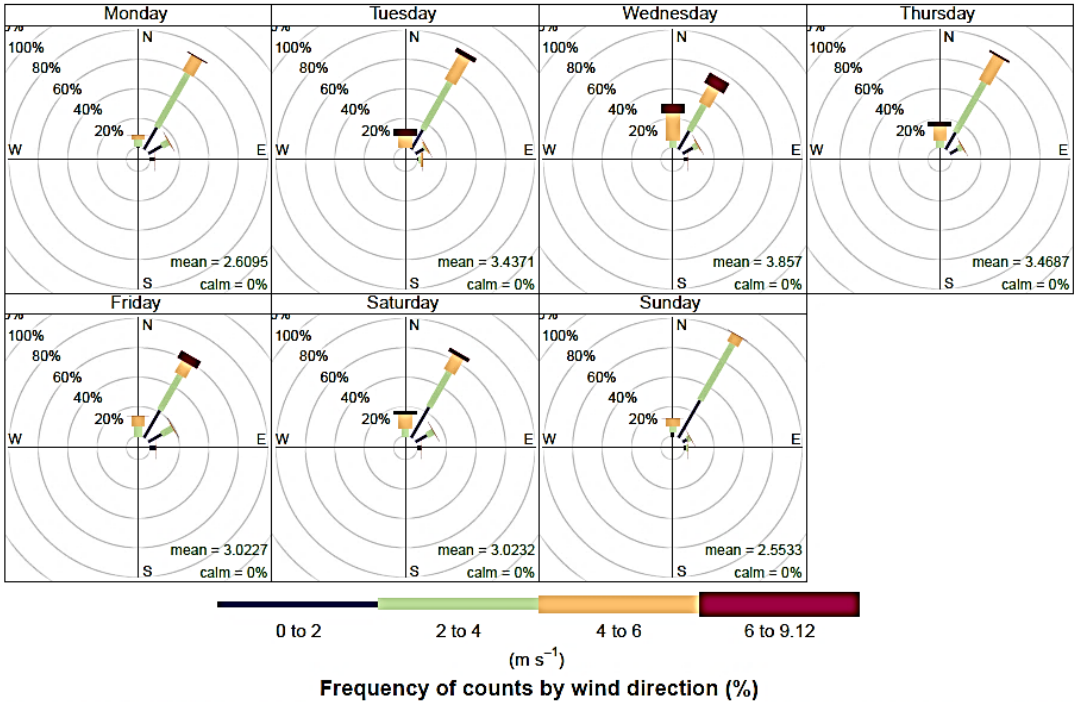

b.)

Figure 3-18. Wind roses showing the wind speed and wind direction for the “weekday” including the mean and frequency (%) distribution at NSFB during a) winter and b) summer (2017).

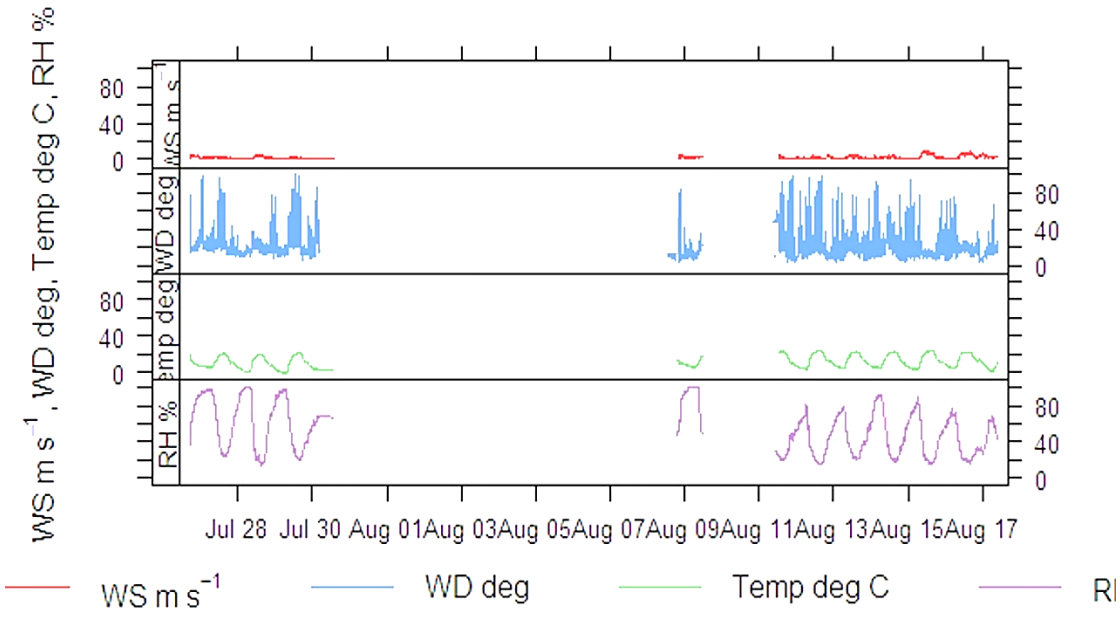

a.)

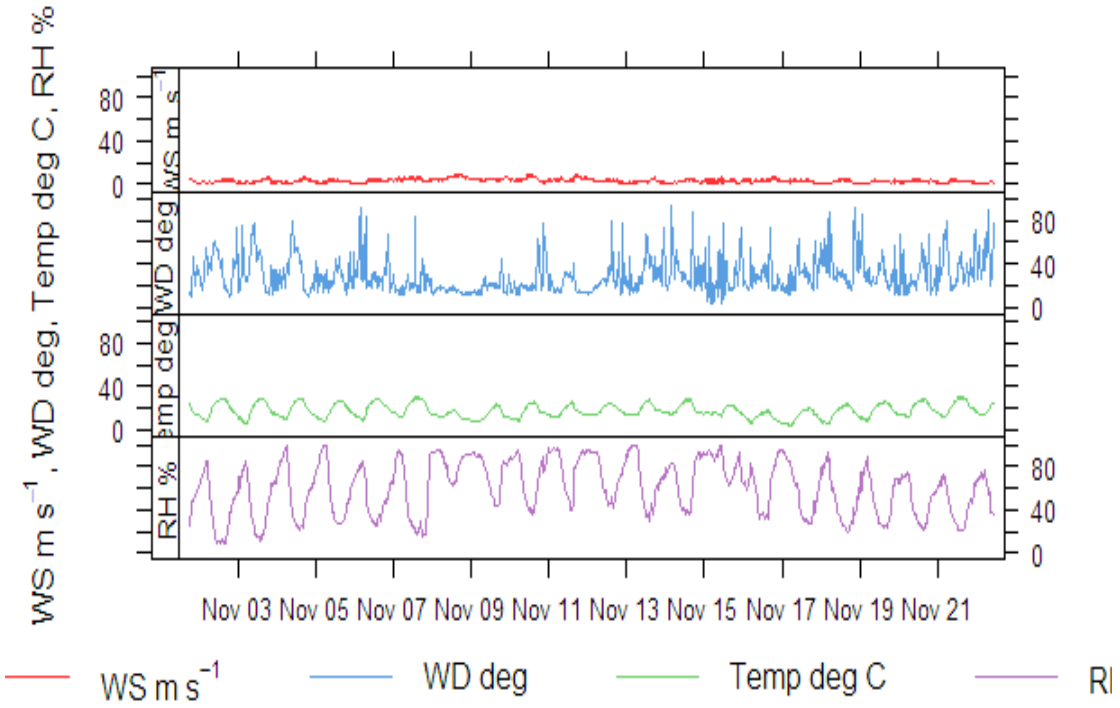

b.)

Figure 3-19. Temporal variability of wind speed, wind direction, temperature and relative humidity at NSFB during a) winter and b) summer (2017).

3.3.5. Solid fuel burning house (SFB)

House SFB shares similar meteorological characteristics as the previously discussed location, however, it is interesting to note that RH levels are very similar between winter and summer here (see Table 3-4), this could be due to the instrument error at NSFB as noted earlier. It is generally expected that winter RH levels will be lower due to prevailing dry conditions over the interior of South-Africa. The wind speed and direction (Figure 3-20) are similar to NSFB and also indicate winds with a predominantly North, North-Eastern origin. A comparison between conditions at this location and NSFB winter campaign is not possible due to instrument error in the non-solid fuel burning house.

Summer conditions again show maximum recorded temperatures and as discussed earlier this impacts PBL height and stable layer. Temperatures are on average 8 degree Celsius warmer between the seasons at SFB and show similar mean conditions to NSFB. The diurnal variation indicated in Figure 3-21 a and b is also similar to NSFB where temperature levels peak at noon and RH at night due to drop temperatures which causes air to become saturated and form dew.

Table 3-4. Descriptive statistics for the meteorological conditions (wind speed, wind direction, temperature, and relative humidity) recorded at NSFB during winter and summer, 2017.

Variable	Min	1st Q	Median	Mean	3rd Q	Max
Winter (26 July to 17 August)						
WS (m/s)	0.3	1.2	1.7	2.2	3.3	6.2
WD (deg)	11.2	19.5	23.9	31.5	37.4	97.1
Temp (°C)	-2.5	5.5	9.2	10.3	16.6	21.4
RH (%)	16.6	35.3	60.3	60.8	89.3	99.9
Summer (1 November to 28 November)						
WS (m/s)	0.4	1.5	2.7	2.8	3.6	8.0
WD (deg)	10.4	19.1	25.9	30.3	36.2	94.2
Temp (°C)	4.8	13.6	16.9	18.1	23.4	30.5
RH (%)	8.3	38.2	62.5	60.3	82.7	100

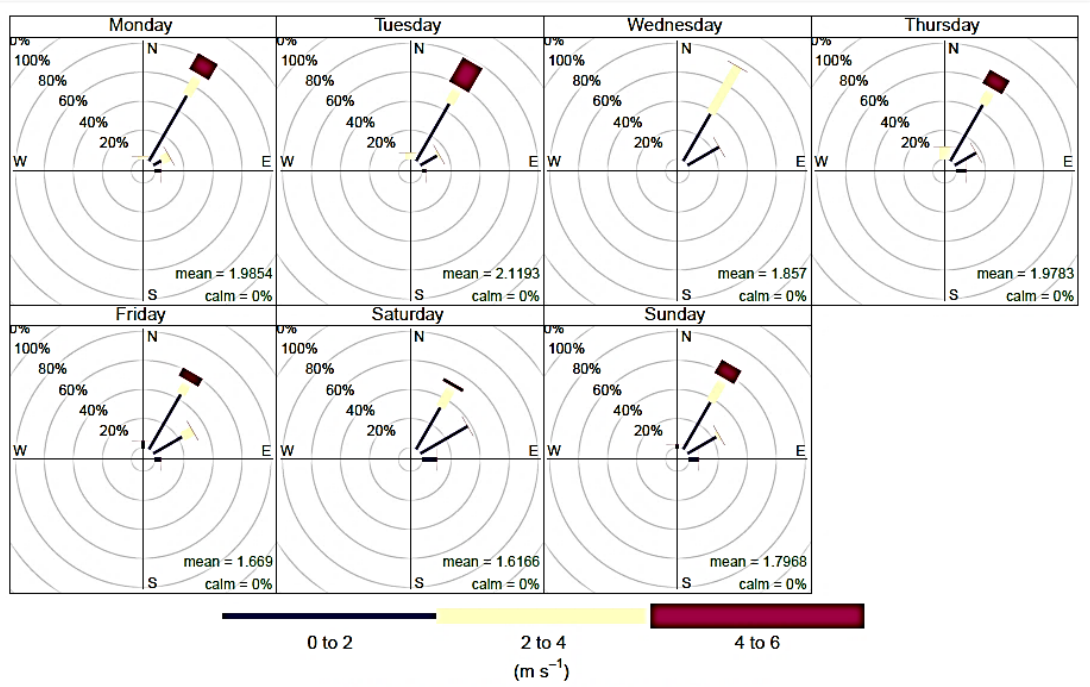

a.)

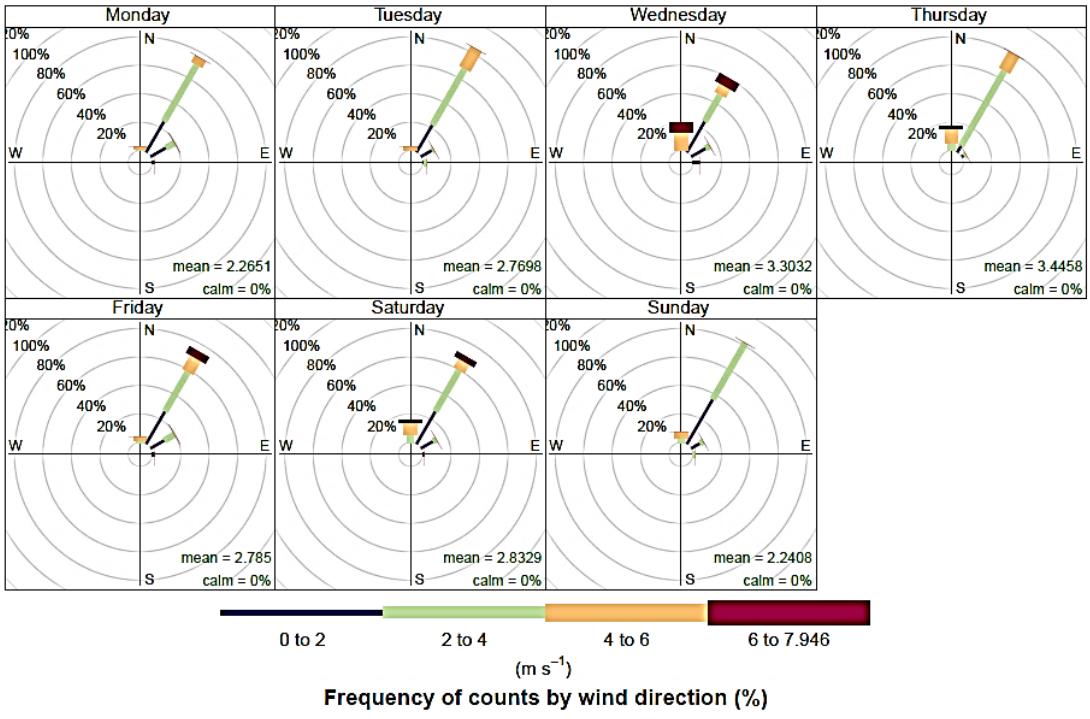

b.)

Figure 3-20. Wind roses showing the wind speed and wind direction for the “weekday” including the mean and frequency (%) distribution at SFB during a) winter and b) summer (2017).

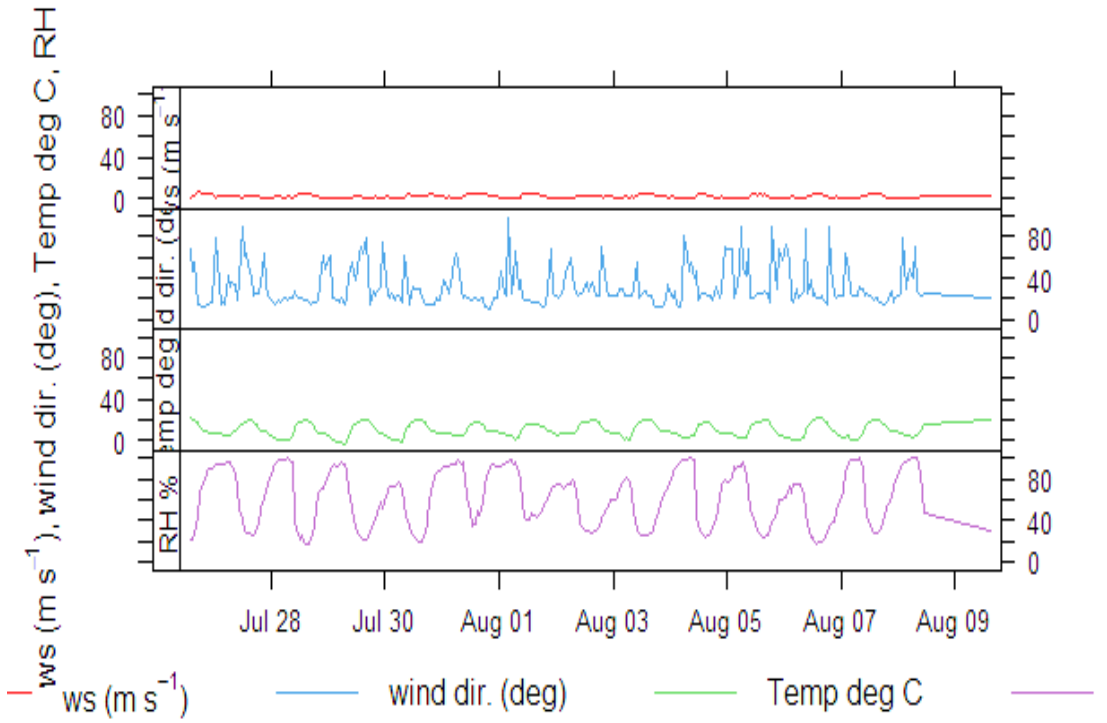

a.)

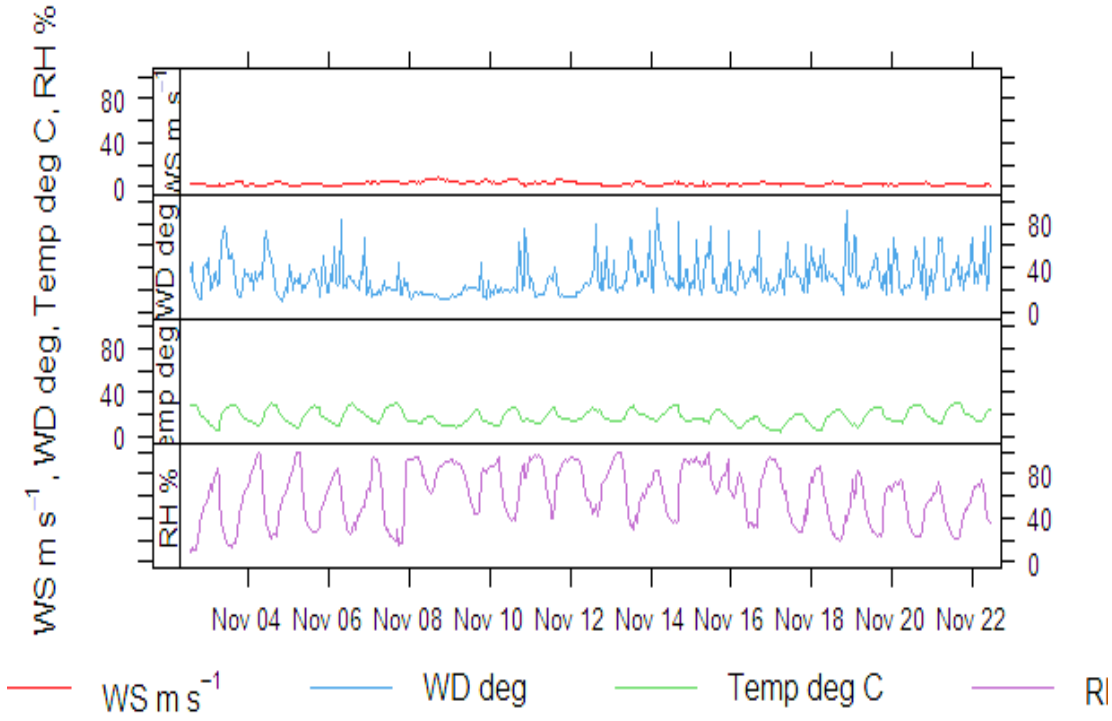

b.)

Figure 3-21. Temporal variability of wind speed, wind direction, temperature and relative humidity at SFB during a) winter and b) summer (2017).

3.4 Data collection

The monitoring campaigns were conducted simultaneously during 2017 in NSFB and SFB for both winter and summer sampling periods (see Table 3-1 and Table 3-5). Various instruments (see Table 3-6) used for collecting data from both the outdoor and indoor environments are discussed in further detail below.

Table 3-5. Information on KwaZamokuhle field campaigns conducted during winter and summer 2017.

Settlement	Coordinates	Year	Season	Sampling Type	Installation	Decommission
KwaZamokuhle	26,13°S 29,73°E	2017	Winter	Continuous	26 July	17 August
				Gravimetric		
			Summer	Continuous	1 November	28 November
				Gravimetric	1 November	20 November

Table 3-6: Instruments used for indoor and outdoor air quality monitoring in KwaZamokuhle in during sampling conducted in the winter and summer of 2017.

Parameter	Sample equipment	Indoor location	Outdoor
PM_4 (µg)	TSI SidePak AM510 monitor. (2)	Kitchen	-
Temp. (°C)	DS1932-F5# Thermochron iButton (10)	Stove Chimney Bedroom Kitchen Living Room	Yes, South facing wall.
PM_4 (µg), RH (%)	MetOne ES-642 (8)	-	Yes, various directions around the house
WD (deg), WS (m/s), Temp (°C), RH (%)	Campbell Weather Station	-	Yes (on the roof of the house)

3.3.6. Indoor environment data collection

Indoor PM_4 levels were measured using a SidePak AM510 instrument. These instruments are light-scattering nephelometers that utilise a long-wavelength laser (λ = 760 nm). A lens perpendicular to both the aerosol stream and laser beam collects the

scattered light within the scattering angle (90 ± 62°) and focuses it onto a photodetector. The signal from the photodetector is processed by the photometric direct current (DC) voltage offset analyser and is converted to mass concentration, based on a conversion constant set during calibration at the factory. The conversion constant represents the ratio of the monitor optical signal to a known mass concentration of Arizona Test Dust. Detailed information about the photometer optical response and its relationship with the aerosol characteristics such as density, refractive index, size and size distribution is provided by Jiang *et al.,* (2010). Air is sampled through a PM_4 inlet at 1.7 $L.min^{-1}$, providing output in $mg.m^{-3}$ (Watson *et al.*, 2011). The instruments were used in conjunction with a 10-mm Nylon Dorr-Oliver Cyclone (placed at an average breathing height of 1.6m) which is able to discriminate between the respirable fraction and larger aerosols. The instruments were set to a logging interval of 5 minutes. The exact locations where the instruments were placed in the NSFB and SFB households can be viewed in Figure 3-4 and Figure 3-5 respectively.

Figure 3-22: Indoor photometric measurements are collected with TSI AM510 Sidepak (far left in the image) personal monitor placed in the kitchen area of the house.(photograph was taken by M.Qhekwana, 2017).

3.3.7. Quality control

Several quality assurance procedures were followed as per manufacturer specifications before field deployment of sampling equipment including: i) factory calibrations; ii) flow

calibrations; iii) zero calibrations; iv) leak tests; and iv) internal filter changes. The photometric samplers used for this research had undergone annual factory calibration which involved the use of a reference photometer (Model 8587) that was gravimetrically calibrated to Arizona Test Dust (ISO 12103-1, A1 Test Dust). The samplers' flows were calibrated with the Jar Method. The latter method complies with the Occupation Safety and Health Administration requirements as set out in ISO 19001. Sampling inlets and cyclones were inspected for any cracks or faults and replaced if found to be damaged in any way. A leak tests using the "pump-fault leak test" were completed to check the O-ring, tubing and pump. This was done by connecting the cyclone to the selected instrument or pump at the relevant 1.7 $L.m^{-1}$ flow rate, and then closing the inlet with a finger. The system passed the leak test if the instrument gave a flow fault error. During the sampling campaigns, the cyclones were regularly cleaned by unscrewing the grit pot from the cyclone and tapping it upside down on a solid surface. The grit pot was then rinsed with isopropyl alcohol (Occupational Health and Safety Administration, 1999).

The zero calibration was done for all instruments prior to each sampling event by attaching the zero filter and following the procedure as described in the individual instrument operating manuals. Zeroing the instruments allowed for higher accuracy at low aerosol concentrations (TSI Incorporated, 2012b). The final activity was that of changing the internal filter of the DustTrak instruments (the SidePak doesn't have an internal filter). Due to the nature of the measurement, the results were found to be 2 to 3 times higher than measurements taken with standard gravimetric sampling (Kim, *et al.,* 2004; Watson *et al.,* 2011). Data in this study were corrected with a previously-calculated correction factor for Townships of 0.715 (Language *et al.,* 2016).

3.3.8. Gravimetric PM_4

Gravimetric samples were collected with two Gillian GilAir pumps which operated at 12hour (10h00–22h00) intervals between filter changes. The pumps collected air samples at a flow rate of 2.0 L/min (±5% uncertainty) and the flow was checked once a week using a Sensidyne Gilibrator II wet flow cell meter. A 10 mm Dorr-Oliver Nylon Cyclone was attached to each of the sample pumps. The gravimetric PM_4 samples were collected on 37 mm mixed cellulose esther (MCE) and quartz fibre filters which were enclosed in filter-holder cassettes sealed with shrink seals. The filters were prepared in a temperature-constant and RH-constant laboratory before use in the field.

3.3.9. Preparation of samples before sampling

The pre-sampling preparations are essential. The filters were equilibrated in the weighing lab for approximately two hours before weighing commenced. Calibration weights of 1 g and 20 g were used to calibrate the microbalance prior to each weighing session. These calibrations were recorded in a logbook so as to provide traceability. Before weighing each filter, the balance was zeroed to reduce the possibility of incorrect reading of mass. Each filter was weighed three times and the average was used for all relevant calculations. It was deemed unnecessary to use an external anti-static radiation source, as the XP26 DeltaRange Microbalance (Mettler-Toledo AG, Greifensee, CH) used during this study has an internal anti-static source. The 37 mm cassettes, consisting of three parts, were then loaded with the weighed filters and sealed with caps at the inlet and outlet ends. Shrink seals of 37 mm were used to prevent the infiltration of contaminated air into the cassette while being handling. The loaded cassettes were sealed in airtight containers to prevent contamination.

3.3.10. Field sampling

During the field sampling campaigns, the sampling pumps were calibrated using the Gillian Gilibrator II calibration systems, as described previously, by making use of the Jar Method. The pumps were calibrated to a flow of 2.2 $L.m^{-1}$ ± 5%, while connected to a 37 mm filter cassette, so as to obtain the 50% 4 µm cut associated with the cyclones. Additionally, to prevent leakages the sampling heads were assembled so the filter cassettes and cyclones were aligned and not obstructed. Cyclones inlets were fixed at a height of ~1.6 m, which is representative of an approximate breathing height. The samples for collocated setup were collected in intervals of ~12-hours. The sampling time (10h00–22h00) was specifically selected so as to prevent the sample from collecting PM over more than one peak burning period experienced within the settlements, thus preventing the filters from overloading. Attention was also focused on ensuring the cyclone was upright so that larger non-respirable PM in the grit pot would not be deposited onto the filters. After each sampling event, the 37 mm cassettes were removed from the sampling head and the caps were placed back on the inlet and outlet ports of the cassettes. The cassettes that were exposed were then stored in an airtight container to prevent any additional PM accumulating on the filter.

3.3.11. Post-sampling

The filters were offloaded in the weighing lab and left to equilibrate overnight, after which they were weighed using the procedure used during pre-sampling. If the filter was damaged in any way, it was noted and excluded from the analysis. The weighed filters were individually stored in Petri-slides until further analysis could take place. The filters were then analysed with wavelength-dispersive x-ray fluorescence (WD-XRF) spectrometry as described below.

The WD-XRF analysis techniques provide the ability to analyse filters without being subjected to any pre-treatment process. The analysis technique is predisposed to aspects such as enhancement- and matrix effects; however, these effects are minimal for thin film samples such as aerosol filters (Vanhoof *et al.*, 2000, 2003:129–138). A PANalytical Axios^{maX} WD-XRF was used for the analysis. The spectrometer implements a sequential analysis method; it thus only analyses a single element at a time. The spectrometer has a rhodium x-ray tube with a 4 kW generator. The instrument had been retrofitted with a system that has helium gas as a medium in the analysis chamber. This system provides the ability to analyse extremely vulnerable samples, such as the filters implemented in air quality source apportionment studies. There were two available detectors, namely the flow- and scintillation-detectors. The sample changer was fitted with seven trays, each capable of holding eight ×37 mm stainless steel sample cups, thus a total of 56 positions were available for use during analysis. A 20 mm collimator mask was selected, thus an area with a 20 mm diameter was analysed. The elements included in the WD-XRF analysis were Li, Na, Mg, Al, Si, P, S, Cl, K, Ca, Ti, V, Cr, Mn, Fe, Co, Ni, Cu, Zn, Ga, Ge, As, Se, Br, Rb, Sr, Y, Zr, Nb, Mo, Pd, Ag, Cd, In, Sn, Sb, I, Cs, Ba, Ce, W, Pt, Au, Hg, Tl, Pb, and Bi (see Table 3-7). These elements range from metals to metalloids and included non-metallic elements; however, most lanthanoids, actinoids and noble gases were excluded from the analysis. MICROMATTER^{TM} calibration standards were used for calibration purposes. These standards are National Institute of Standards and Technology (NIST) traceable reference materials and have a Nucleopore ® polycarbonate aerosols membrane backing mounted in a 25 mm ring mount. Each element had two calibration points that were obtained from a very light standard ranging from 3–8 µg.cm^{-2} and a heavier standard ranging between 40–60 µg.cm^{-2}

Table 3-7. Elements included in the WD-XRF analysis and the associated MICROMATTER™ - XRF Standards applied during the calibration of the PANalytical Axios^{maX} spectrometry instrument as used for the filter application.

Element	Metals					Metalloids	Non-metals	Description	(µg.cm^{-2}) ± 5%	
	A	AE	PT	T	L				H	VL
Li	√							Lithium as LiF	53.6	4.1
Na	√							Sodium or Chlorine as NaCl	519	7.5
Mg		√						Magnesium as MgF2	51.8	6.6
Al			√					Aluminum as Al metal	53.1	7.1
Si						√		Silicon as SiO	58.5	5.3
P							√	*Gallium or Phosphorus as GaP ; Ga=31.5 and 3.1 P=11.8 and 3.8	43.3	6.9
S							√	Sulphur as CuSx Cu=31.9 S=10.5 and as InSx In=5.6 S=1.4	42.4	7.0
Cl							√	Chlorine as KCl	47.9	7.3
K	√							Potassium or Chlorine as KCl	46.4	7.2
Ca		√						Calcium as CaF2	45.4	6.8
Ti				√				Titanium as Ti metal	51.8	6.6
V				√				**Vanadium as V metal	38.3	7.8
Cr				√				Chromium as Cr metal	39.0	6.0
Mn				√				**Manganese as Mn metal	54.8	6.3
Fe				√				**Iron as Fe metal	46.1	6.7
Co				√				Cobalt as Co metal	46.5	4.8
Ni				√				Nickel as Ni metal	50.3	7.1
Cu				√				Copper as Cu metal	48.9	6.0
Zn				√				*Zinc as ZnTe	53.2	7.1
Ga			√					*Gallium or Phosphorous as GaP; Ga=41.0 and 4.2 P=9.4 and 4.4	50.4	78.6
Ge						√		Germanium as Ge metal	49.4	6.3
As						√		*Arsenic or Gallium as GaAs; Ga=19.2 and 3.0 As=30.8 and 4.0	50.0	7.0
Se							√	Selenium as Se metal	46.8	4.5

Element	Metals				Metalloids	Non-metal	Description	(µg.cm^{-2}) ± 5%	
Br						√	Bromine or Cesium as CsBr	46.6	6.5
Rb	√						Rubidium or Iodine as RbI	42.8	7.0
Sr		√					Strontium as SrF_2	50.9	5.9
Y			√				Yttrium as YF_3	51.8	5.27
Zr			√				Zirconium as ZrF_4	59.2	4.17
Nb			√				Niobium as Nb_2O_3	50.1	6.6
Mo			√				Molybdenum as MoO_3	59.8	6.8
Pd			√				Palladium as Pd metal	52.1	6.1
Ag			√				**Silver as Ag metal	52.3	7.0
Cd			√				*Cadmium as CdSe	53.0	5.72
In		√					Indium as In metal	52.6	6.0
Sn		√					Tin as Sn metal	55.5	5.3
Sb					√		Antimony as Sb metal	53.5	6.7
I						√	Iodine or Rubium as RbI	54.0	
Cs	√						Bromine or Cesium as CsBr	46.6	6.5
Ba		√					Barium as BaF2	48.9	6.5
Ce				√			Cerium as CeF3	51.0	7.23
W			√				Tungsten as WO_3	47.9	6.4
Pt			√				Platinum as Pt Metal	51.3	6.0
Au			√				Gold as Au metal	48.6	4.7
Hg			√				Mercury as AgHg; Ag=28.5 Hg=27.5 and *HgTe; Hg=3.7 Te=2.5	56.0	6.2
Tl		√					Thallium as TlCl	45.1	5.9
Pb		√					**Lead as Pb metal	52.3	7.1
Bi		√					Bismuth as Bi metal	51.6	7.7

A- Alkali; AE – Alkali Earth; PT –Post Transition; T – Transition; L - Lanthanoids* may not be stoichiometric; ** will oxidize; H – Heavy Standard; VL – Very Light Standard

The filter samples were placed in the 37 mm sample cup holders. Filters were kept in place by making use a Teflon filter holder. The filter holder consists of three parts, namely: the i) filter holder bottom; ii) filter hold top; and iii) the filter support. The cups were placed on the trays and loaded into the spectrometer. Using the SuperQ software,

the measurement queue was created for the 56 available positions. Each filter was analysed for an average of 1294 seconds, while an additional 10 seconds were needed as a medium flush time and an added two seconds were used as delay time between measurement samples. Each sample was thus analysed for ~22 minutes.

3.3.12. Indoor temperature and relative humidity

Thermochron® iButton RS1923I-F5 temperature and relative humidity sensors were distributed throughout the indoor environment (living room, kitchen and bedroom) of the NSFB and SFB households at a height of 1.6m to record the temperature and relative humidity profiles for each house. In addition to the kitchen sensor, a sensor was placed at a distance of 10 cm from the chimney of the SFB stove (see Figure 3-23 b). This distance prevents the plastic casing of the sensor from melting. The south-facing external wall of both houses had an allocated iButton to record the outdoor ambient temperatures (Figure 3-23 a). The purpose of these sensors was to record the spatial variability in temperature and relative humidity in the house. The relative locations at which the iButtons were placed in the NSFB and SFB households respectively can be viewed in Figure 3-4 and Figure 3-5 respectively. The temperature sensors have a range of −20 °C –85 °C at a 0.5 °C resolution with a temperature accuracy of ±0.5 °C and timing accuracy of ±2 minutes per month (Table 3-8). ColdChain TD Multiprofiler CTMD software was selected as an interface for programming and downloading the data from the sensors. The sensors logged temperatures in 10-minute intervals.

Table 3-8. Specifications for the Thermochron RS1923L-F5 iButtons.

	RS1923L-F5	
	Temp. (°C)	RH (%)
Operating Range	-20 to +85	0 to 100
Range Accuracy	±0.5: -10 to +65	±5
Resolution	0.0625 or 0.5	0.04 or 0.6
Battery Life	~7 years	
Calibration	NIST-Traceable	
Software	ColdChain TD Multiprofiler CTMD	

a)  b) 

Figure 3-23. Examples of iButtons placed in the SFB house on the a) south facing the exterior wall and b) at a 10 cm distance from the chimney of the stove (photograph taken by M. Qhekwana, 2017).

3.3.13. Outdoor environment data collection

The ES-642 measures particulate concentration using a highly sensitive forward-scatter laser nephelometer, having a measurement range of 0–100 mg/m^3 or 0–100,000 µg/ m^{-3}. Optional sharp-cut cyclones were used to set the measure level of the ES-642. As supplied, it provides particulate monitoring for TSP; with the addition of the sharp-cut cyclone it can be set for particulate smaller than $PM_{10,}$ $PM_{2.5}$ or PM_1. The accuracy of the instrument is ± 5% based on a traceable PSL 0.6-micron reference standard. The ES-642 has a heated inlet to handle high humidity that may be encountered outdoors. PM_4 concentrations are recorded at one-minute time intervals.

Four ES-642 were placed outside the houses (Figure 3-24) being investigated to establish: a) the detailed ambient concentrations of $PM_{4;}$ and b) to determine if the highest concentrations in the ambient environment had a directional bias due to sources located upwind of the houses in each of the four main cardinal sectors. There was the potential that ambient environmental sources could be highly localised or could be associated with more regional scale sources.

Figure 3-24: Outdoor PM_4 measurements around the house using the ES642 sampler. Samples were collected during winter (26 July–17 Aug 2017) and summer (02–28 November 2017).

3.3.14. Meteorological condition

An automatic weather station was placed on the roof of each of the two houses where meteorological measurements were made (Figure 3-25). The parameters that were recorded included wind speed, wind direction, ambient temperature, ambient relative humidity and average rainfall. Weather stations are used on land and sea for a variety of operational and research purposes. Rugged design, low power requirements and long-distance communications methods allow modern (automated) weather stations to operate remotely for long periods without the need for human intervention. They offer the convenience of unattended, long-term monitoring at multiple remote locations, thereby reducing the time and cost associated with frequent measurements. In addition, the possibility of human error in data collection is minimized (Tanner, 1990).

Figure 3-25: The Campbell Scientific Automated Weather Station installed at the top of the roof of one of the houses used for the campaign. It was run on battery which is charged by a solar panel.

3.3.15. Indoor and Outdoor (I/O) continuous monitoring of PM_4.

Continuous I/O PM_4 monitoring was carried out over the two periods mentioned in Table 3-1. Indoor PM_4 measurements were collected in the kitchen area of each home and outdoor measurements were collected around the house in all four cardinal directions. The indoor PM sampler used for the study was a *TSI* Sidepak AM510 personal aerosol monitor and for the outdoor measurements, a Metone ES642 remote dust monitor was used. Both instruments were fitted with a 10 mm Dorr-Oliver Nylon Cyclone to take measurements at a height of 1.6 m above the ground – considered to be the average breathing height of most individuals.

3.3.16. Other parameters measured.

Further measurements taken included indoor and outdoor air temperature (AT) and Relative Humidity (RH). The ES642 has the capability to measure, PM concentrations, AT and RH at the same time. Indoor AT and RH readings were collected with the DS1923-F5# Hygrorchron temperature and humidity data loggers by *Maxim Integrated*

Products. Temperature readings of all rooms in both of the houses were collected. A thermocouple was placed near the electric stoves of both the houses, and a thermocouple was placed 10 cm away from the chimney of the coal stove in the SFB house. This was to allow for the identification of burning cycles in the coal stove.

3.5 Indoor and Outdoor PM_4 temporal variation

Indoor and outdoor PM_4 measurements were recorded on average every five minutes to ensure good resolution. The daily time-series of indoor and outdoor PM_4 concentrations were plotted to determine which days had the highest or lowest concentrations. Diurnal plots were also created to show when the highest concentrations of PM_4 are observed during the day. The measurements presented were from photometric instrumentation and were thus corrected using the gravimetric counterpart of the experiment. The calculated correction factor obtained from gravimetric concentrations was 0.756 µg m^{-3} and was applied to the photometric results.

Indoor PM_4 temperature and relative humidity

The indoor temperature and relative humidity were measured using periods averaging 10 minutes. The measurements were obtained in the living room, kitchen and bedroom and near the stoves of both house types. The diurnal (24-hourly) variation in temperature and relative humidity is plotted in Figure 4-7 and Figure 4-8 respectively, where the changes in temperature and relative humidity can be observed at an hourly rate for the 2017summer and winter sampling campaigns.

Indoor and outdoor infiltration coefficient

Infiltration into the house is due to the penetration of air from outside into the building structure (Chaloulakou *et al*., 2003; Milner *et al.,* 2005; Lv *et al*., 2005). The infiltration occurs due to the passage of air from the outside into the building through cracks in the walls, windows, roof or the outside doors (Milner *et al.,* 2005). Liddament, (1996) also termed the flow/loss of air from the indoor to the outdoor environment “exfiltration”. The reduction of air infiltration into a building structure holds many benefits including energy saving and largely reduces the impact of outdoor sources of air pollution inside the house (Liddament, 1996; Chaloulakou *et al.,* 2003). According to Liddament, (1996), an

airtight building provides more comfort to occupants and ventilation can be achieved through the intentional opening of windows and doors when desired. Stephen, (2000) noted that the largest database of air leakage rates was conducted in the UK by BRE and covers 471 houses and the study helps to better understand air exchange rates and the correlation between airtightness and ventilation (Dimitroulopoulou *et al.,* 2005).

The extent to which outdoor air pollution affects the indoor was represented by the infiltration coefficient (F_{in}). A linear regression model was used to get the relationship between indoor and outdoor PM and is also referred to as the RCS (Random component superposition model), expressed as follows:

$$C_{in} = F_{in}C_{out} + C_s \quad \text{Equation 3-1}$$

where $\boldsymbol{C_{in}}$ is the indoor particles concentration (μg.m^{-3}), $\boldsymbol{C_{out}}$ the outdoor particles concentration (μg.m^{-3}), $\boldsymbol{C_s}$ the indoor source strength (μg.m^{-3}) and $\boldsymbol{F_{in}}$the infiltration coefficient. This suggests that sources can be attributed to the indoor and outdoor environment as a function of infiltration.

Bivariate correlation analysis

The relationship between two known variables was determined through a bivariate correlation analysis. The validity of the correlation is determined the (r) value which is known as the Pearson correlation coefficient. The expression can be denoted as Equation 3-2:

$$r = \frac{\sum(X-\bar{X})(Y-\bar{Y})}{\sqrt{(X-\bar{X})^2(Y-\bar{Y})^2}} \quad \text{Equation 3-2}$$

where X and Y represent variables, and $\bar{X}$ and $\bar{Y}$ represent the mean of the variables., the Pearson coefficient (r) is utilized to show the correlation between indoor particles concentration, outdoor particles and other meteorological parameters.

Calculating the gravimetric particulate mass concentration

The gravimetric mass refers to the collected particulate mass after exposure of the collection substrate. The gravimetric PM_4 concentration was calculated from the

laboratory data and the sampler volume using Equation 3-3 gravimetric mass concentration in microgram per cubic meter (µg m^{-3})

$$PM = \frac{\left((M_f - M_i) - (B_f - B_i)\right)}{V_T} \times 10^6, \mu g.m^{-3} \quad \text{Equation 3-3}$$

where PM is the gravimetric PM_4 concentration in $\mu g.m^{-3}$ M_f is the post-exposure filter weight in g, M_i is the pre-exposure filter weight in g, B_f is the mean post-exposure blank filter weight in g, B_i is the mean pre-exposure blank filter weight in g, and V_T is the total volume of air sampled in m^3. The result is then converted from g to µg by multiplying with 10^6 (NIOSH, 1998; WHO, 1976).

Calculating element mass concentrations

The elemental mass concentrations were given in $\mu g.cm^{-2}$ after which it was converted to µg m^{-3} using Equation 3-4: Conversion of element mass concentration for µg cm^{-2} to µg m^{-3}

$$Element\ Mass\ (\mu g.cm^{-3}) = \frac{(EM_S - EM_B)A}{V_T} \quad \text{Equation 3-4.}$$

where EM_S is the element mass concentration of the sample in µg cm^{-2}, EM_B is the average element concentration of the blank filters in $\mu g.cm^{-2}$, A is the exposed area of the 37mm filter in cm^{-2}, and V_T is the total volume of air sampled in m^3. The exposed area of the filter was calculated to be 8.4 cm^{-2} by using Equation 3-5: Exposed area of 37mm filter in µg cm^{-2}.

$$Exposed\ Area\ (\mu g.cm^{-2}) = \pi r^2 \quad \text{Equation 3-5.}$$

, where r is the radius of the exposed part of the filter in centimetre.

Calculating element enrichment factors

Median enrichment factors (EF) for individual elements in the PM_4 fraction relative to Mason's average crustal rock composition (Mason, 1966) were calculated using Al as the reference element (Equation 3-6): Enrichment factor using crustal Fe as a reference element.

$$Enrichment\ Factor\ (EF) = \frac{[C(X)/C(Al)]_{PM4\ aerosol}}{[C(X)/C(Al)]_{crust}}$$ Equation 3-6.

where *C(X)* is the concentration of a selected element and *C(Al)* the concentration of iron in the aerosol sample or the reference crustal rock.

3.6 Source Identification

Principal Component Analysis (PCA)

The Principal Components Analysis (PCA) is a statistical factor analysis technique with an origin stemming from the law of conservation of mass. It functions by way of initially extracting a sequence of principal factors (components) from the measured data on pollutant concentrations, on the basis of the shared correlation between the different species. These were then interpreted as putative sources, and the contribution from each estimated from the factor scores. The PCA is a multivariate modelling method which does not require information on the composition of sources as an input. It can thus be used to identify sources, and estimate contributions, where detailed information on characteristics of sources is unavailable, but where a considerable amount of measured concentration data exists (Wolff *et al.,* 1985)

PCA, like other multivariate receptor models, is founded on the analysis of the correlation between measured concentrations of chemical species in a number of samples, assuming that the highly correlated compounds come from the same source. The method can therefore be utilised to detect the hidden source information from ambient measurement datasets. Ambiguities inevitably arise during interpretation of the factors, and the validity of the interpretation depends on good prior understanding of possible source characteristics, in the absence of such knowledge the results derived can be somewhat hypothetical and tentative (Jollife, 1996; Paatero *et al.,* 2005). Various assumptions are made by the PCA multivariate method. The composition of sources is assumed to be constant over the period of sampling at the receptors; chemical species used in PCA do not interact with each other and their concentrations are linearly additive; source profiles f_{pj} are linearly independent of each other. The marker elements (tracers) for each source should be included; measurement errors are random and uncorrelated; the numbers of species(j) is greater than or equal to the number of

sources (p); the number of samples is much greater than the number source types to ensure statistically meaningful calculations; variability of the concentrations from sample to sample is primarily due to differences in source contribution and not due to measurement uncertainty or changes in source composition; the effect of processes that affect all sources equally (e.g. atmospheric dispersion) is much smaller than the effect of processes that influence individual sources (e.g. wind direction and changes in emission rates.

As input, the PCA model requires concentration data from a large number of samples (n>100) analysed for chemical constituents. In order to interpret the resulting components, information is also needed on the characteristics of putative sources, derived either from the literature or available measurements of emission composition. The output from a PCA model is a series of factors (components), which can be interpreted as emission sources. Interpretation is based on the elements/species which characterise each component. The amount of variance explained by each factor is then used as the basis for estimating the contribution associated with each putative source. PCA also provides qualitative source profiles, which can be used as input to other receptor models such as CMB. Principal Component Analysis (PCA) is a form of factor analysis. Its aim is to identify structures in the pattern of relationships among the variables (i.e. measured concentrations of different pollutant species) in order to. Determine whether the observed variables can be explained largely or entirely in terms of a much smaller number of (inferred) variables, or factors (Jollife, 1996; Paatero *et al.,* 2005). These are then interpreted and allocated to identifiable sources by reference to prior information on, or knowledge about, possible origins of the emissions (e.g. based on literature or independent measurement data). Estimates of the contribution of each of these source categories to the measured pollutant mixture are then made on the basis of the percentage of variance explained by each factor at each measurement location (Jollife, 1996; Paatero *et al.,* 2005).

PCA models can be expressed as follows:

$$C_{ij} = \sum_{p=1}^{n} g_{ip} f_{pj} + e_{ij}$$ Equation 3-7.

p is the number of sources;

j is the number of species, with $j \geq p$;

C_{ij} is the measured ambient concentration of species j in sample i;

f_{pj} (source profiles) is the fractional concentration of species j in the emissions from source p;

g_{ip} is the concentration contribution of source p to sample i and

e_{ij} is the portion of the measured elemental concentration that cannot be explained by the model.

CHAPTER 4 RESULTS AND DISCUSSION

Chapter 4 presents the results showing the temporal variation and loading of particulate matter (PM) at the representative sites. The ratios between indoor and outdoor PM are presented and discussed herein. The data represented is from the indoor and outdoor environment during winter and summer sampling campaigns.

4.1 Characterization of indoor and outdoor PM_4

The 24-hr limit value set by the Department of Environmental Affairs (DEA) for ambient concentrations for $PM_{2.5}$ is 40 µg m^{-3} (RSA, 2009), whereas there is no indoor standard for $PM_{2.5}$ and PM_4. Moreover, indoor air standards are available for industrial workplaces but are not available for household air. Thus the ambient standard set by DEA is adopted for the indoor environment as well in this study.

Indoor PM_4

Indoor measurements were collected in two houses in KwaZamokuhle during sampling periods in the winter and summer of 2017. The winter sampling was conducted from 26 July—17 August 2017 and in summer from 1 November–28 November. Summary statistics of the indoor PM_4 concentrations for the two seasons are given in Table 4-1. The 5-minute averaged data collected during winter show a mean PM_4 mass concentration of 105 (± 62) and 172 (± 120) µg m^{-3} for NSFB and SFB, respectively. The mean PM_4 mass concentrations collected during summer showed means of 38 (± 12) and 43 (± 23) µg m^{-3} for NSFB and SFB were measured respectively, this indicates that the mean PM_4 mass concentrations in the non-solid fuel-burning household were lower than those measured in the solid fuel burning household by 40% and 20% for winter and summer respectively. The winter/summer ratios were a factor of three and four times higher for NSFB and SFB, respectively. This indicates that PM_4 mass concentrations were a factor of 2 and 3 times higher during winter, for both NSFB and SFB, compared to the summer measurements.

Table 4-1. Descriptive statistics for the 5-min averaged indoor PM_4 mass concentrations (μg m^{-3}) for each individual household during winter and summer, 2017.

House	Valid N	Mean	SD	Min	Median	Max	NSFB/SFB Ratio	Winter/Summer Ratio
Winter (26 July–17 August)								
NSFB		*105	62	40	84	255	1	3
SFB		*172	120	48	123	447		4
Summer (1 November–28 November)								
NSFB		38	12	25	32	66	1	
SFB		*43	23	17	33	98		

Mean concentrations represented in the table with (*) are higher than the 40 μg m^{-3} $PM_{2.5}$ 24-hr limit.

The time-series box-plots for daily indoor PM_4 mass concentrations for summer and winter are presented in Figure 4-1 and Figure 4-2. Outliers are represented in the time series plot with a red cross to indicate the extreme values that can sometimes be measured by light-scattering monitoring equipment. Daily PM_4 concentrations were a factor of 2 and 3 times higher during the winter in NSFB and SFB, respectively. For approximately 90% of the days sampled during winter, concentrations inside the SFB house were 3 orders of magnitude higher than the National Ambient Air Quality Standard (NAAQS) $PM_{2.5}$ 24-hr limit value. A maximum value of ± 910 μg m^{-3} was recorded on 15 August 2017 with the minimum of ± 30 μg m^{-3} measured on the same day, this showed a high variability of PM_4 in the household in a single day.

In the household that did not practice any solid-fuel burning, PM_4 concentrations were also observed to be higher than the NAAQS $PM_{2.5}$ limit for more than 50% of the days sampled in winter. The maximum value of ± 280 μg m^{-3} was measured on the 8 August 2017 and the minimum on the same day was ± 40 μg m^{-3} showing pronounced variability of PM_4 in house NSFB as well. The winter period is the time when residents are exposed to the greatest amount of PM and are at greatest risk of the health impacts associated with poor air quality. The daily PM_4 concentrations in both dwellings for summer was within the prescribed $PM_{2.5}$ guidelines for ± 75% of the days sampled. Only five days out of the 28 days sampled in November 2017 had concentrations that were considered to be detrimental to health when compared to the NAAQS $PM_{2.5}$ 24-hr-limit. The reason for

lower concentrations of PM_4 in the households during the summer can be attributed to less use of solid fuel and no need for space-heating during the warmer months.

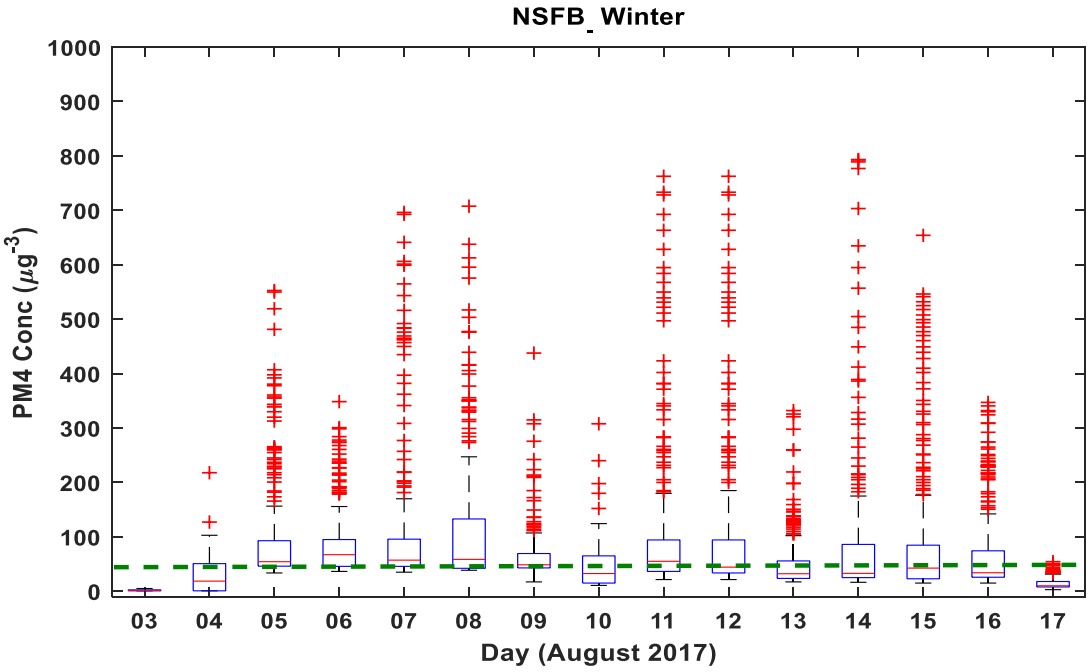

a.)

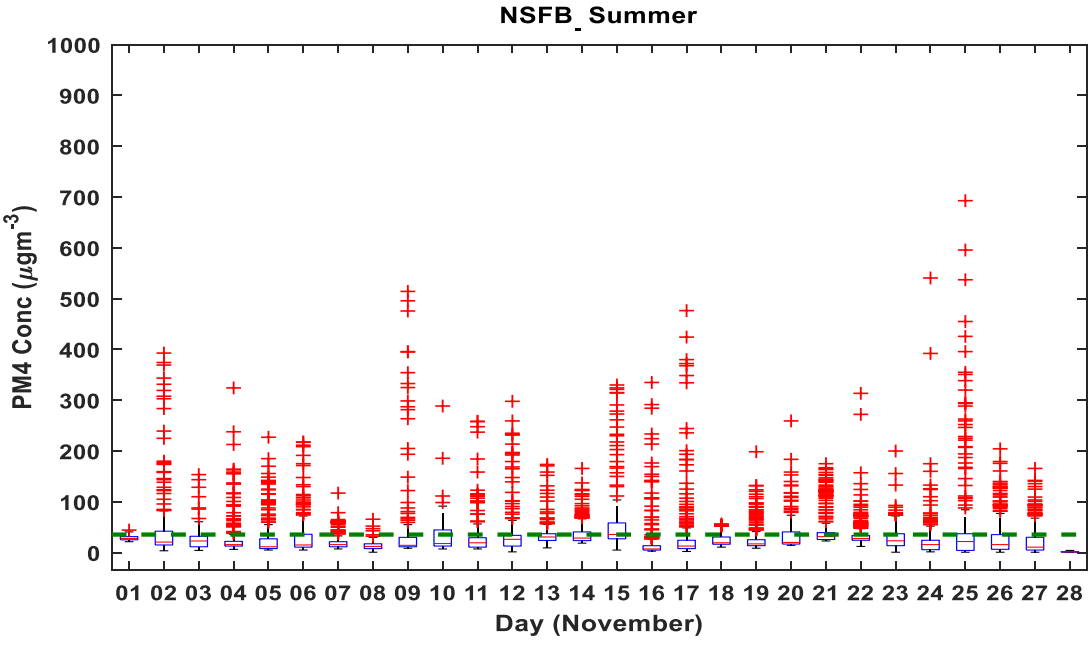

b)

Figure 4-1. Time series of the daily median indoor PM_4 mass concentrations in the non-solid fuel burning (NSFB) during a.) winter and b.) summer (2017). (Mean: red line; Box: 25%-75%; Whisker: min-max; Green Dotted line: NAAQS 24-hr $PM_{2.5}$ at 40 μg m^{-3}).

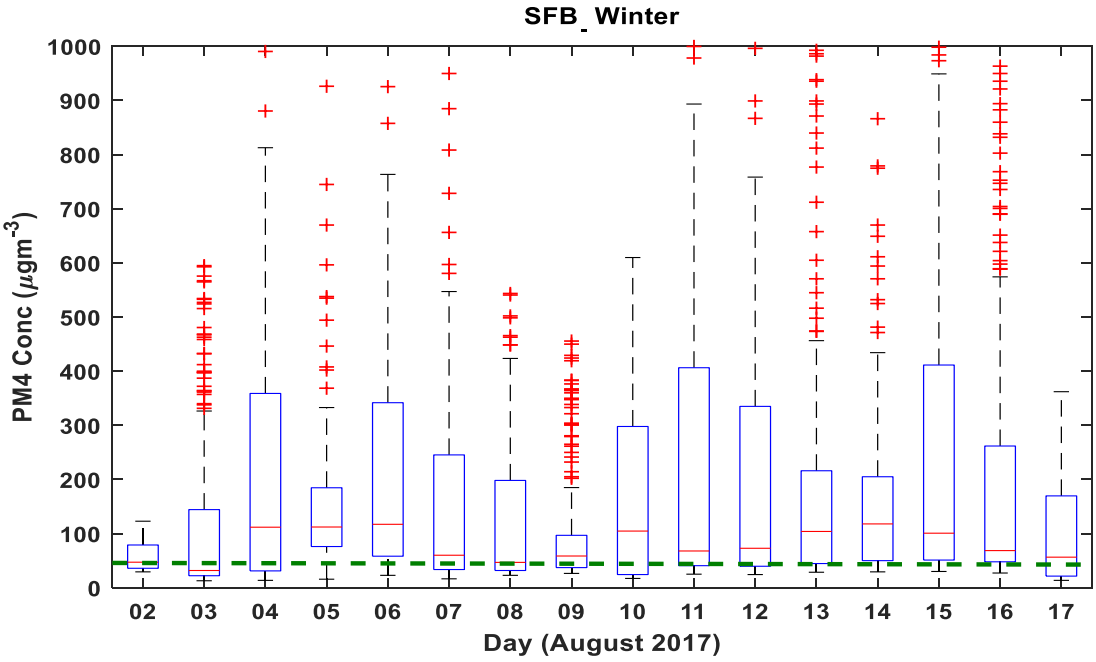

a.)

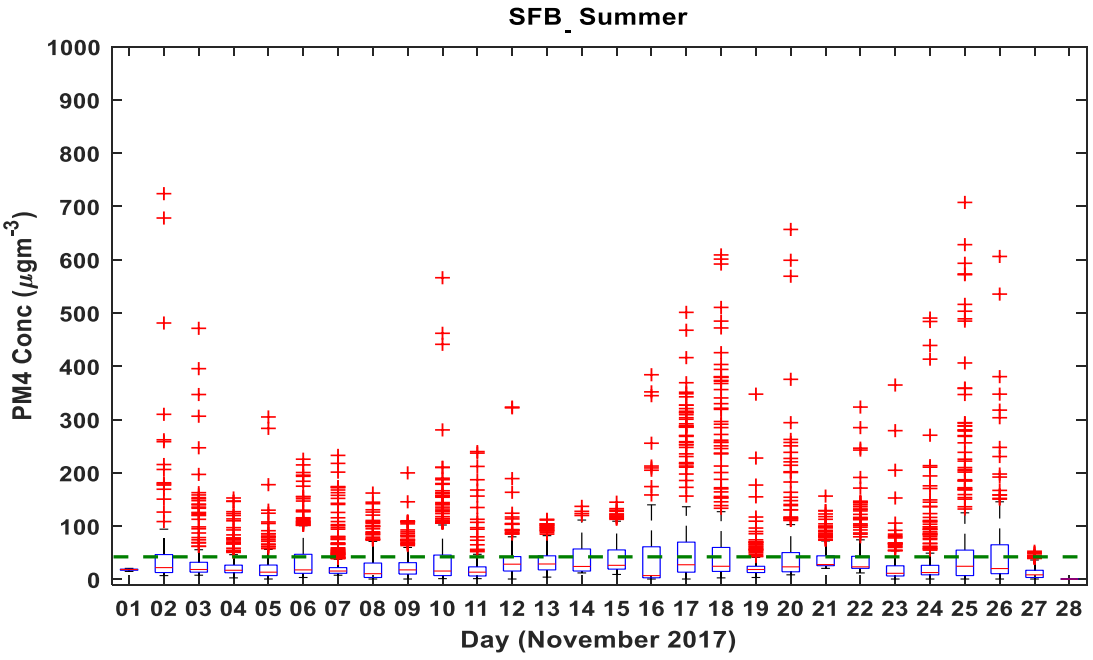

b.)

Figure 4-2. Time series of the daily median indoor PM_4 mass concentrations in the solid fuel burning (SFB) during a) winter and b) summer (2017). (Mean: red line; Box: 25%–75%; Whisker: min–max; Green Dotted line: NAAQS 24-hr $PM_{2.5}$ at 40 μg m^{-3}).

The medians of the daily averaged indoor PM_4 mass concentration are presented in Figure 4-3. It shows that the 24-hour averaged medians were generally above the NAAQS 24-hr $PM_{2.5}$ standard of 40 µg m^{-3}. This is true for both NSFB and SFB during winter; however, during summer the median for NSFB fell below and SFB was above the set standards. Thus, SFB PM_4 concentrations were found to exceed the standards irrespective of the season.

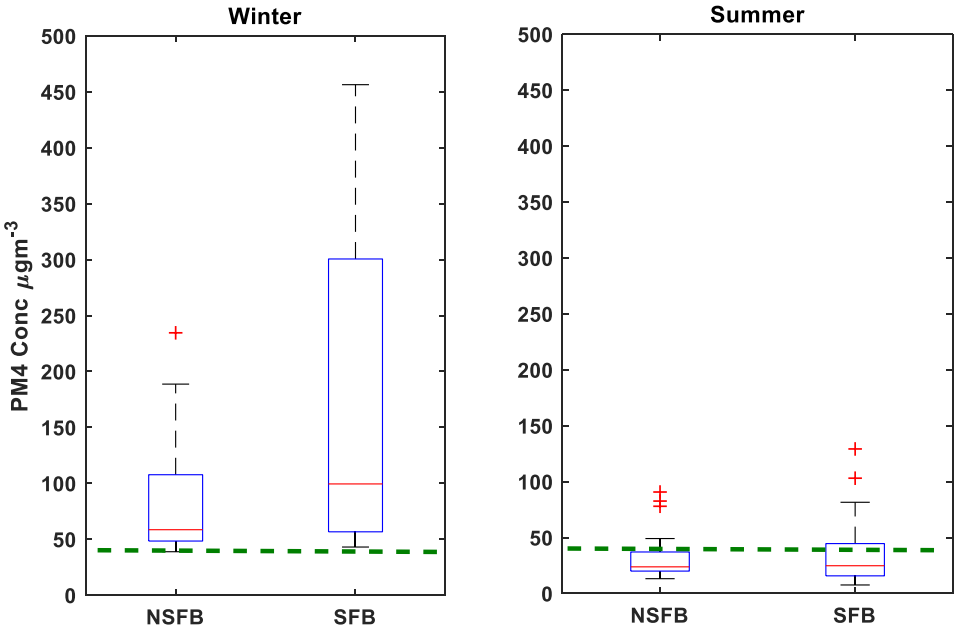

Figure 4-3. Box and whisker plot of the median indoor PM_4 daily concentrations, at the non-solid fuel burning (NSFB) and solid fuel burning (SFB) households during winter and summer (2017) (Mean: red line; Box: 25%-75%; Whisker: non-outlier range; Star: outliers; Green Dotted line: NAAQS 24-hr $PM_{2.5}$ at 40 µg m^{-3}).

The average diurnal pattern of the indoor PM_4 mass concentrations for NSFB and HSFB are shown in Figure 4-4 (a and b). The NAAQS 24-hr $PM_{2.5}$ value is also indicated on the graphs.

A clear bimodal pattern can be identified, with the two peaks, morning and evening, potentially associated with domestic activities, such as residents' waking-up activities such as breakfast preparation, boiling water, preparations for work or school and cleaning. The evening peak is often ascribed to meal preparation in summer and in

colder winter months' solid fuel burning for space-heating was also considered. It is also important to note that the peaks coincided with peak traffic periods that might also contributed to particulate loading through the mobilising and resuspending of dust present on road surfaces. The peak in each house was studied in further detail.

The bimodal peaks, were easily identified in the non-solid fuel burning house (NSFB) (Figure 4-4 a). The morning peak occurred between 03h00 and 08h00 (peaks around 05h00 at ±130 µg m^{-3}) and in the evening between 15h00 and 20h00 (peaks around 17h00 at ±220 µg m^{-3}) during the winter months. Thus, there was increased particulate loading for approximately 5-hours during the morning and evening. In summer these peaks were less pronounced, but were still identifiable. The morning peak for the summer months occurred between 05h00 and 08h00 (peaks around 07h00 at ±40 µg m^{-3}) and in the evening between 17h00 and 21h00 (peaks around 19h00 at ±100 µg m^{-3}). There was a 3 and 4-hour period, respectively, in the morning and evening where increased levels of PM_4 could be identified. There was a noticeable difference in the time period that residents were exposed to increased levels of respirable PM during winter and summer.

The bimodal peak, mentioned earlier, was easily identified in the solid fuel burning house (SFB) (Figure 4-4 b). The morning peak occurred between 05h00 and 12h00 (peaks around 09h00 at ±500 µg m^{-3}) and in the evening between 17h00 and 23h00 (peaks around 20h00 at >1000 µg m^{-3}) during winter. There was an increased particulate loading for approximately a 7-hour period during the morning and evening, respectively. The extended evening peak could be attributed to space-heating that occurred at night during winter. In summer these peaks were less pronounced but could still identifiable. The morning peak occurred between 05h00 and 09h00 (peaks around 07h00 at ±65 µg m^{-3}) and in the evening between 16h00 and 21h00 (peaks around 18h00 at ±100 µg m^{-3}). There was a four- and five-hour period, respectively, in the morning and evening where there were increased levels of PM_4.

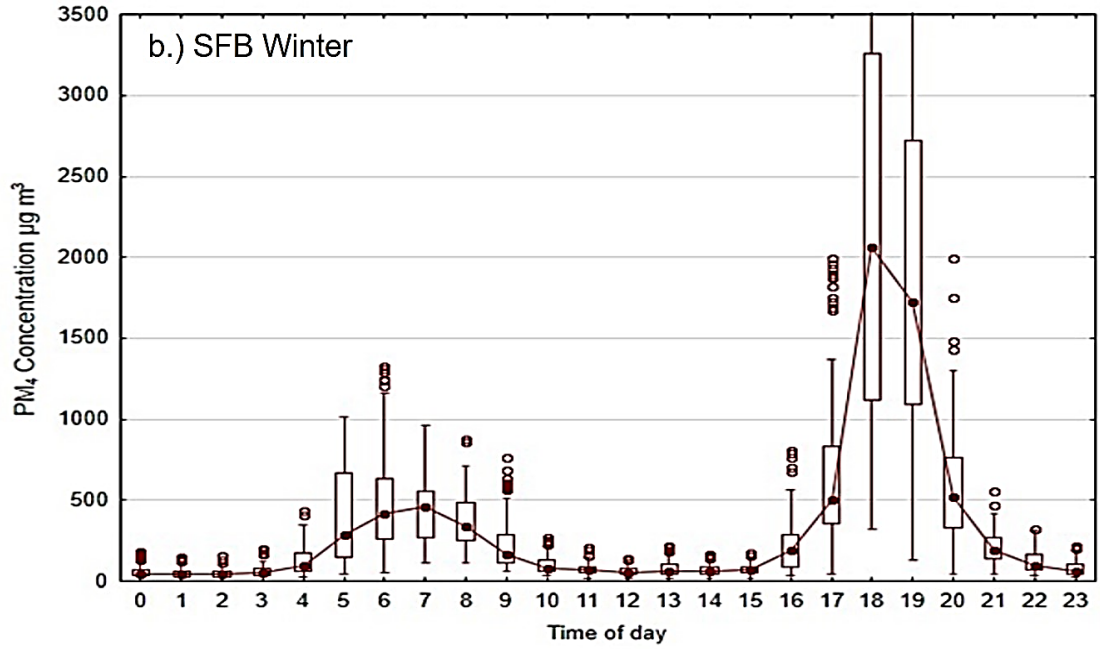
b.) SFB Winter
PM4 Concentration µg m3
Time of day

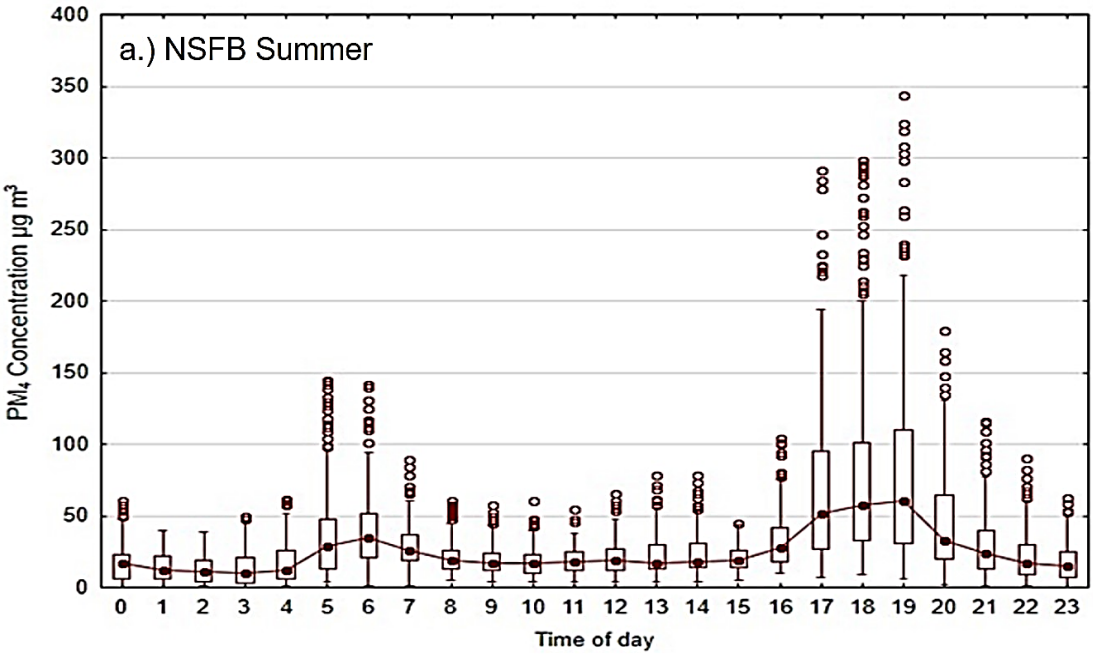
a.) NSFB Summer
PM4 Concentration µg m3
Time of day

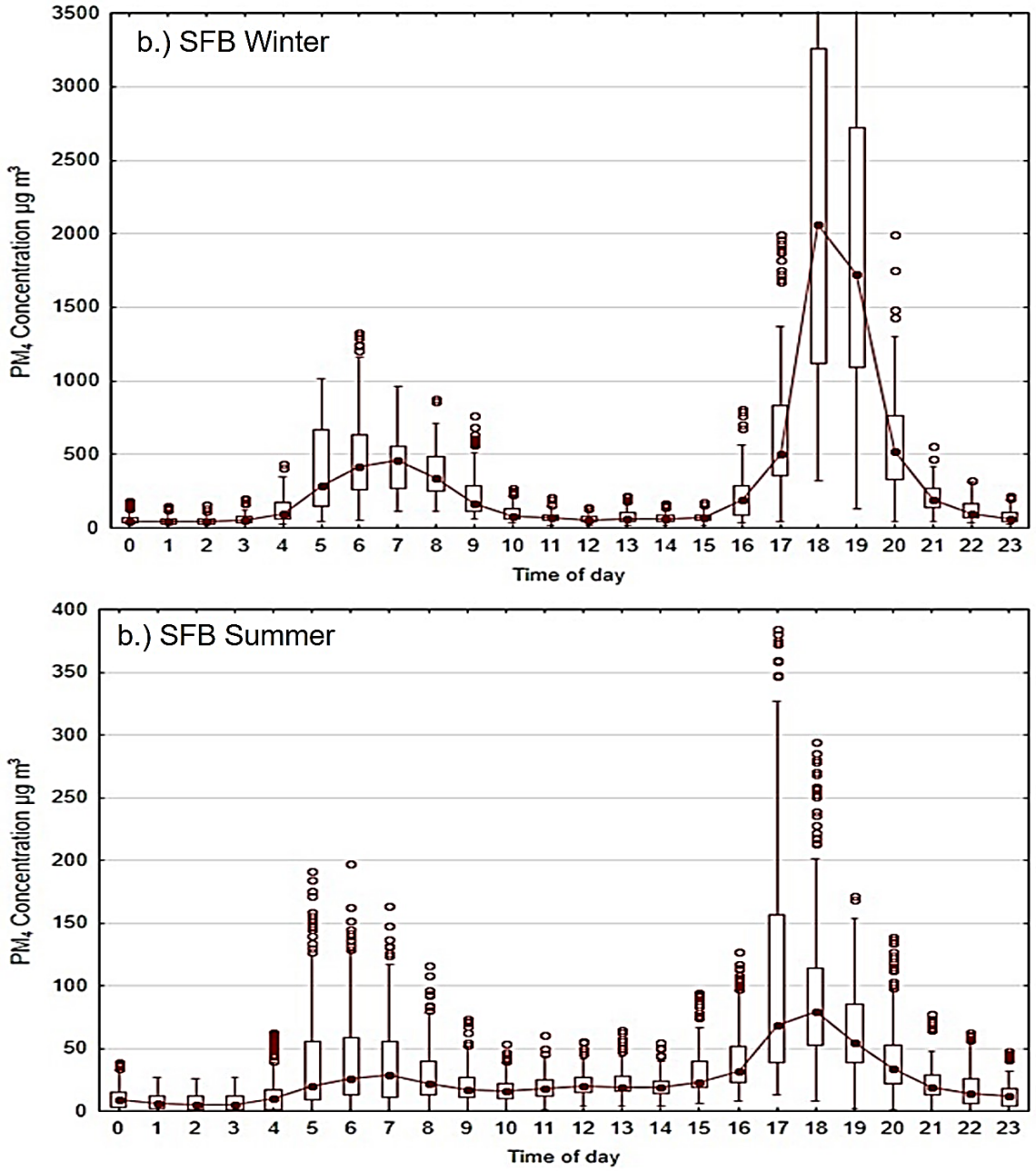

Figure 4-4. Diurnal pattern of the mean hourly averaged indoor PM_4 mass concentrations (µg m^{-3}) measured in a) non-solid fuel burning (NSFB) and b) solid fuel burning (SFB) during winter and summer (2017). Mean: solid dot; Box: 25%–75%; Whisker: min–max; *Note: difference in scale between graphs for winter and summer.

Gravimetric mass characterisation

Gravimetric filter samples were collected for the respirable size fraction (PM_4) during two sampling campaigns (winter and summer) at the two sampling sites (NSFB and SFB) within KwaZamokuhle. A total of 152 valid filter samples were collected over the two campaigns. Particulate loadings ranged up to 348 µg m^{-3}, with a mean PM_4 loading of 84 (±75) µg m^{-3}. The particulate loadings showed large variations between day and night in NSFB and SFB. The gravimetric PM_4 mass concentrations for each site are discussed in further detail below.

The descriptive statistics for day and night-time periods for each house, categorised by season, are given in Table 4-2 and are also presented in Figure 4-5. The winter PM_4 mass concentration in the non-solid fuel burning household (NSFB) was < 300 µg m^{-3} during both day and night-time, with means of 79 (±82) and 70 (±70) µg m^{-3}, respectively. The PM_4 mass concentration in the solid fuel burning household (SFB) reached maximum loadings > 300 µg m^{-3} during both day and night-time, with means of 149 (±99) and 103 (±99) µg m^{-3}, respectively. The mean PM_4 loading in SFB was ~80% and ~50% higher during day- and night-time respectively, when compared to NSFB. This also indicates that on average, during winter, the mean PM_4 loading was above the NAAQS 24 hour $PM_{2.5}$ standards for both NSFB and SFB.

During summer, PM_4 mass concentration in the NSFB household was < 150 µg m^{-3} both during day and night-time, with means of 71 (±24) and 51 (±18) µg m^{-3}, respectively. The PM_4 mass concentration in the SFB household reached maximum loading of > 300 and < 100 µg m^{-3} during the day and night-time, with means of 72 (±73) and 65 (±25) µg m^{-3}, respectively. The mean PM_4 loading in the SFB household during the day was similar to that of the NSFB household while the mean night-time PM_4 loadings in SFB were ~30% higher compared to NSFB. This also indicates that on average, during summer, the mean PM_4 loadings were above the NAAQS 24-hour $PM_{2.5}$ standards for both NSFB and SFB.

Table 4-2. Respirable PM descriptive statistics (μg m^{-3}) showing the mean, standards deviation, median, min, max and percentiles (25th, 75th, and 99th) at non-solid fuel burning (NSFB) and solid fuel burning (SFB) households for day-time and night-time periods during summer and winter 2018.

Season	House	Time of day	N	Minimum	25th %	Mean	SD	Median	75th %	99th%	Maximum
Winter	NSFB	Day	20	4	28	79	82	41	111	270	270
		Night	20	4	26	70	70	39	90	224	224
	SFB	Day	20	21	60	149	99	125	219	333	333
		Night	20	15	41	103	99	55	169	309	309
Summer	NSFB	Day	18	36	53	71	24	68	85	132	132
		Night	18	7	40	51	18	52	65	79	79
	SFB	Day	18	0	41	72	73	60	68	348	348
		Night	18	5	49	65	25	68	87	99	99

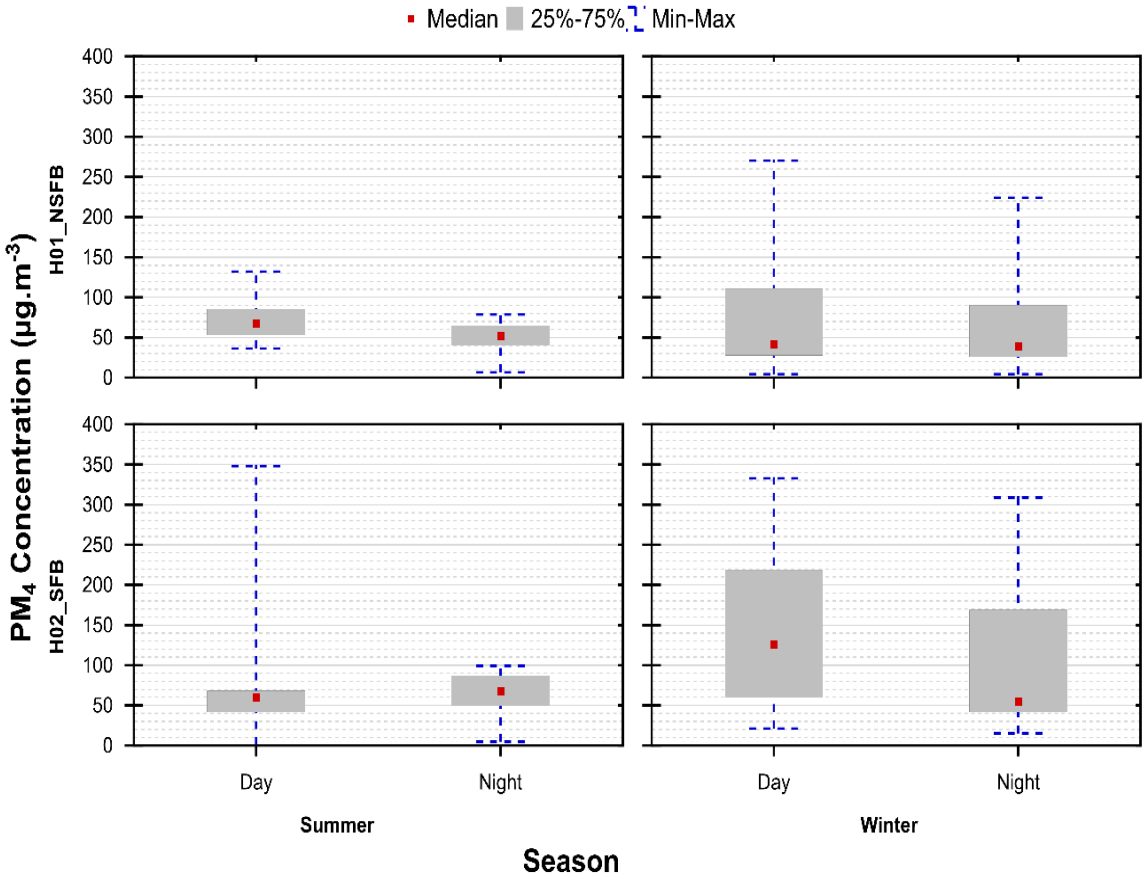

Figure 4-5. Box plots showing the median respirable fraction particulate aerosol mass concentration (µg m^{-3}) during winter and summer 2017 at non-solid fuel burning (NSFB) and solid fuel burning (SFB) in KwaZamokuhle.

The time series of the respirable size fraction particulate mass concentrations are presented in Figure 4-6 (a and b), for winter and summer respectively. The winter period shows a district pattern with gradually increasing PM_4 loadings accruing from 10–15 August (Figure 4-6 a). This is true for both the NSFB and SFB households. The solid fuel burning house had higher PM_4 mass loadings for 35 (88%) of the 40 × 12-hour samples collected from 26 July–16 August, 2017, when compared to the NSFB household. The time-integrated average for the day and night samples shows that burning of non-solid fuel exceeds the 24-hr $PM_{2.5}$ NAAQS for 10 days and burning of solid fuel for 20 of the 22 days sampled. During summer the solid fuel burning house had higher PM_4 mass loadings for 19 (53%) of the 36 × 12-hour samples collected from 1–19 November, 2017 (Figure 4-6 b), when compared to the 47% where the non-solid fuel burning household

had higher PM_4 concentrations. The time-integrated average for the day and night samples shows that NSFB exceeds the 24-hr $PM_{2.5}$ NAAQS for 18 days and SFB for 15 of the 19 days sampled. It is important to note that solid fuel burning was not the only contributing source of PM. Varying sources exist and could be responsible for the higher PM concentrations measured on several days at house NSFB. The NSFB dwelling was located near an unpaved road and this could have contributed to increased PM loadings. There were 3 days where NSFB PM_4 concentrations were higher than the SFB household, Figure 4-6 b . Some houses around NSFB practiced solid fuel burning and may have had an influence on the increase of PM inside the dwelling. Another possible contributing factor could be the ventilation methods practiced by the house during summer, i.e. opening of doors and windows during the day/night time. While SFB did not practice solid fuel burning but used an electric stove instead for food preparation during the warmer summer months. Solid fuels were more frequently used during the colder winter months when space heating was required by residents. These days of higher PM loading in NSFB were mostly noticeable in summer and are not as frequent during the winter.

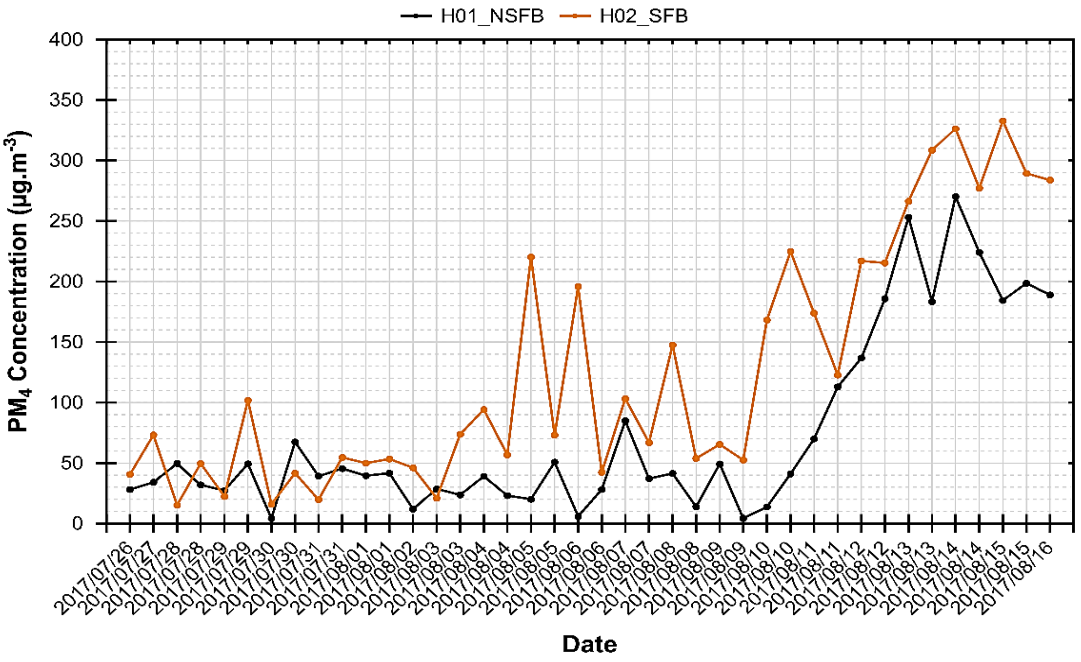

a.)

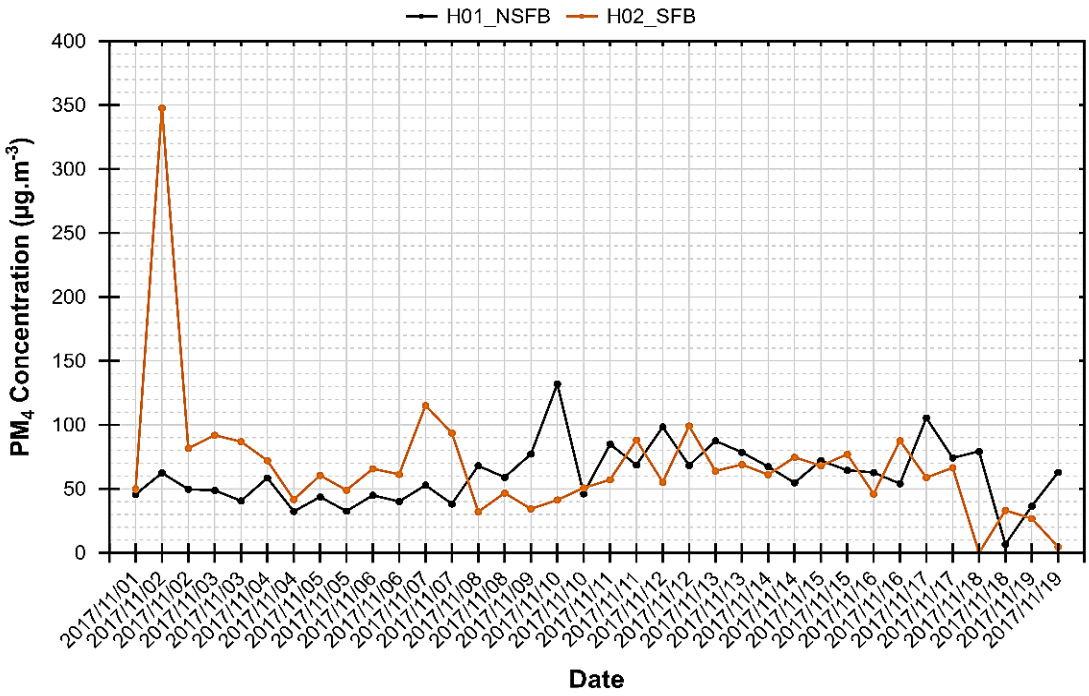

b.)

Figure 4-6. Time series of the respirable fraction particulate aerosol mass concentration (µg m^{-3}) during a.) winter and b.) summer 2017 at non-solid fuel burning (NSFB) and solid fuel burning (SFB) in KwaZamokuhle.

Indoor temperature and relative humidity

Table 4-3 shows the temperature comparison between the two houses. During the winter the NSFB and the SFB house had an indoor temperature higher than the ambient temperature but the minimum temperature in the NSFB was higher than the SFB by a factor of two. The minimum temperature was below the WHO standard for thermal comfort. The temperature graphs represented below represent the diurnal pattern for the total number of days which were sampled in summer and winter.

Table 4-3. Descriptive statistics for the 10-min averaged temperatures (°C) and relative humidity (%) for NSFB and SFB during winter and summer, 2017.

House	Location	Valid N	Mean	Median	Minimum	Maximum	Std.Dev.
		Winter (26 July–17 August)					
	Ambient	4096	11.8	10.1	-0.4	26.7	7.1
	Bedroom	4096	17.8	18.6	12.1	24.1	2.2
NSFB	Kitchen	4096	18.5	18.1	15.1	27.6	2.1
	Living room	4096	18.7	18.6	14.6	23.1	1.8
	Stove	4096	19	19.0	14.5	27.5	2.3
	Ambient	4170	11.4	10.0	-0.5	24.1	6.8
	Bedroom	4096	15.6	15.6	5.6	24.6	4.8
SFB	Kitchen	4096	17.6	17.7	7.1	28.7	4.9
	Living room	4096	15.7	15.6	6.5	25.1	4.6
	Stove	4096	18.0	18.1	6.6	30.6	5.7
		Summer (1 November–28 November)					
	Ambient	7987	19.6	17.7	4.6	38.1	7.7
	Kitchen	7990	24.1	24.1	18.6	31.6	2.3
NSFB	Stove	7991	24.3	24.0	19.0	32.5	2.3
	Living room	7988	23.6	23.6	18.1	30.1	2.4
	Bedroom	7989	23.4	23.6	18.6	31.1	2.1
	Ambient	7701	19.9	18.1	4.0	37.6	7.8
	Kitchen	7700	23.5	22.7	11.6	36.7	5.0
SFB	Stove	7698	23.3	22.1	10.6	38.6	5.9
	Living room	7701	23.2	21.6	9.1	40.1	6.5
	Bedroom	7700	23.1	22.1	10.1	37.1	5.6

The maximum indoor temperature in the NSFB was in the kitchen area at the stove, followed by the bedroom and then the living room. In contrast, in the SFB it is the stove, the kitchen area followed by the living room and finally the bedroom. This implies that the SFB household depends on heating from the stove to heat up the whole house while the NSFB household probably uses an electric heater to heat rooms since they depend on electricity. The mean indoor temperature at all locations (bedroom, kitchen, living room and stove) in both houses was above the mean ambient temperature. However,

the standard deviation in the temperature indicated a wider variation in the indoor temperature at the SFB than the NSFB household. This could be explained by the fact that the indoor temperature in the SFB house depends purely on solid-fuel burning for space heating and this was limited to certain periods, while the NSFB household relies on electricity and so can maintain space-heating for as long as they wish to. During the summer, the average temperature in both houses was comparable (about 23 °C) and was generally above the average ambient temperature which was about 20 °C. The maximum indoor temperature was found to be higher in the SFB house than the SFB house and the minimum indoor temperature in the SFB house was lower than that of the NSFB household. The standard deviation showed that the temperature variation in the SFB house is a factor of two times higher than the NSFB household. This implies that the insulation in the NSFB house regulates the indoor temperature. For the SFB house, the variation in the indoor temperature is comparable to the ambient temperature variation while that of the NSFB is lower than the ambient variation by a factor of two. The diurnal pattern of the temperature inside the houses collected using the temperature buttons showed variability with the hours of the day. The temperature started at a low point (12 °C) and reached a peak (25 °C) during the day; the temperature then later reduced again in the evening. This variability is to be expected as the temperature depends on the amount of solar radiation.

Though the average ambient temperature outside the NSFB during winter was 11 °C, which is lower than the WHO standard (18 °C), the indoor average temperature was maintained at a value above the standard. This could be a result of the household having access to electricity for space-heating. Furthermore, the house has a ceiling which helps to conserve the heat. Thus, for the NSFB house, the indoor average temperature is maintained within an acceptable standard of minimum comfort. On the other hand, the average indoor winter temperature in the SFB house closely follows the temperature of the stove with observed stove temperatures suggesting that burning stops sometime around 00h00. Consequently, the indoor temperature drops below the 15 °C mark till it reaches a minimum of 8.6 °C. For approximately 10hrs (00h00–10h00) the occupants are thus exposed to thermal discomfort. This may be due to lack of money to buy enough coal to keep up the space-heating. During the summer the SFB house recorded an indoor average temperature as high as 32.5 °C during the day and a temperature generally above 25 °C from 10h00–20h00 (10hrs) even when the ambient

temperature had decreased. Thus the decrease in indoor temperature lags behind the ambient temperature in reaching the minimum warm weather thermal comfort standard.

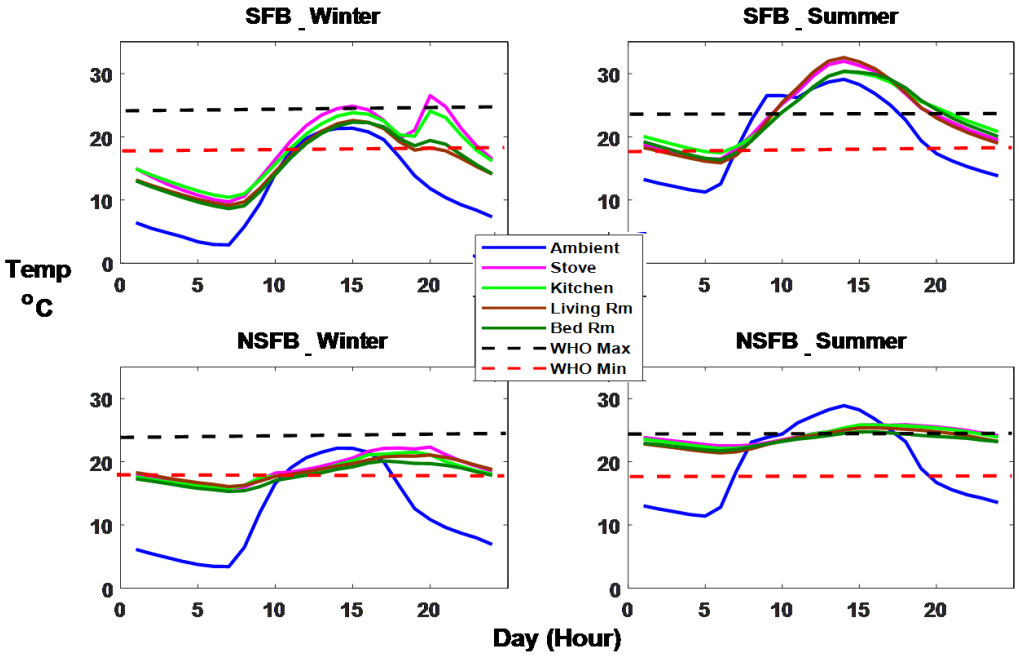

Figure 4-7. Mean indoor temperature measured during winter and summer at solid fuel burning (SFB) and non-solid fuel burning (NSFB) households. The Blue line = the ambient temperature and relative humidity measurement, black line (dotted) World Health Organisation (WHO) maximum and redline (dotted) WHO minimum temperature guideline ranges for thermal comfort.

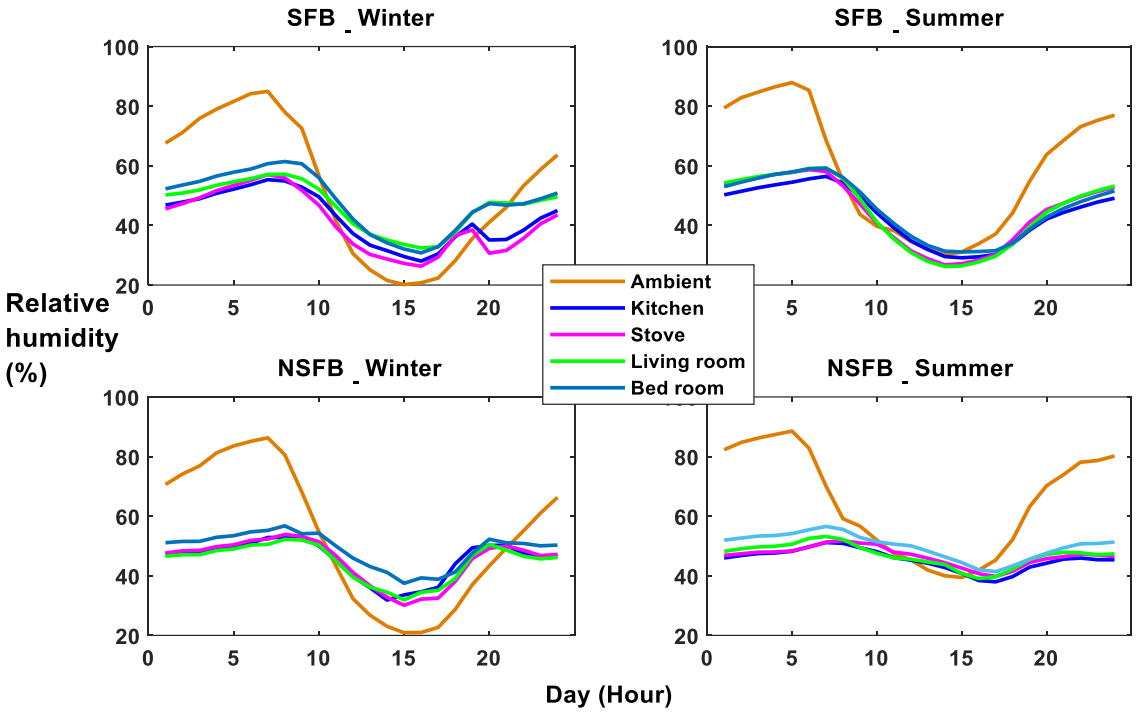

Figure 4-8. Mean indoor relative humidity measured during winter and summer at solid fuel burning (SFB) and non-solid fuel burning (NSFB) households. The Blue line = the ambient temperature and relative humidity measurement, black line (dotted) World Health Organisation (WHO) maximum and redline (dotted) WHO minimum temperature guideline ranges for thermal comfort.

Outdoor PM_4

Winter and summer outdoor measurements taken during 2017 in the two houses in KwaZamokuhle. Summary statistics of the outdoor PM_4 concentrations for the two seasons are given in Table 4-4. Summer easterly direction data for the NSFB house are missing, as well the SFB house's easterly and southerly direction data. This missing data is attributable to instrumentation failure. Regarding the available data, mean PM_4 recorded during winter was two and three orders of magnitude higher than the NAAQS $PM_{2.5}$ in all cardinal directions of the dwellings irrespective of the fuel choice of the residents. This is expected due to the general practice of solid fuel combustion in the greater KwaZamokuhle community.

Table 4-4. Descriptive statistics for the outdoor PM_4 mass concentrations (µg m^{-3}), in all cardinal directions, for NSFB and SFB during winter and summer, 2017.

House	Direction	Mean	SD	Min	Median	Max	NSFB/SFB Ratio	Winter/Summer Ratio
Winter (26 July–17 August)								
NSFB	N	104	112	13	45	385	0.3	3
	E	126	155	20	45	559	2	6
	S	144	162	20	84	702	2	4
	E	177	206	21	131	927	-	-
SFB	N	321	214	88	233	940		19
	W	75	83	11	33	256		1
	S	63	45	17	52	174		-
	E	-	-	-	-	-		-
Summer (1 November–28 November)								
NSFB	N	34	35	10	20	128	0.3	
	E	23	33	4	7	131	0.2	
	S	38	107	1	11	1493	-	
	E	-	-	-	-	-	-	
SFB	N	17	10	9	14	40		
	W	147	50	75	141	322		
	S	-	-	-	-	-		
	E	17	8	8	14	38		

The median winter and summer outdoor PM_4 mass concentrations measured in each cardinal direction are presented in Figure 4-9. Of the eight (8) ambient monitors used to sample PM_4, only one instrument recorded median PM_4 concentrations below the NAAQs $PM_{2.5}$ 24hr-limit during winter. During the winter period, outdoor concentrations around the SFB household were a factor of two and three times higher than $PM_{2.5}$ NAAQS at instruments SFB-S and SFB-E respectively. Concentrations at the instrument SFB-N with the highest PM_4 values recorded means of 321 (±214) (range: 940–80 µg m^{-3}) and 177 (±206) (range: 927–21 µg m^{-3}) µg m^{-3} at the SFB and NSFB households respectively. Although the instruments measured at equal distances (2 m) around the dwellings in the same low-income settlement, the median concentrations recorded were highly variable from one direction to another and between seasons. Winter presented the worst-case scenario for both houses where outdoor PM_4 concentrations exceeded

the $PM_{2.5}$ standard by a factor of two as seen in the median concentrations presented in Figure 4-9 a.

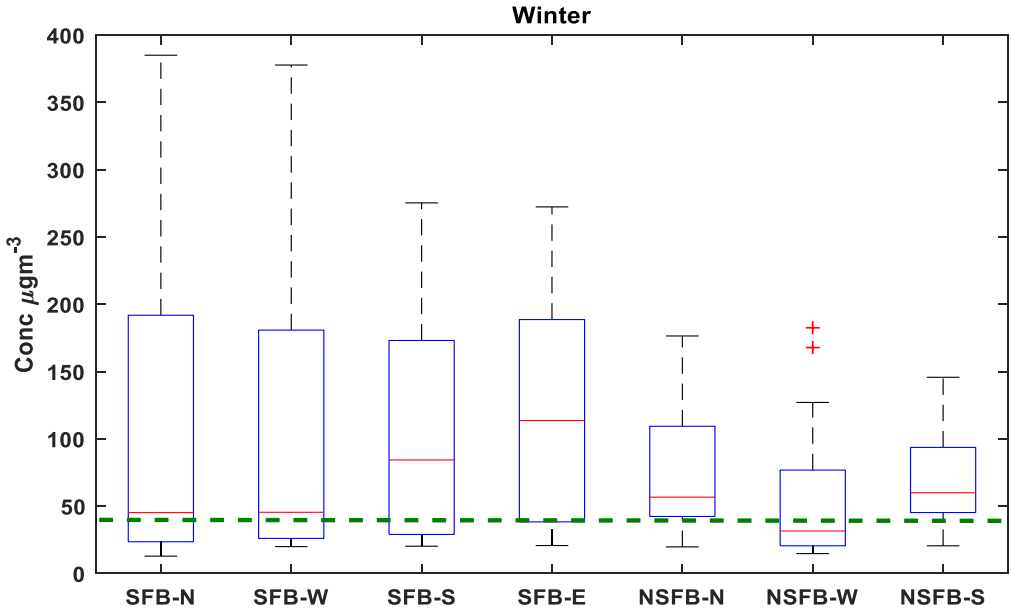

a.)

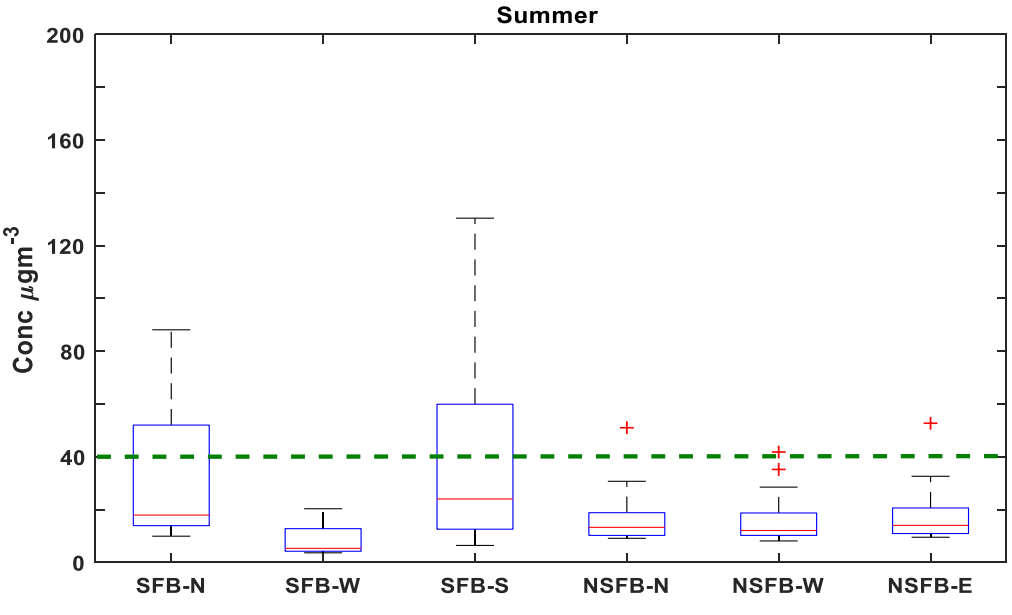

b.)

Figure 4-9. Box and whisker plot of the median outdoor PM_4 daily concentrations, at the non-solid fuel burning (NSFB) and solid fuel burning (SFB) households, in all cardinal direction, during a) winter and b) summer (2017) (Mean: red line; Box: 25%-75%; Whisker: non-outlier range; Star: outliers; Green Dotted line: NAAQS 24-hr $PM_{2.5}$ at 40 µg m^{-3}).

Figure 4-10 and Figure 4-11 show the NSFB and SFB houses' winter and summer averaged mean hourly diurnal patterns for outdoor PM_4 mass concentration, for each cardinal direction. During the winter period around the SFB household, PM_4 concentrations displayed a bimodal peak distribution, which has been attributed to anthropogenic daily human activities (see earlier section 3.1.4.).

The two peaks are noticeable in the early morning for ±5 hours (04h00–09h00) and late afternoon until evening for ±five hours (15h00–20h00). The evening peak was found to be two times higher than the morning peak, reaching maximum concentrations of ±650 µg m^{-3} during winter The PM_4 concentrations during the day between 10h00 and 14h00 were found to be 45 (±15) µg m^{-3}. The instruments SFB-south and SFB-west around the solid fuel burning dwelling were the ones where the highest concentrations of PM_4 were measured

Around the NSFB dwelling instrument, NSFB-north and NSFB-south instrument data displayed a three-peak distribution not observed in the other monitored directions. The first peak was noticeable from 06h00–10h00 (four hours) the second peak was from 12h00–16h00 and the third peak was from 18h00–21h00. The source of the second peak requires further investigation in order to explain the source in full detail. The NSFB-west instrument presented results with a bimodal pattern, where the second peak was consistent with the second peak in the latter two ambient monitors. Mean concentrations around the NSFB dwelling were ±175 µg m^{-3}

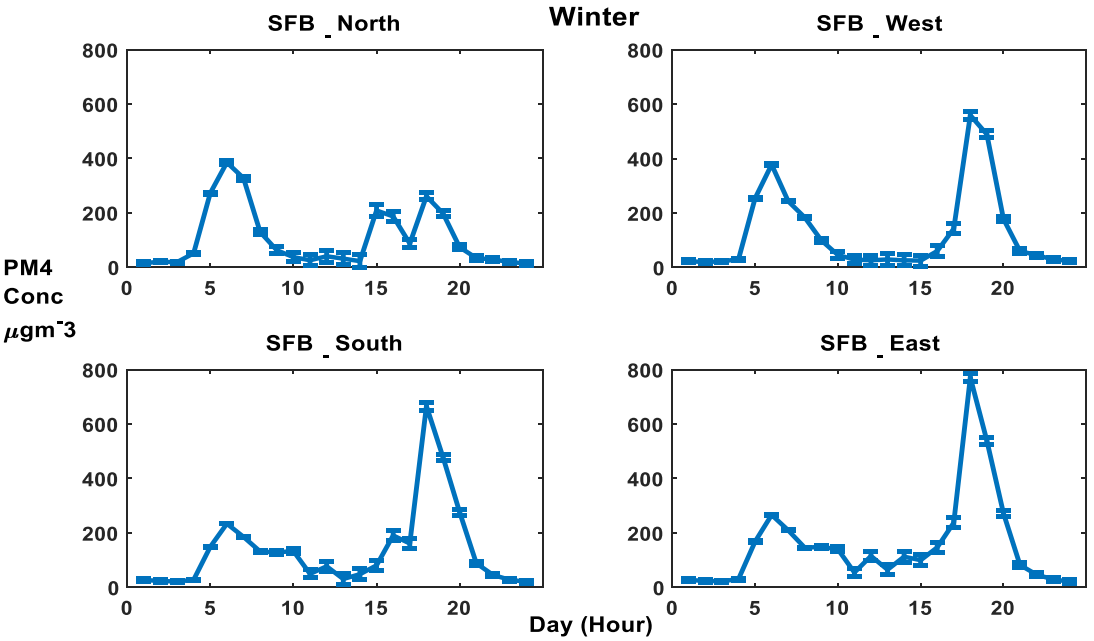

a.)

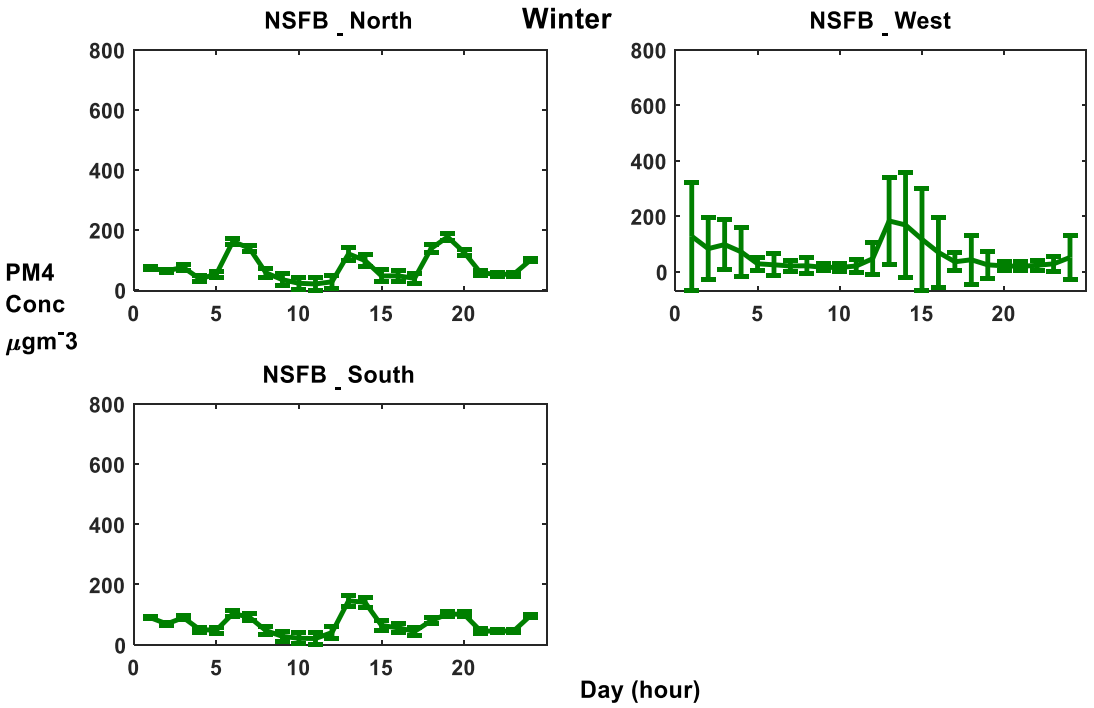

b.)

Figure 4-10. Diurnal pattern of the mean hourly averaged indoor PM_4 mass concentrations (μg m^{-3}) measured in a.) solid fuel burning (SFB) (blue) and b.) non-solid fuel burning (NSFB) (green) households during winter (2017). (Whiskers: standard deviation).

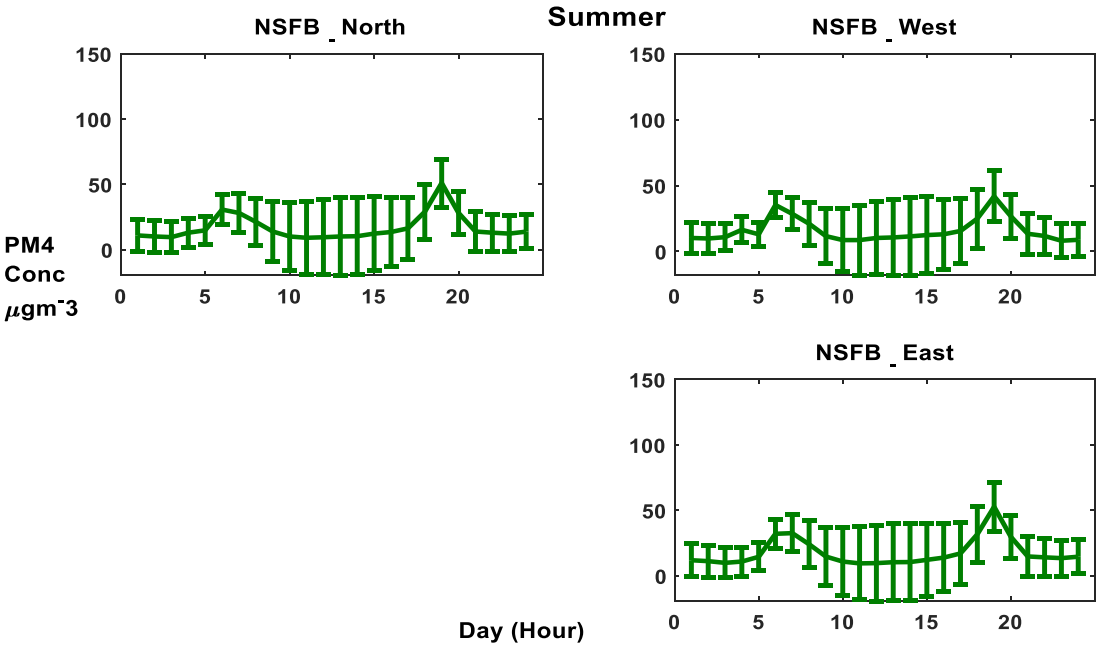

a.)

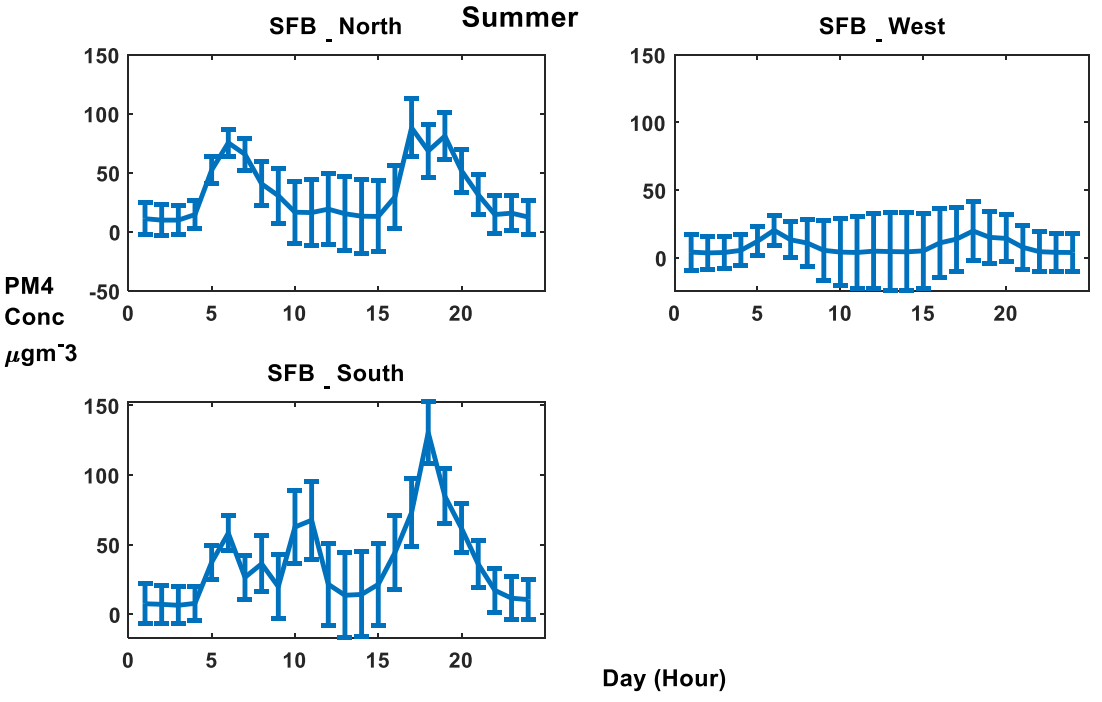

b.)

Figure 4-11. Diurnal pattern of the mean hourly averaged indoor PM_4 mass concentrations (μg m-3) measured in a.) solid fuel burning (SFB) (blue) and b.) non-solid fuel burning (NSFB) (green) households during summer (2017). (Whiskers: standard deviation).

4.2 Relationship between indoor and outdoor PM_4

The indoor and outdoor diurnal mean concentrations of PM_4 measured during summer and winter in the two domestic households are presented in Figure 4-12. The mean diurnal indoor PM_4 concentrations in winter were ±172 µg m^{-3} (range: 447–48 µg m^{-3}) and ±105 µg m^{-3} (range: 255–40 µg m^{-3}) in the SFB and NSFB households respectively. The corresponding mean outdoor levels were ±115 µg m^{-3} (range: ±350–65 µg m^{-3}) and ±93 µg m^{-3} (range: 160–21 µg m^{-3}), respectively. The respective diurnal PM_4 indoor concentrations exceeded the NAAQs $PM_{2.5}$ 24-hr limit value for 70% and 85% during summer of the measured days in NSFB and SFB. High indoor PM levels can be caused by indoor, as well as outdoor factors. Both households are situated in a low-income settlement where 75% of the community practices domestic use of solid fuel. Unpaved roads, waste and biomass burning are also prevalent factors that generate PM and which could also penetrate structures and contribute to the total indoor PM_4 loading. The infiltration is also dependant on meteorological conditions, insulation of the building and ventilation methods/patterns which in turn influenced the air exchange between the indoor and the ambient air.

In both summer and winter, the indoor PM_4 concentration in the SFB house was around two to four orders of magnitude higher than the outdoor levels surrounding the building. This was expected as the indoor burning of solid fuel is likely to have caused the interior PM_4 concentration to increase above the ambient environment. On the other hand, at the NSFB household, the indoor PM_4 concentration was two orders of magnitude higher than the outdoor in the summer but not in the winter. During the winter the influence of solid fuel being burnt in the majority (75%) of households throughout the community makes the outdoor PM_4 concentration higher than the indoor level. In contrast, in the summer, less solid fuel is being burnt so the outdoor concentration is slightly less than the indoor PM_4 concentration. During the winter, the outdoor PM_4 concentration is sometimes higher especially during the afternoon when it is raised by a factor of three. In the morning hours (08h00 to 10h00) the indoor PM_4 level increased by a factor of three compared to the outdoor levels. In the evening the PM_4 level again increases, but at this time (about 16h00) by a factor of up to five times that of the outdoor level. During the summer, in the SFB household the indoor PM_4 concentration was generally higher than the outdoor concentration by a factor of seven especially in the evening at about 18h00.

During the winter, the outdoor concentrations were at times higher than the indoor concentration before the burning hours in the morning (04h00 to 05h00) and also in the evening (15h00 to 16h00) by a factor of three in the morning and a factor of two in the evening. The indoor PM_4 level was higher during the morning (08h00 to 10h00) and evening (19h00 to 21h00) burning periods. The PM_4 level increased five-fold in the morning but by as high as 12-fold in the evening.

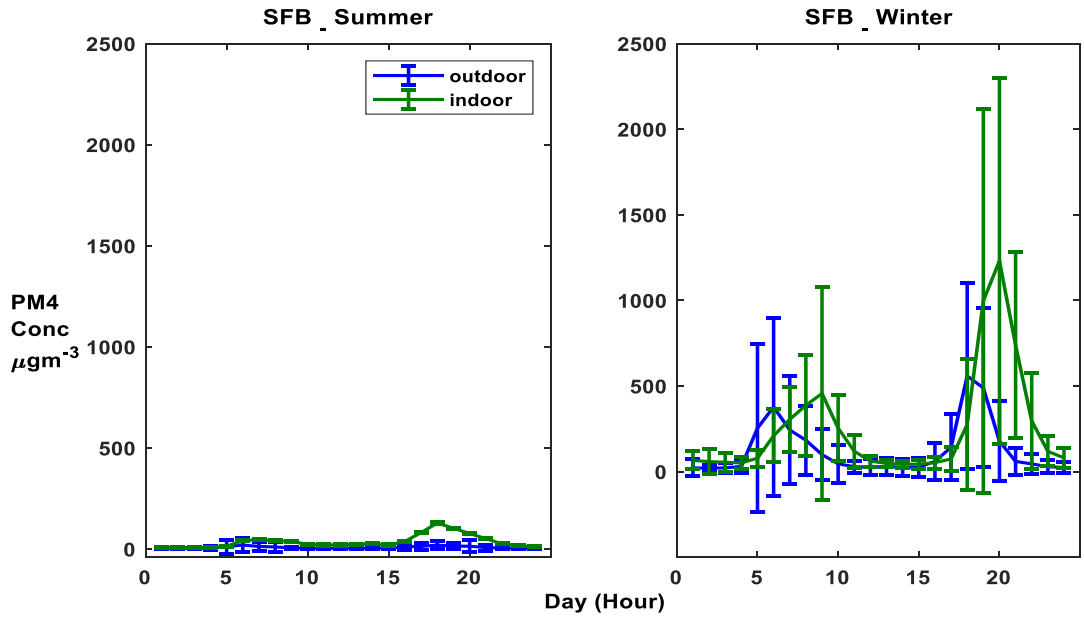

a.)

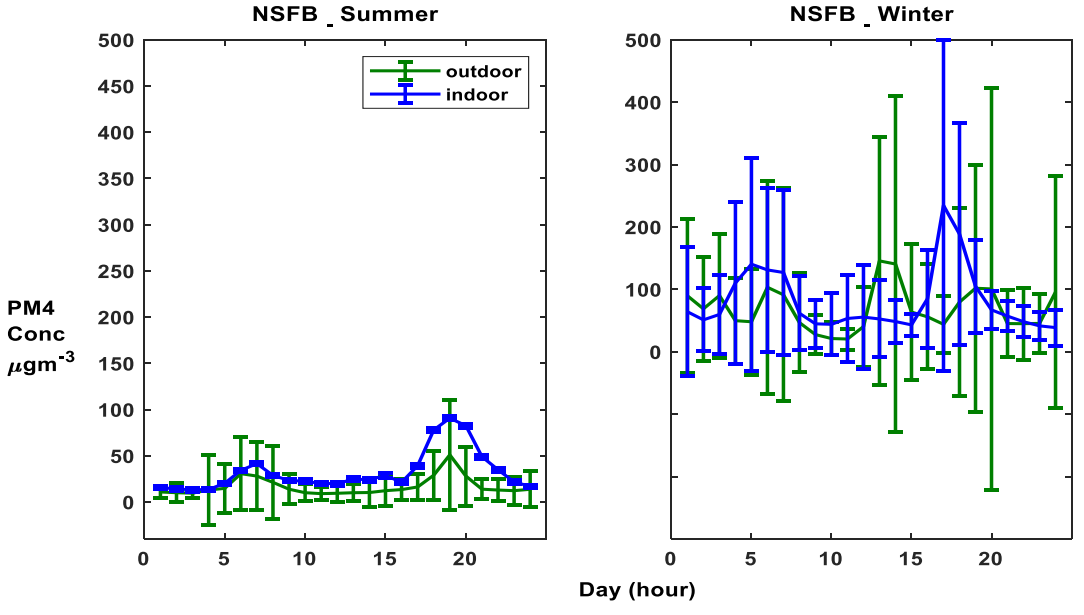

b.)

Figure 4-12. Diurnal pattern of the mean hourly averaged indoor and outdoor PM_4 mass concentrations (μg m^{-3}) measured in a) solid fuel burning (SFB) (blue) and b) non-solid fuel burning (NSFB) (green) households during winter and summer (2017). (Whiskers: standard deviation).

Figure 4-13 represents the 24-hr averaged PM_4 concentration measured outdoors and indoors at the NSFB and SFB households respectively. In the NSFB house during winter

the maximum/minimum 24-hr averaged PM_4 indoor concentration was 80.5 μg m^{-3} (15.3 μg m^{-3}) while the maximum/minimum outdoor level was 73.5 μg m^{-3} (18.9 μg m^{-3}). For SFB, the PM_4 level was 207.5 μg m^{-3} (60.9 μg m^{-3}) while the maximum/minimum outdoor level was 110.0 μg m^{-3} (34.5 μg m^{-3}). During the summer, the NSFB household had a maximum/ minimum 24-hr averaged indoor PM_4 concentration of 39.8 μg m^{-3} (14.2 μg m^{-3}) while the maximum/minimum outdoor level was 21.2 μ m^{-3} (11.2 μg m^{-3}). For the SFB household, the PM_4 level was 36.6 μg m^{-3} (17.4 μg m^{-3}) while the maximum/minimum outdoor level was 9.2 μg m^{-3} (5.1 μg m^{-3}). Overall the data shows that the indoor PM_4 concentrations are higher than the outdoor levels in all seasons across both houses. However, during the winter, the indoor PM_4 level at the SFB household is twice as high on most days and even higher on certain days. In contrast, the NSFB household has a PM_4 level only slightly higher than the outdoor level. During summer, both the indoor and the outdoor PM_4 concentrations are low for both houses.

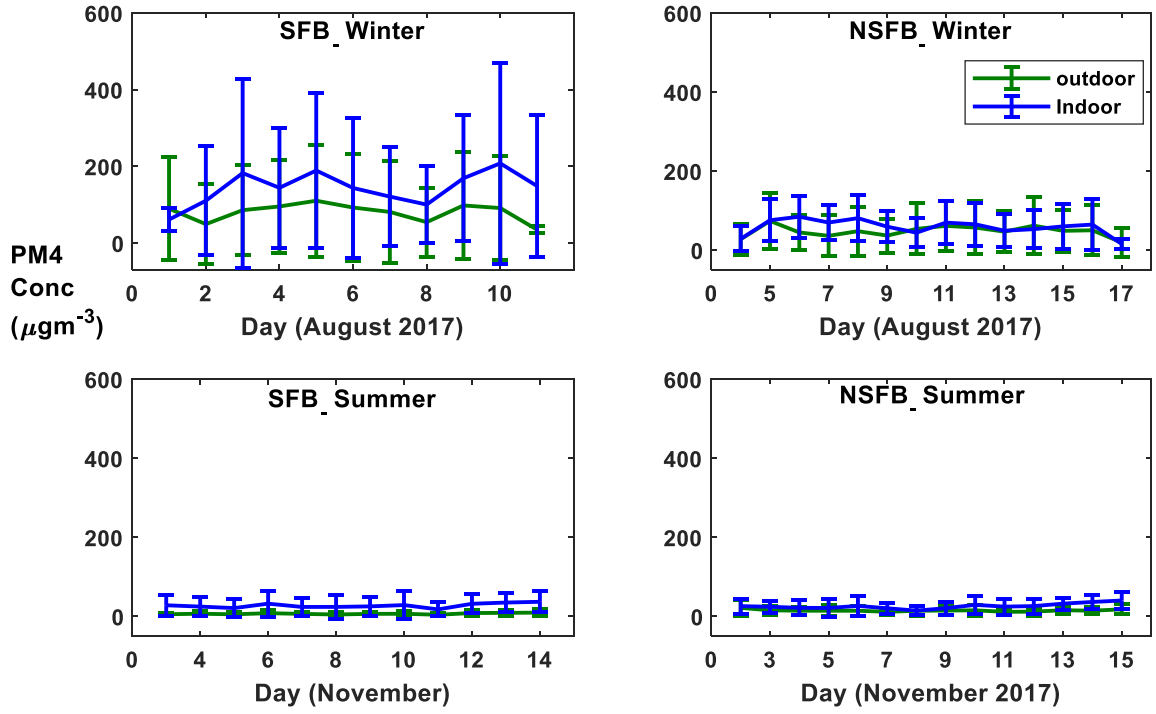

Figure 4-13. The daily pattern of the mean 24 hours averaged indoor/outdoor PM_4 mass concentrations (μg m^{-3}) measured in non-solid fuel burning (NSFB) and solid fuel burning (SFB) households during winter and summer (2017). (Whiskers: standard deviation).

The coefficient of determination (R^2) is an index that can be used to explain to what degree the outdoor is affected by the indoor concentration. The slope of the regression line corresponds to the fraction of the indoor-generated PM_4 passing through the walls and other openings to the outdoor and the intercepts is taken as the contributions from other sources. Penetration of particles of small aerodynamic diameter is expected to occur through the wall easily (Milner *et al.,* 2005). Using the Pearson paired t-test, R^2 ranges between 0.00 – 0.19 during the winter and 0.57 to 0.73 during the summer Table 4-5 and Figure 4-14 . The outdoor PM_4 during the winter did not correlate to the indoor which implies that ambient pollution comes from the surrounding than directly from the indoor. The slope during the winter ranges between -0.23 to 0.25 suggesting that only a little contribution is made from pollution penetrating the wall from the indoor to the outdoor (Milner et al., 2005). Also the larger intercept of 55.04 to 97.15 also confirms that the outdoor concentration comes from contribution from other sources other than those from indoor. On the other hand, during the summer the correlation presented that there is likelihood that the outdoor PM concentration gets some influence from the indoor concentration. The R^2 in both houses ranges from 0.57 to 0.73 which indicates a good correlation supported by the low p-values. There are increments in the values of the intercept showing more contributions from the indoor to the outdoor and less values of intercepts confirming less contributions from other sources.

The ratio between the indoor and outdoor concentration was used to evaluate the variance (Chaloulakou *et al*., 2003; Milner *et al.,* 2005; Lv *et al*., 2005). The I/O ratios of PM_4 at both dwellings for winter and summer ranges between 1.01 to 4.42, respectively. During the winter the NSFB ratio ranges between 1.08 and 1.46 and for SFB 1.62 and 2.40. These show that the ratio is higher at the SFB as more PM_4 concentration is present indoor. During the summer NSFB ranges between 1.82 and 2.04 while SFB ranges between 1.01 and 4.42 with the highest ratio still occurring at SFB. The ratio during summer is higher than winter probably because the outdoor pollution during winter receives contribution from surrounding households as most houses were involved in burning activities both for cooking and space heating. Hence the ratio is less because the difference between outdoor and indoor is comparable. The ratio was greater in the SFB than the NSFB, this was anticipated as air pollution indoors has higher concentration than outdoor. During the winter the meteorology also enhances the trapping of the emitted PM_4 as vertical motion of air is suppressed and wind speed is

low. Other related research observed the ratio to be smaller but in their cases the source originates from outdoor rather than indoor (Riain, 2003).

Table 4-5 The statistical relationship between the indoor and outdoor hourly mean measurements indicating the intercept, slope, p-value, R^2 and the indoor/outdoor ratio.

House	Season	Location	Intercept	Slope	*p*-value	R^2	I/O
NSFB	Winter	North	55.04	0.25	0.19	0.07	1.08
		West	68.76	0.01	0.96	0.00	1.17
		East	74.43	-0.23	0.27	0.05	1.46
SFB	Winter	North	97.13	0.03	0.66	0.01	2.40
		West	72.15	0.21	0.03	0.18	2.02
		South	76.51	0.24	0.01	0.24	1.85
		East	95.64	0.24	0.03	0.19	1.62
NSFB	Summer	North	04.61	0.38	0.00	0.69	1.93
		West	05.73	0.31	0.00	0.57	2.04
		East	04.65	0.41	0.00	0.69	1.82
SFB	Summer	North	09.42	0.64	0.00	0.63	1.11
		West	03.48	0.13	0.00	0.61	4.42
		South	05.50	0.84	0.00	0.73	1.01

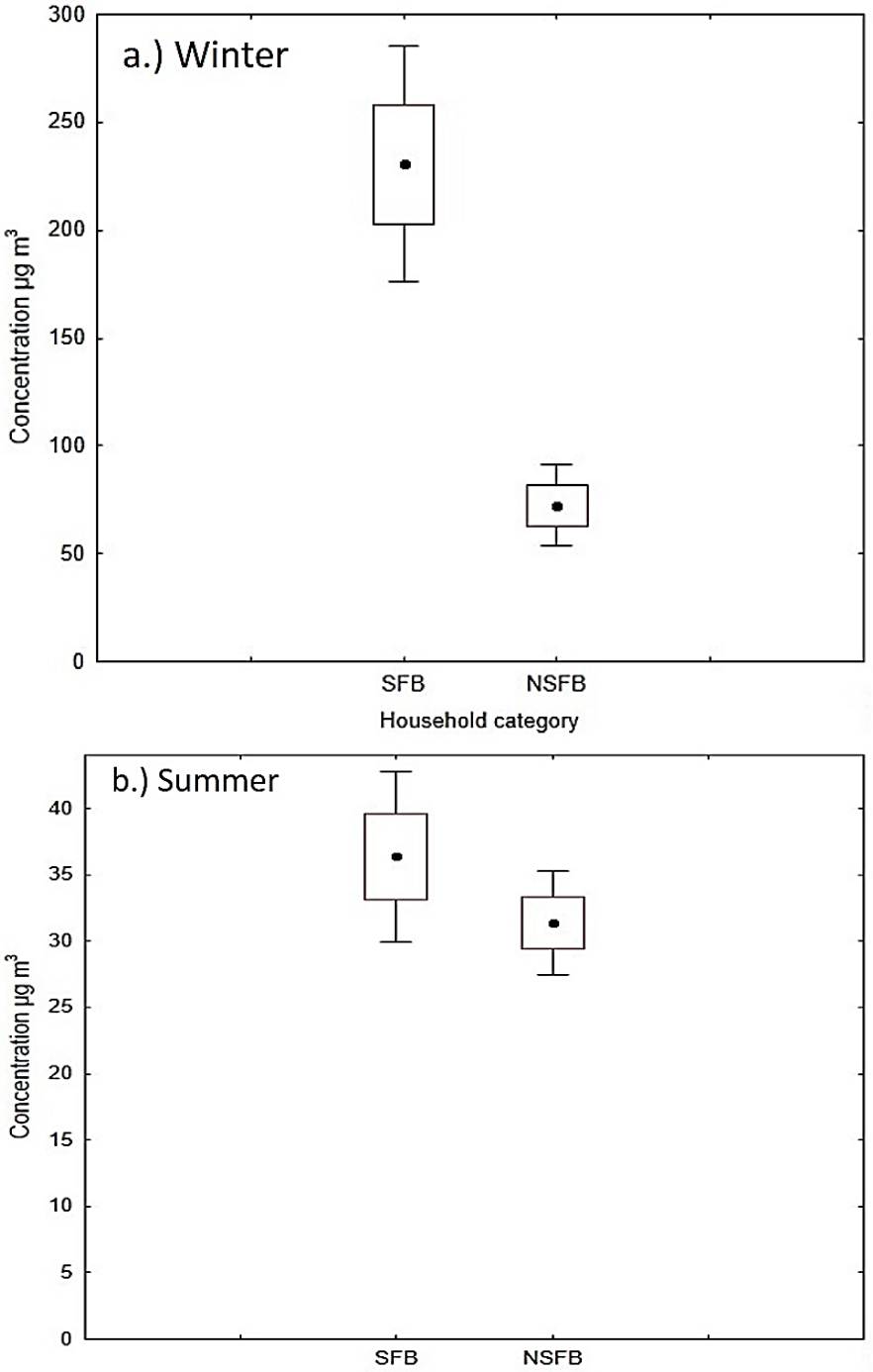

Figure 4-14 The statistical significance between the indoor and outdoor represented with box and whisker plots.

4.3 Indoor source identification

The day-to-night (D/N) ratios have been used to evaluate if gravimetric PM_4 mass loadings changed or were consistent during daytime and night-time periods. The D/N ratios of the mean mass concentrations for the respirable size fraction for winter and summer are given in Figure 4-15. The D/N ratios are above one for both NSFB and SFB, irrespective of the season. Thus, PM_4 mass concentration is more prominent during the day-time in both the NSFB and SFB houses during winter and summer.

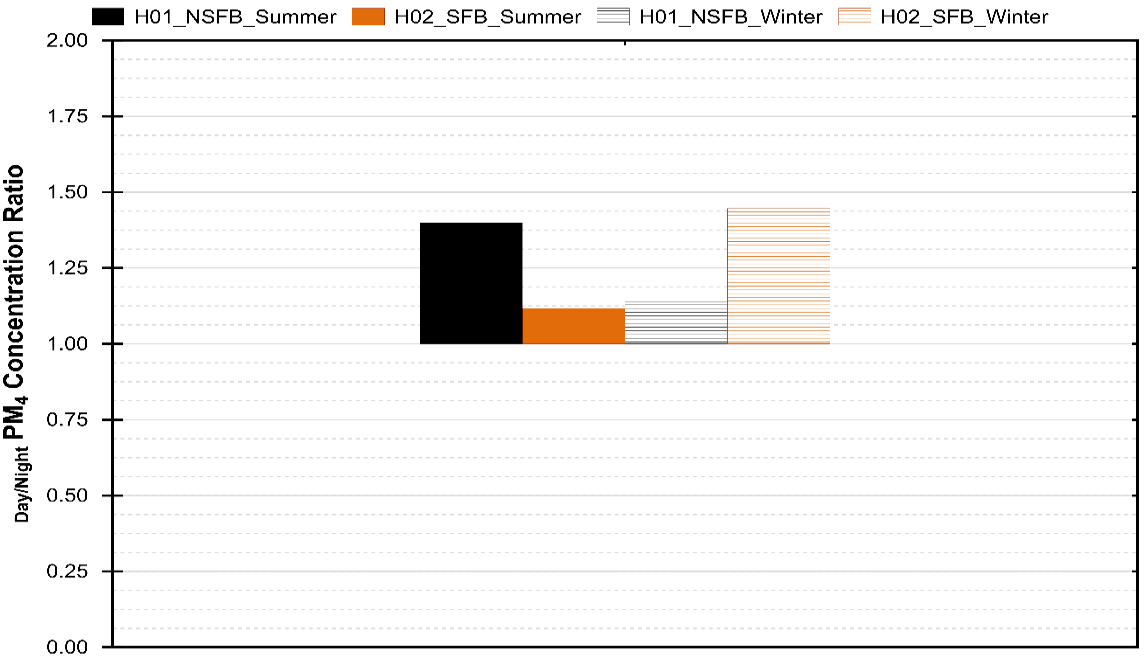

Figure 4-15. Ratio of the mean day-to-night respirable fraction particulate aerosol mass concentration (μg m^{-3}) during winter and summer 2017 for NSFB and SFB in KwaZamokuhle.

The summer-to-winter (S/W) ratios have been used to evaluate if the gravimetric PM_4 mass loadings changed or were consistent during daytime and night-time periods across seasons. The S/W ratios of the mean mass concentrations for the respirable size fraction for winter and summer are given in Figure 4-16. The S/W ratios are below one for both NSFB and SFB, irrespective of the time of day. Thus, PM_4 mass concentrations are higher during winter in both the NSFB and SFB houses for both days and nights.

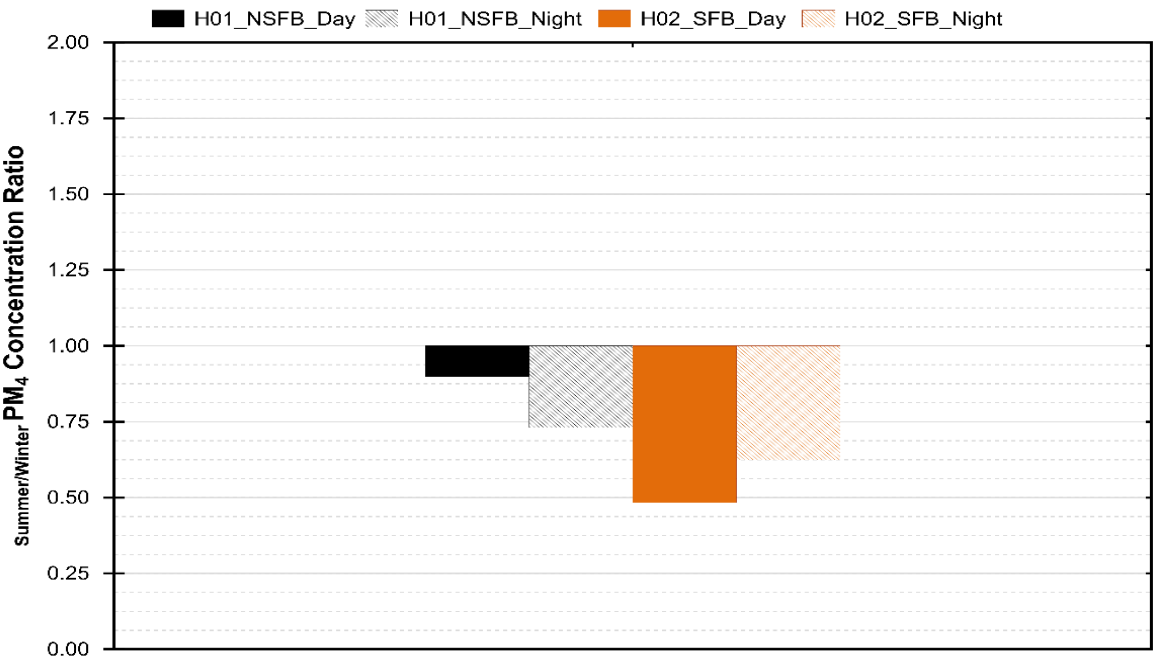

Figure 4-16. Ratio of the mean summer-to-winter respirable fraction particulate aerosol mass concentration (µg m^{-3}) during daytime and nigh-time 2017 for NSFB and SFB in KwaZamokuhle.

4.3.1. Elemental characterisation

Atmospheric element concentrations (µg m^{-3}), were derived by wavelength dispersive x-ray fluorescence (WD-XRF) for the filters exposed in NSFB and SFB, during winter and summer 2017. The element mass concentration, day-to-night seasonal elemental ratios, summer-to-winter ratios and elemental enrichment factors are discussed in detail for each monitoring site (NSFB and SFB).

4.3.2. Element mass concentrations

The elemental mean concentrations (and standard deviation) for day and night in winter and summer (2017) collected on each filter, for NSFB and SFB, in the respirable size fraction is given in Table 4-6. The data is categorised by season (winter and summer) as well as by the time the sample was collected, namely, day (10h00-22h00) and night (22h00-10h00).

Dust related elements

Magnesium (Mg) is an element commonly found in coarse fraction of natural soils and was detected in both NSFB and SFB households. The mean daytime (*winter:* 0.813±0.212 µg m^{-3}; *summer:* 0.656±0.281 µg m^{-3}) and night-time (*winter:* 0.867±0.427 µg m^{-3}; *summer:* 0.697±0.136 µg m^{-3}) concentration in NSFB were lower than that of the SFB during both daytime (*winter:* 1.206±0.471 µg m^{-3}; *summer:* 1.489±2.286 µg m^{-3}) and night-time (*winter:* 1.305±0.630 µg m^{-3}; *summer:* 0.983±0.601 µg m^{-3}) periods (Table 4-6).

A time-series of the Mg concentration and associated enrichment factors, for both NSFB and SFB, for winter (Figure 4-17 a) and summer (Figure 4-17 b) are given below. During winter SFB had higher concentrations of Mg on most days, except during three night-time measurement periods were the concentrations were approximately the same (27-, 28 July, and 1 August). There was a single night (30 July) where the Mg concentration was higher in NSFB. From the night of 10- to 13 August, Mg was not detected. The associated enrichment factors are for most part below one or very close to unity. The non-solid fuel burning house showed enrichment of Mg on 6 samples, 5 of which are night-time samples (26 July, 3-, 6-, 7-, and 8 August) and 1 daytime sample (31 July). The solid fuel burning household only showed enrichment on 28 July during the day.

During summer NSFB Mg concentration range from 0.3 µg m^{-3} to just above 1 µg m^{-3}, while SFB ranged between 0.2- and 10 µg m^{-3}. The solid fuel burning house had increased levels of Mg from 3- to 8 November. During the before mentioned dates, the enrichment factors are close to unity, in some cases being above one and others below. It is clear that there is daily variability in the Mg concentrations in both households, however, during summer Mg had a higher level of enrichment compared to winter were the enrichment factor is below one for most days, indicating Mg depletion.

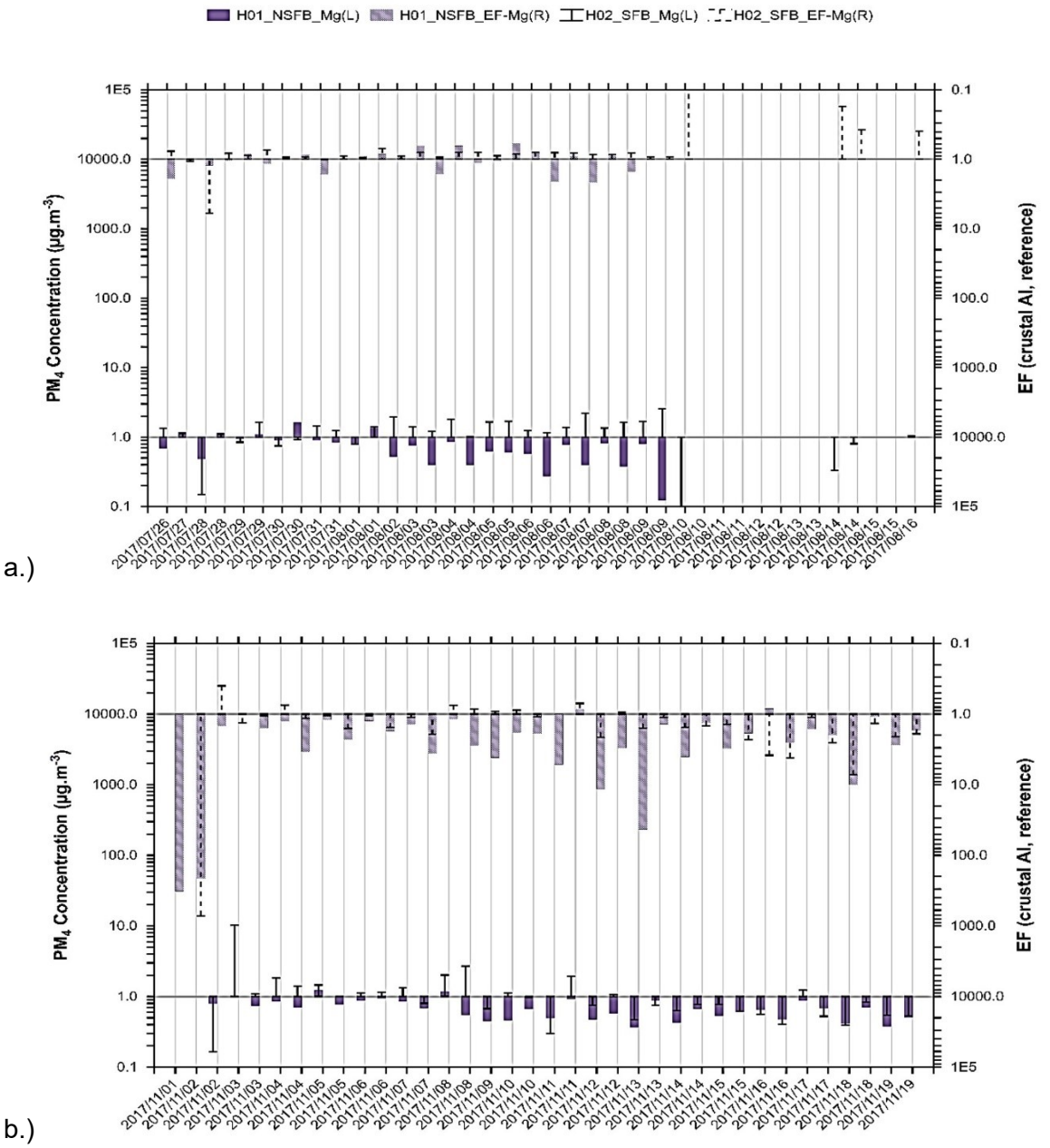

Figure 4-17. Time-series of the detected Mg element concentrations (µg m^{-3}) (left y-and bottom x-axis) and the associated enrichment factors (right y- and top x-axis) at NSFB and SFB in KwaZamokuhle during winter and summer 2017.

Aluminium (Al) is an element commonly found in the course fraction (1-10% of mass) of paved road dust, unpaved road dust, construction soils, agricultural soils, and natural soils while in the fine fraction (0.1-1% of mass) it is present in motor vehicle emissions and marine aerosols. Aluminium was detected in both NSFB and SFB households. The

mean daytime (*winter:* 3.007±1.983 µg m^{-3}; *summer:* 1.600±1.383 µg m^{-3}) and night-time (*winter:* 2.357±1.843 µg m^{-3}; *summer:* 1.602±0.907 µg m^{-3}) concentration in NSFB were lower than that of the SFB during both daytime (*winter:* 6.047±2.106 µg m^{-3}; *summer:* 5.229±7.147 µg m^{-3}) and night-time (*winter:* 5.764±2.802 µg m^{-3}; *summer:* 3.237±3.274 µg m^{-3}) periods (Table 4-6). Soil dust has an Al-to-Si ratio of 2:1. The correlation of Al-to-Si is presented in Figure 4-18 for both NSFB and SFB in both seasons. The correlation indicates that both Al and Si are a result of a single source, namely dust.

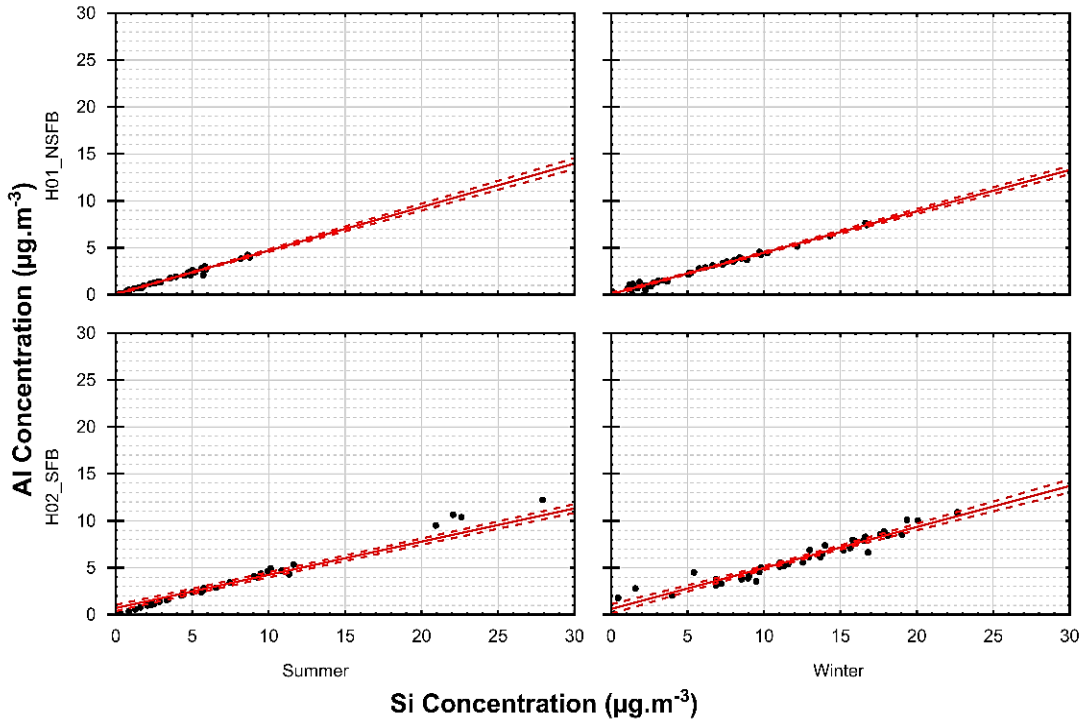

a.)

Figure 4-18. Correlation matrix of detected Al-to-Si element concentrations (µg m^{-3}) at NSFB and SFB in KwaZamokuhle during winter and summer 2017.

Silicon (Si) is an element commonly found in coarse fraction (>10% of mass) of paved road dust, unpaved road dust, construction material, agricultural soils, and natural soils while in the fine fraction (0.1-1% of mass) it is present in motor vehicle emissions, residential oil combustions, and marine aerosols. Silicon was detected in both NSFB and SFB households. The mean daytime (*winter:* 6.717±4.310 µg m^{-3}; *summer:* 3.323±2.995 µg m^{-3}) and night-time (*winter:* 5.173±4.301 µg m^{-3}; *summer:* 3.327±1.885 µg m^{-3}) concentration in NSFB were lower than that of the SFB during both

daytime (*winter:* 12.806±4.697 µg m^{-3}; *summer:* 12.073±20.464 µg m^{-3}) and night-time (*winter:* 11.458±6.116 µg m^{-3}; *summer:* 7.113±7.243 µg m^{-3}) periods (Table 4-6).

A time-series of the Si concentration and associated enrichment factors, for both NSFB and SFB, for winter (Figure 4-19 a) and summer (Figure 4-19 b) are given below. During winter SFB had higher concentrations of Si on most days, except during two (2) measurement periods (daytime and night-time) were the concentrations were approximately the same (29- and 30 July). There were three (3) samples were the Si concentrations were higher in NSFB than in SFB, these included one (1) daytime sample (28 July) and two (2) night-time samples (30 July and 12 August). The increased Si concentration during the night of 30 July in NSFB, this corresponds to the higher Mg level in NSFB described previously. In NSFB between 28 July and 1 August the night-time Si concentrations are higher than daytime levels, however, this trends is reversed from 3- to 13 August (with the exception of 5- and 10 August). The final two days (15- and 16 August) also show higher night-time Si concentrations. The Si mass concentrations in SFB shows similar variations with most night-time periods having higher Si levels than days, except for (31 July, 3- , 4-, 6, 12-, and 13 August). It is important to note that there is less variation between day- and night-time Si in SFB than in NSFB. The associated enrichment factors are for most part below one. The NSFB house showed enrichment of Si on two (2) daytime sample (12- and 14 August). The SFB household had no indication of any Si enrichment.

During summer NSFB Si concentration ranged from <0.1 to 10 µg m^{-3} while SFB ranged up to 100 µg m^{-3}. In NSFB between 3- and 8 November the daytime Si concentrations are higher than night-time levels, however, this trends is reversed from 10- to 19 November (with the exception of 16- and 17 November). The Si mass concentrations in SFB shows similar trends to NSFB. It is important to note that there is less variation between day- and night-time Si in SFB than in NSFB. The associated enrichment factors are for most part below one except for the SFB house that showed enrichment of Si for a single daytime sampling period (11 November). The NSFB household had no indication of any Si enrichment.

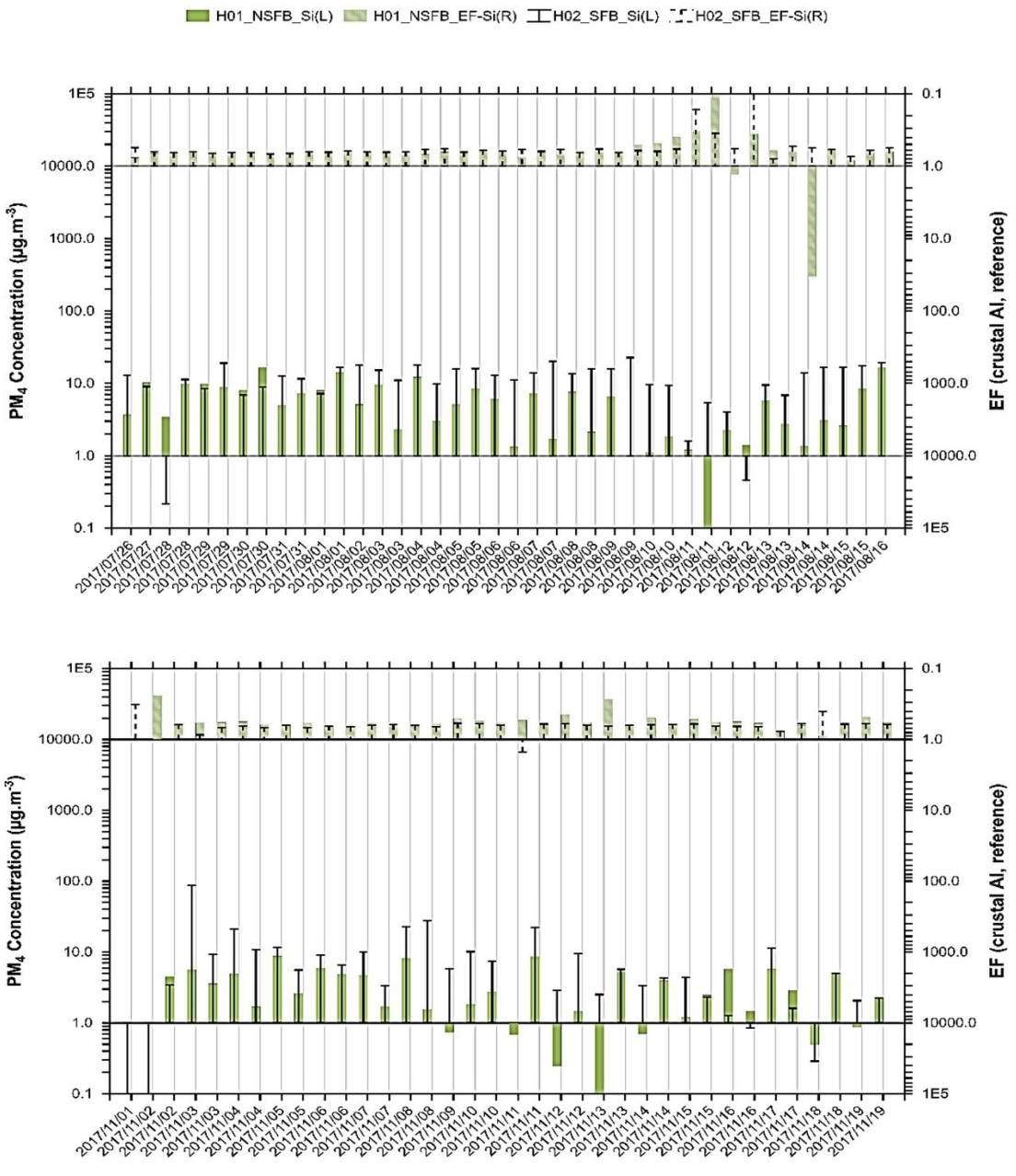

Figure 4-19. Time-series of the detected Si element concentrations (µg m^{-3}) (left y-and bottom x-axis) and the associated enrichment factors (right y- and top x-axis) at NSFB and SFB in KwaZamokuhle during winter and summer 2017.

Calcium (Ca) has similar origins as Mg, Al, and Si discussed above. Calcium was detected in both NSFB and SFB households. The mean daytime (*winter:* 1.161±0.781 µg m^{-3}; *summer:* 0.483±0.364 µg m^{-3}) and night-time (*winter:* 1.169±1.080 µg m^{-3}; *summer:* 0.646±0.425 µg m^{-3}) concentration in NSFB were lower

than that of the SFB during both daytime (*winter:* 4.733±1.844 µg m^{-3}; *summer:* 5.039±11.825 µg m^{-3}) and night-time (*winter:* 7.605±5.927 µg m^{-3}; *summer:* 2.505±3.148 µg m^{-3}) periods (Table 4-6).

A time series of Ca concentration and the associated enrichment factors, for both NSFB and SFB, for winter (Figure 4-20 a) and summer (Figure 4-20 b) are given below. During winter SFB had higher concentrations for Ca on all days, with the associated EFs above one in most cases while others are close to unity, compared to NSFB. The day- and night-time concentration variation in the SFB household shows less variability on the same day than the NSFB household. The EFs for NSFB is below one rom 26 July to 8 August, after which the EFs are at unity or above one. Calcium has the highest enrichment on 9 August in NSFB during the night.

The Ca concentration during summer in NSFB are almost always <1 µg m^{-3} except for three (3) days where it is just <1 µg m^{-3}. Between 2- and 12 November Ca in SFB were high compared to NSFB. After the previously mentioned dates the variability in the Ca concentrations in SFB is more erratic. The associated enrichment factors are for most part above one in NSFB, however, it is noticeable that at lower Ca concentrations there is a lower Ca EF indicating depletion.

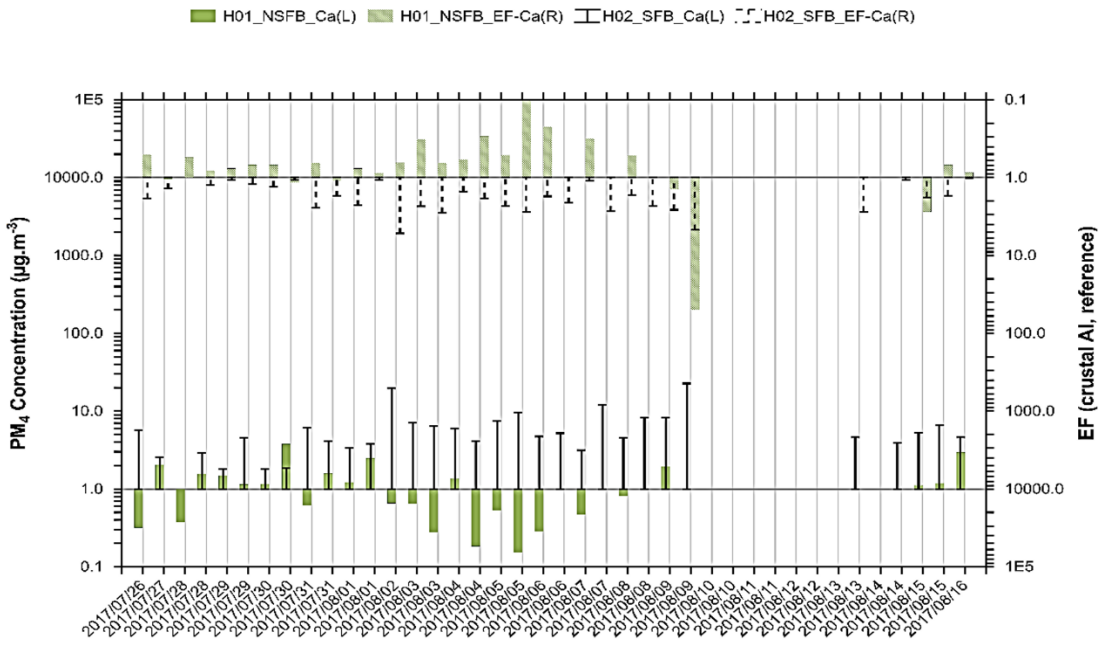

a.)

b.)

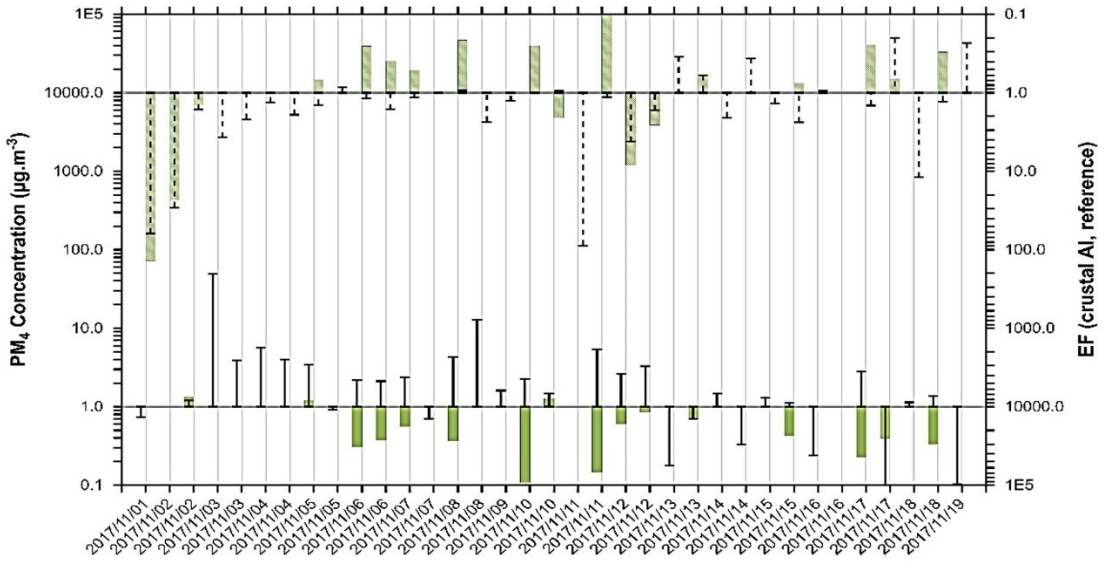

Figure 4-20. Time-series of the detected Ca element concentrations (µg m^{-3}) (left y-and bottom x-axis) and the associated enrichment factors (right y- and top x-axis) at NSFB and SFB in KwaZamokuhle during winter and summer 2017.

Iron (Fe) was detected in both NSFB and SFB households. The mean daytime (*winter:* 1.151±0.493 µg m^{-3}; *summer:* 0.589±0.561 µg m^{-3}) and night-time (*winter:* 0.836±0.616 µg m^{-3}; *summer:* 0.526±0.315 µg m^{-3}) concentration in NSFB were lower than that of the SFB during both daytime (*winter:* 2.103±0.635 µg m^{-3}; *summer:* 1.637±2.315 µg m^{-3}) and night-time (*winter:* 1.428±0.449 µg m^{-3}; *summer:* 1.049±1.072 µg m^{-3}) periods (Table 4-6).

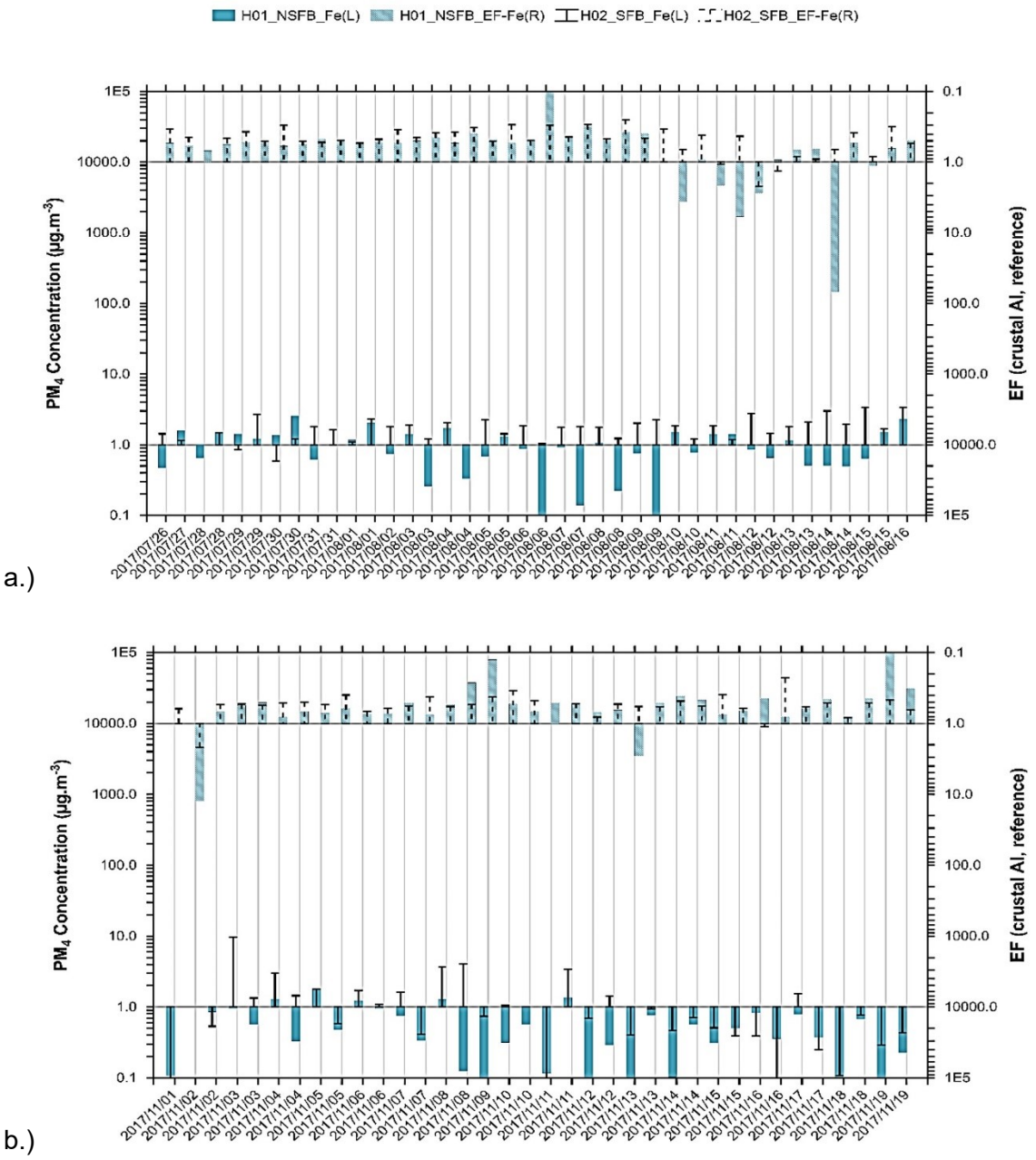

Figure 4-21. Time-series of the detected Fe element concentrations (µg m^{-3}) (left y-and bottom x-axis) and the associated enrichment factors (right y- and top x-axis) at NSFB and SFB in KwaZamokuhle during winter and summer 2017.

4.3.2.1. Coal and biomass combustion

Sulphur (S) was detected in both NSFB and SFB households. The mean daytime (*winter:* 1.852±1.046 µg m^{-3}; *summer:* 0.632±0.677 µg m^{-3}) and night-time (*winter:*

1.920±0.983 µg m^{-3}; *summer:* 0.918±0.881 µg m^{-3}) concentration in NSFB were lower than that of the SFB during both daytime (*winter:* 3.384±1.136 µg m^{-3}; *summer:* 1.238±0.723 µg m^{-3}) and night-time (*winter:* 2.638±1.040 µg m^{-3}; *summer:* 1.313±0.917 µg m^{-3}) periods (Table 4-6).

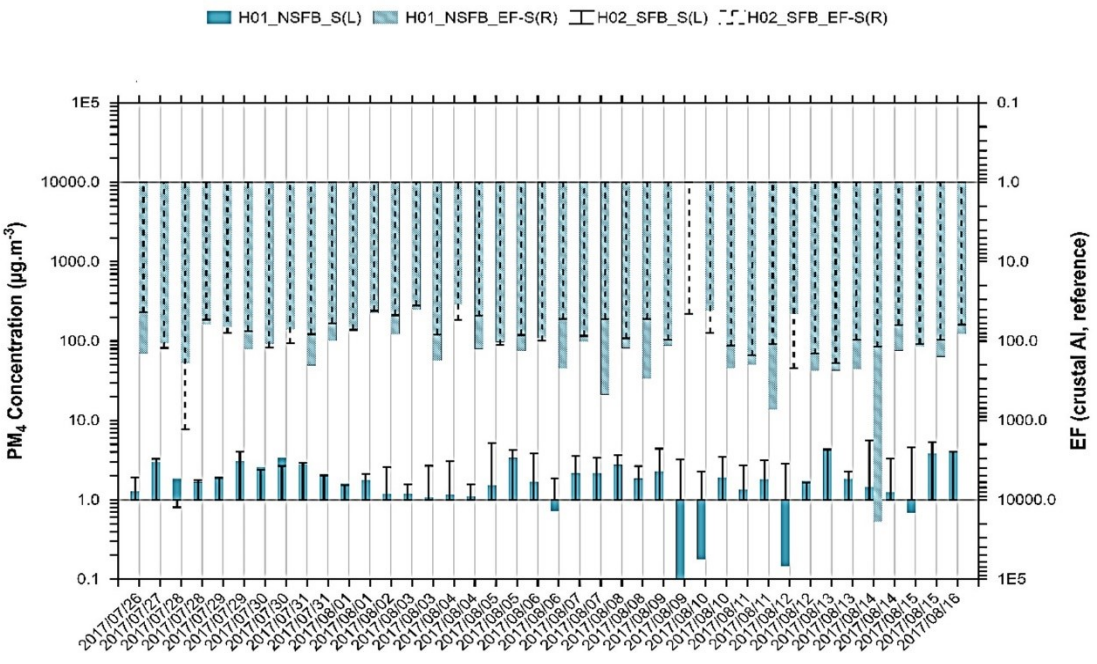

a.)

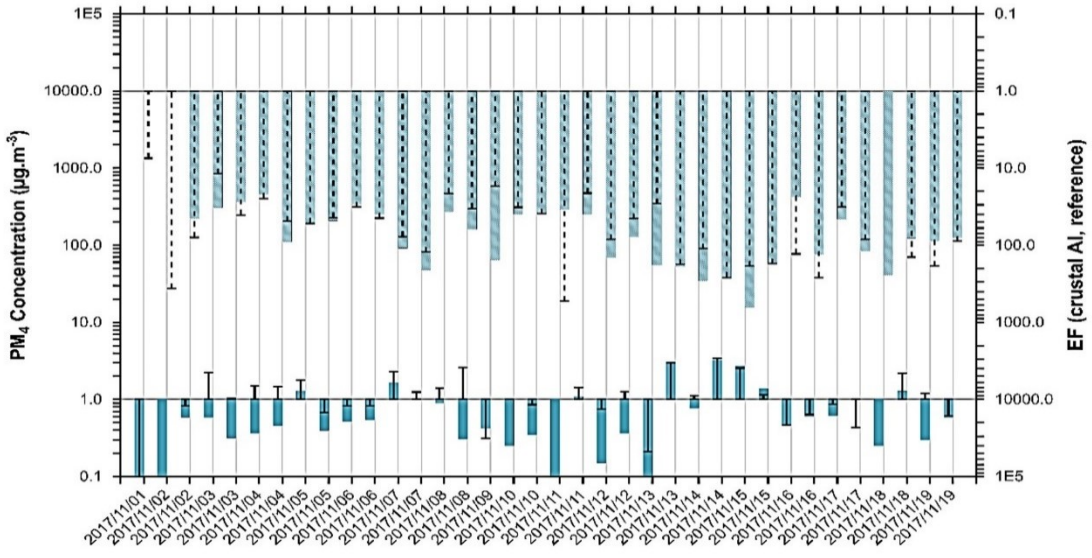

b.)

Figure 4-22. Time-series of the detected S element concentrations (µg m^{-3}) (left y-and bottom x-axis) and the associated enrichment factors (right y- and top x-axis) at NSFB and SFB in KwaZamokuhle during winter and summer 2017.

4.3.2.2. Other Sources

Lead (Pb) was detected in both NSFB and SFB households. The mean daytime (*winter:* 0.239±0.132 µg m^{-3}; *summer:* 7.114±0.787 µg m^{-3}) and night-time (*winter:* 0.223±0.162 µg m^{-3}; *summer:* 6.547±1.736 µg m^{-3}) concentration in NSFB were similar than that of the SFB during both daytime (*winter:* 0.203±0.122 µg m^{-3}; *summer:* 6.957±0.709 µg m^{-3}) and night-time (*winter:* 0.206±0.152 µg m^{-3}; *summer:* 6.249±1.699 µg m^{-3}) periods (Table 4-6).

a.)

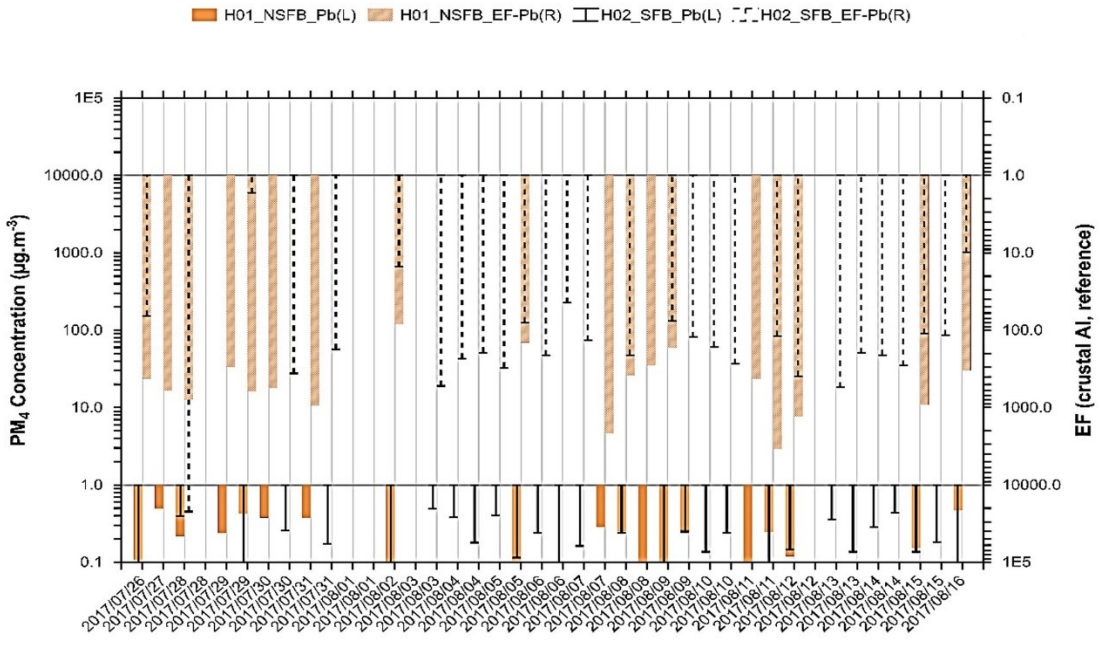

b.)

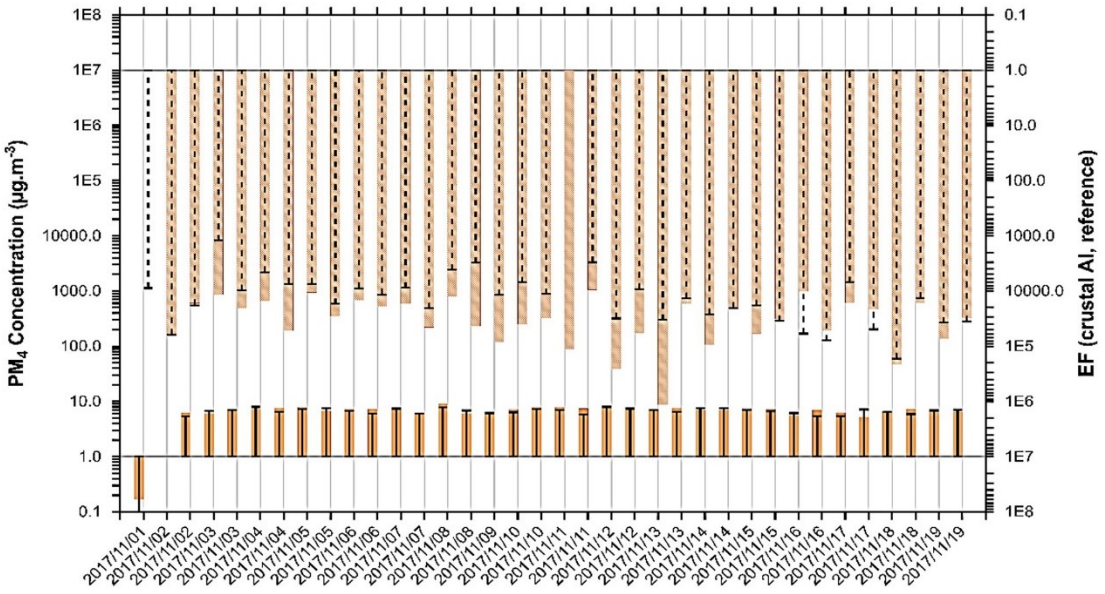

Figure 4-23. Time-series of the detected Pb element concentrations (µg m^{-3}) (left y-and bottom x-axis) and the associated enrichment factors (right y- and top x-axis) at NSFB and SFB in KwaZamokuhle during winter and summer 2017.

Table 4-6. Mean atmospheric concentrations and standard deviation in µg m^{-3} of selected elements and PM_4 as measured in in NSFB and SFB during summer and winter 2017 in KwaZamokuhle.

Variable	Time of Day	NSFB								SFB							
		Winter				Summer				Winter				Summer			
		Valid N	Mean	±SD	Median	Valid N	Mean	±SD.	Median	Valid N	Mean	±SD	Median	Valid N	Mean	±SD	Median
PM 4	Night	20	70	70	39	18	51	18	52	20	103	99	55	18	65	25	68
	Day	20	79.394	81.657	41.488	18	71.335	24.255	67.720	20	149.495	98.903	125.378	18	72.156	73.261	59.676
Na	Night	19	2.793	2.373	1.726	17	2.452	1.049	2.571	19	2.955	1.262	2.963	17	2.537	2.173	2.393
	Day	20	3.404	2.675	3.050	17	1.729	1.500	1.152	19	3.662	1.560	3.595	16	3.257	4.517	1.463
Mg	Night	14	0.687	0.427	0.561	17	0.697	0.136	0.689	15	1.305	0.630	1.226	17	0.983	0.601	0.835
	Day	13	0.813	0.212	0.806	16	0.656	0.281	0.509	16	1.206	0.471	1.297	17	1.489	2.286	0.773
Al	Night	19	2.357	1.843	1.412	17	1.602	0.907	1.334	20	5.764	2.802	5.332	18	3.237	3.274	2.400
	Day	20	3.007	1.983	3.014	17	1.600	1.383	0.973	20	6.047	2.106	6.310	16	5.229	7.147	3.472
Si	Night	19	5.173	4.301	3.079	17	3.327	1.885	2.764	20	11.458	6.116	11.035	18	7.113	7.243	5.301
	Day	20	6.717	4.310	6.401	17	3.323	2.995	1.819	20	12.806	4.697	13.753	17	12.073	20.464	5.743
P	Night	18	0.055	0.037	0.047	17	0.028	0.016	0.026	18	0.088	0.047	0.089	18	0.057	0.055	0.045
	Day	17	0.082	0.078	0.074	17	0.027	0.021	0.020	19	0.104	0.054	0.105	16	0.089	0.103	0.055
S	Night	20	1.920	0.983	1.822	18	0.918	0.881	0.589	20	2.638	1.040	2.611	18	1.313	0.917	1.091
	Day	20	1.852	1.046	1.736	18	0.632	0.677	0.440	20	3.384	1.136	3.426	15	1.238	0.723	1.115

Cl	Night	15	1.020	0.538	0.925	0	-	-	-	16	0.740	0.372	0.648	6	0.245	0.410	0.104
	Day	14	1.223	0.742	1.072	1	0.100	-	0.100	15	1.150	0.377	1.165	7	0.522	0.899	0.087
K	Night	17	1.066	0.730	0.961	17	0.687	0.300	0.654	17	1.426	0.662	1.440	18	0.916	0.640	0.808
	Day	16	1.135	0.460	1.224	18	0.554	0.406	0.417	16	2.489	1.139	2.599	18	1.375	2.330	0.721
Ca	Night	11	1.169	1.080	1.141	9	0.646	0.425	0.421	16	7.605	5.927	5.885	16	2.505	3.148	1.287
	Day	15	1.161	0.781	1.109	7	0.483	0.364	0.368	15	4.733	1.844	4.572	16	5.039	11.825	2.203
Ti	Night	17	0.139	0.089	0.123	18	0.395	0.118	0.429	19	0.332	0.124	0.321	17	0.507	0.209	0.457
	Day	19	0.174	0.085	0.159	18	0.422	0.138	0.405	20	0.322	0.107	0.291	17	0.615	0.445	0.503
V	Night	10	0.032	0.025	0.025	9	0.034	0.021	0.030	15	0.049	0.023	0.052	9	0.034	0.037	0.025
	Day	13	0.029	0.025	0.026	9	0.020	0.013	0.020	14	0.040	0.033	0.034	10	0.033	0.031	0.031
Cr	Night	7	0.030	0.017	0.040	1	0.019	-	0.019	12	0.037	0.017	0.040	2	0.018	0.014	0.018
	Day	12	0.028	0.019	0.027	1	0.003	-	0.003	13	0.072	0.145	0.019	3	0.019	0.005	0.019
Mn	Night	17	0.043	0.033	0.042	15	0.039	0.028	0.037	16	0.039	0.022	0.043	13	0.084	0.046	0.074
	Day	18	0.047	0.022	0.044	12	0.093	0.048	0.095	19	0.059	0.036	0.057	18	0.090	0.069	0.074
Fe	Night	20	0.836	0.661	0.701	18	0.526	0.315	0.494	19	1.428	0.449	1.424	18	1.049	1.072	0.737
	Day	20	1.151	0.493	1.110	17	0.589	0.561	0.317	20	2.103	0.635	1.887	17	1.637	2.315	0.742
Co	Night	4	0.016	0.016	0.011	4	0.015	0.014	0.012	5	0.001	0.000	0.001	4	0.013	0.014	0.009
	Day	10	0.016	0.015	0.012	12	0.040	0.034	0.025	7	0.010	0.010	0.007	8	0.032	0.029	0.021
Ni	Night	13	0.030	0.018	0.020	18	0.252	0.085	0.253	17	0.033	0.019	0.031	18	0.239	0.084	0.242
	Day	15	0.030	0.024	0.020	17	0.272	0.067	0.260	14	0.041	0.030	0.033	17	0.280	0.072	0.287
Cu	Night	8	0.043	0.029	0.043	17	0.933	0.101	0.925	11	0.026	0.021	0.024	18	0.870	0.224	0.921
	Day	10	0.022	0.018	0.013	18	0.898	0.244	0.949	11	0.023	0.018	0.013	17	0.929	0.095	0.937
Zn	Night	14	0.236	0.129	0.212	17	0.477	0.164	0.500	20	0.344	0.165	0.357	17	0.669	0.305	0.605

	Day	19	0.197	0.174	0.157	17	0.523	0.235	0.552	20	0.512	0.193	0.558	18	0.888	0.818	0.733
Pb	Night	9	0.223	0.162	0.244	18	6.547	1.736	6.911	13	0.206	0.152	0.180	18	6.249	1.699	6.591
	Day	10	0.239	0.132	0.231	17	7.114	0.787	7.181	15	0.203	0.122	0.174	17	6.957	0.709	7.003

4.3.2.3. Day-to-night ratios

Samples were collected for 12hour periods from 10h00 in the morning to 22h00 at night. The mean day-to-night (D/N) ratios have been used to evaluate if sources changed or were consistent during the daytime and night-time samples collected during summer and winter at NSFB and SFB monitoring sites in KwaZamokuhle. The D/N ratios of the mean concentrations for each element and PM is the respirable size fractions are given in Figure 4-24 a and b, respectively.

In NSFB (Figure 4-24 a), the D/N ratio for the aerosol mass was about 1.1 and 1.4 during winter and summer respectively. This indicates that the particulate loading was higher during the day for both seasons (also shown in Figure 4-15). In winter ratios are lower than one was observed for V, Cr, Cu, and Zn which indicates higher concentrations at night for these elements. In summer V, Cr, and Cu remained elevated at night. The dust elements (Mg, Al, Si, K) were above one during winter indicating prominence during the day, whereas during the summer these elements are close to unity.

In SFB (Figure 4-24 b), the D/N ratio for the aerosol mass was about 1.5 and 1.1 during winter and summer respectively. This indicates that the particulate loading was higher during the day for both seasons (also shown in Figure 4-15). In winter ratios are lower than one was observed for Mg, Ca, V, and Cu which indicates higher concentrations at night for these elements. In summer only V remained elevated at night. The dust elements (Al, Si, K) were above one during winter and summer indicating prominence during the day.

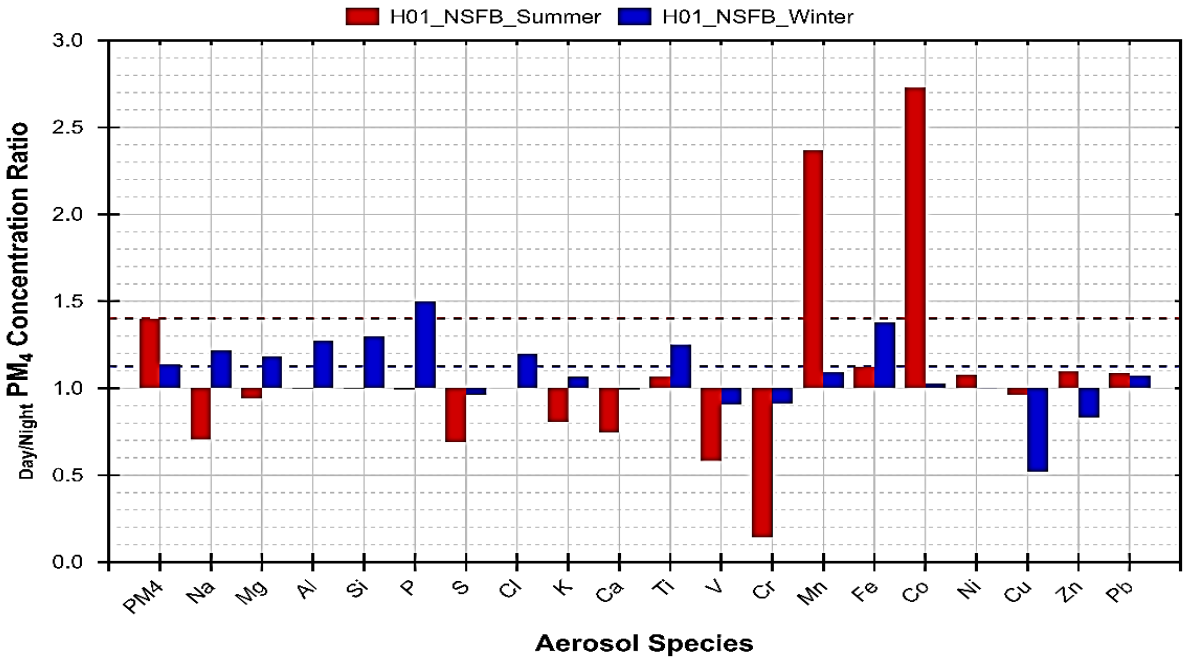

a.)

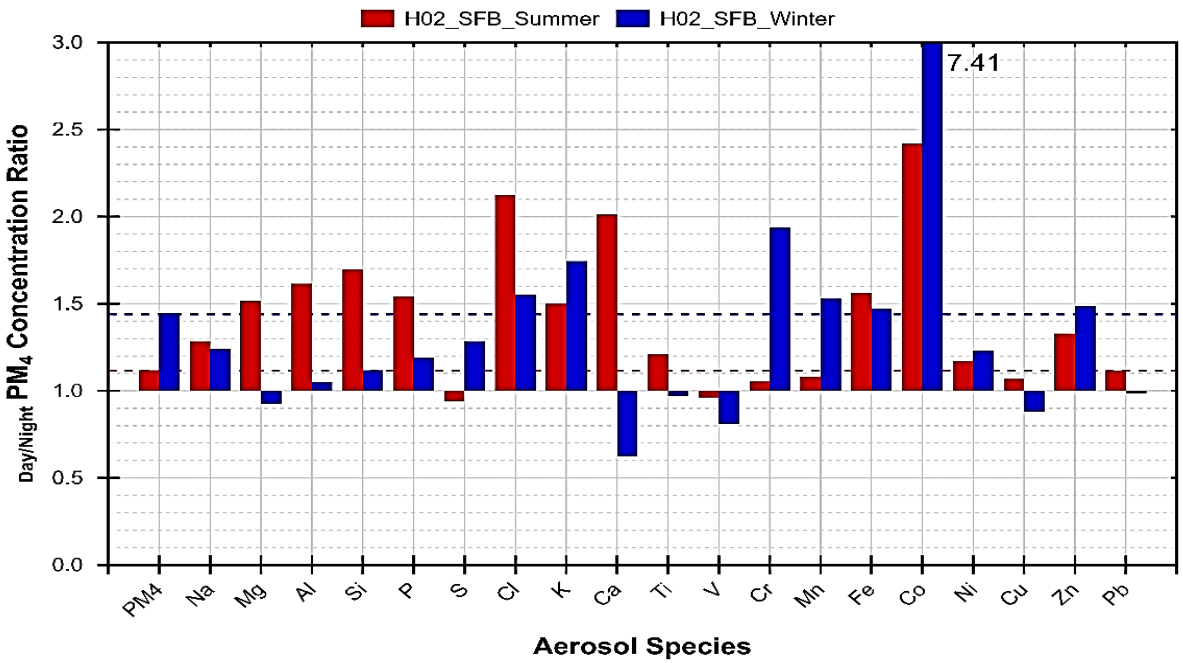

b.)

Figure 4-24. Ratio of mean atmospheric concentration for day-to-night for aerosol species and PM_4 measured at a.) NSFB and b.) SFB during winter and summer 2017 in KwaZamokuhle. The dashed lines indicate the change of the median aerosol mass.

4.3.2.4. Summer-to-winter ratios

The mean summer-to-winter (S/W) ratios have been used to evaluate if sources changed or were consistent during summer and winter, collected during daytime and night-time, at NSFB and SFB monitoring sites in KwaZamokuhle. The S/W ratios of the mean concentrations for each element and PM in the respirable size fractions are given in Figure 4-24 a and b, respectively.

In NSFB the following elements are most prominent during the winter: Na, Mg, Al, Si, P, S, Cl, K, Ca, V, Cr, and Fe in both day- and night-time. The following elements: Ti, Ni, Cu, Zn, and Pb are more prevalent during summer day- and night-time periods. Manganese (Mn) and Co are more complicated as during daytime it is more prominent during summer while at night it is close to unity.

In SFB the following elements are most prominent during the winter: Na, Al, Si, P, S Cl, K, V, Cr, and Fe in both day- and night-time. The following elements: Ti, Mn, Co, Ni, Cu, Zn, and Pb are more prevalent during summer day- and night-time periods. Magnesium (Mg) and Ca are more complicated as during the night-time it is more prominent during winter while at daytime it is close to unity.

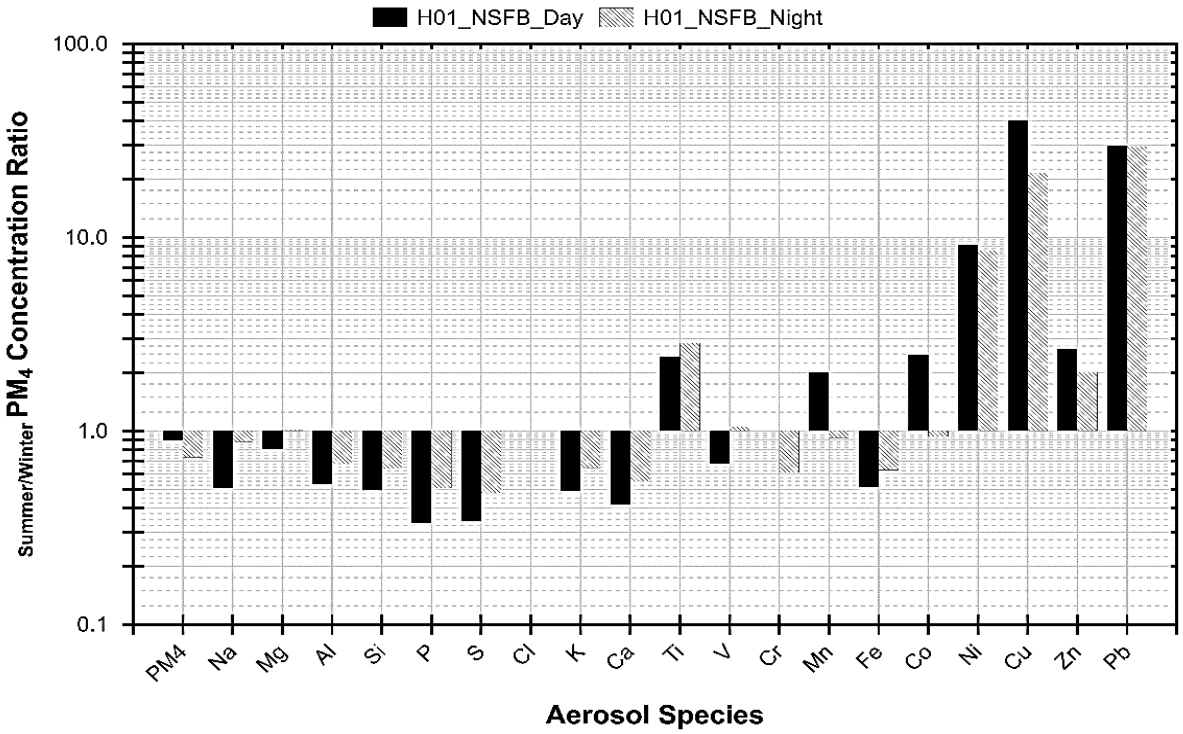

a.)

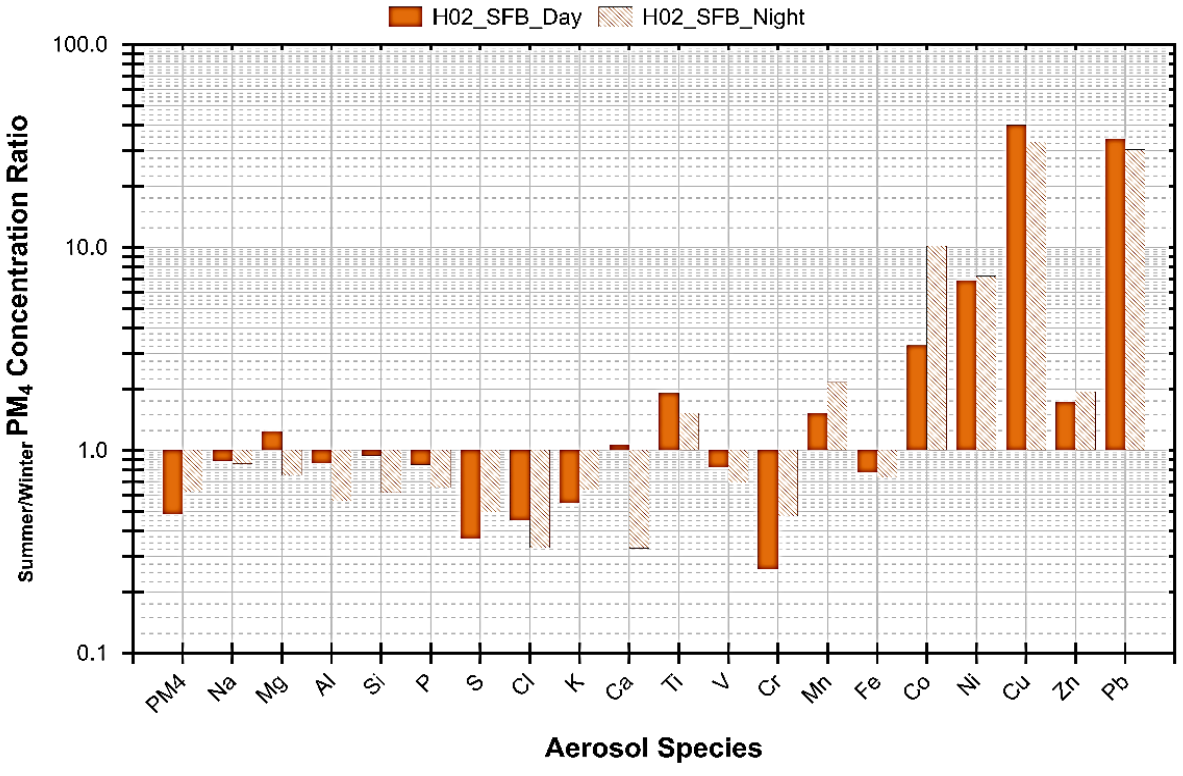

b.)

Figure 4-25. Ratio of the mean summer-to-winter respirable fraction particulate aerosol mass concentration during daytime and nigh-time 2017 for a.) NSFB and b.) SFB in KwaZamokuhle.

4.3.2.5. Enrichment Factors

Median enrichment factors (EFs) for each element in the respirable size fractions collected during winter and summer at NSFB and SFB collected in KwaZamokuhle, calculated relative to Mason's average crustal rock composition with Al as reference element is shown in Figure 4-26 and Figure 4-27, respectively. The elements displaying EFs close to one are mainly attributable to crustal material that is re-suspended and dispersed by natural or anthropogenic activities. Previous studies have indicated that vehicle exhaust is generally dominated by mainly elemental carbon, however, elements such as Cu, Zn, Pb, and Mn which are used as markers for this emission source.

In the non-solid fuel burning house (NSFB) the EFs for the day are given in Figure 4-26 a and nights in Figure 4-26 b. During the winter daytime elements such as Mg, Si, P, K, Ca, Ti, Mn, and Fe are close to one, thus these elements are mainly attributable to crustal dust. Elements that show enrichment include Na, S, Cl, V, Cr, Co, Ni, Cu, Zn, and Pb. Night-time measurements gave similar EFs to that displayed during days.

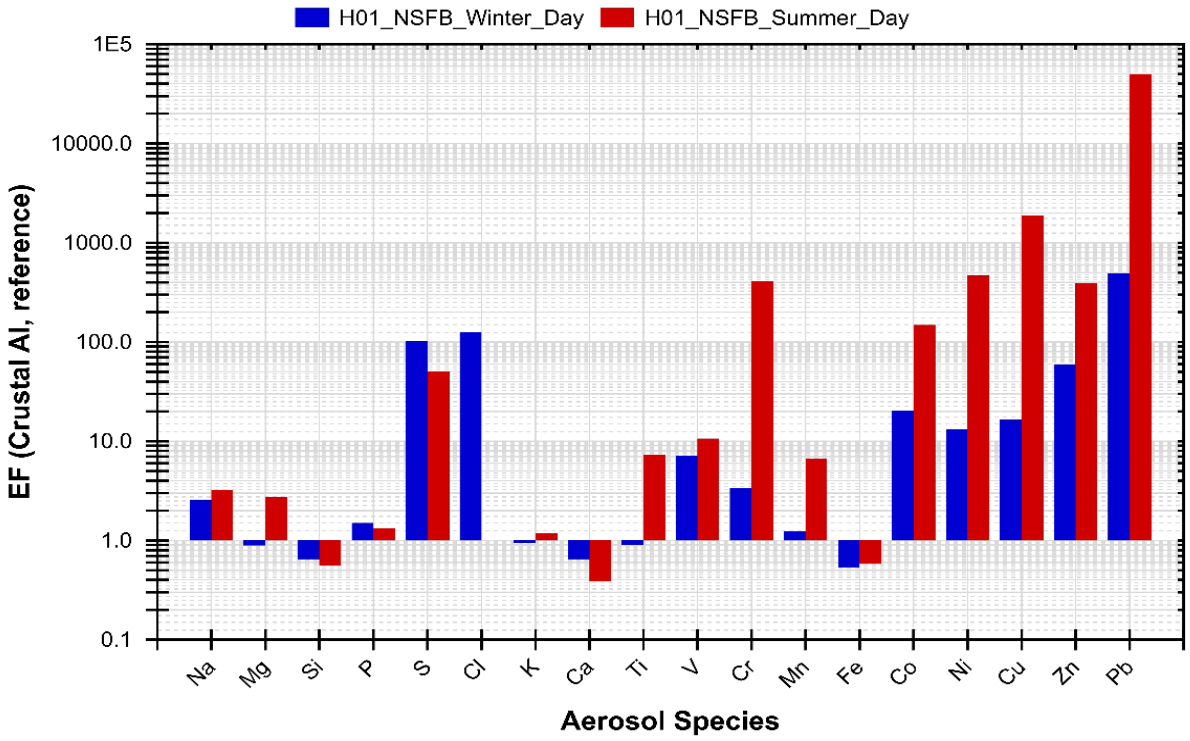

a.)

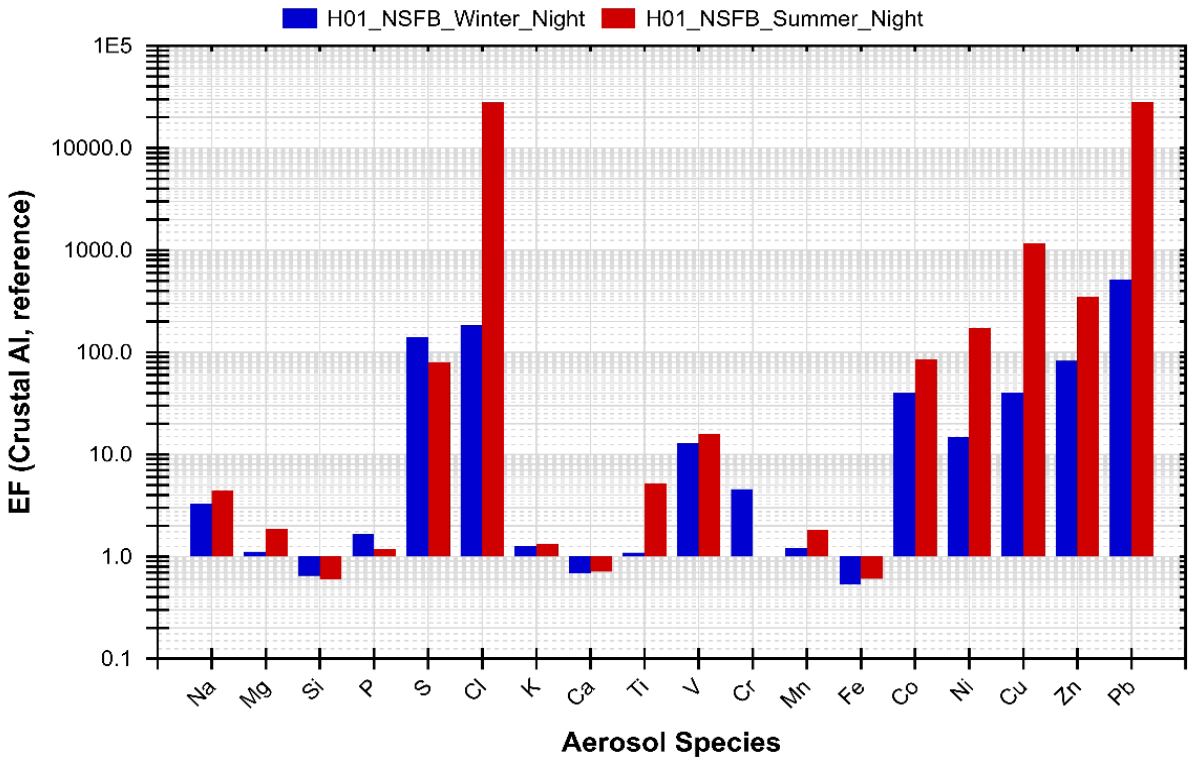

b.)

Figure 4-26. Median crustal enrichment factors (Al as reference element) for NSFB during a.) daytime and b.) nigh-time for the respirable particulate fraction in KwaZamokuhle during winter and summer 2017.

In the solid fuel burning house (SFB) the EFs for the day are given in Figure 4-27 a and nights in Figure 4-27 b. During the winter daytime elements such as Na, Mg, Si, P, K, Ca, Ti, Cr, Mn, and Fe are close to one, thus these elements are mainly attributable to crustal dust. Elements that show enrichment include S, Cl, V, Co, Ni, Cu, Zn, and Pb. Night-time measurements gave similar EFs to that displayed during days, however, the EFs are higher than winter EFs for all elements except for Si and Cl.

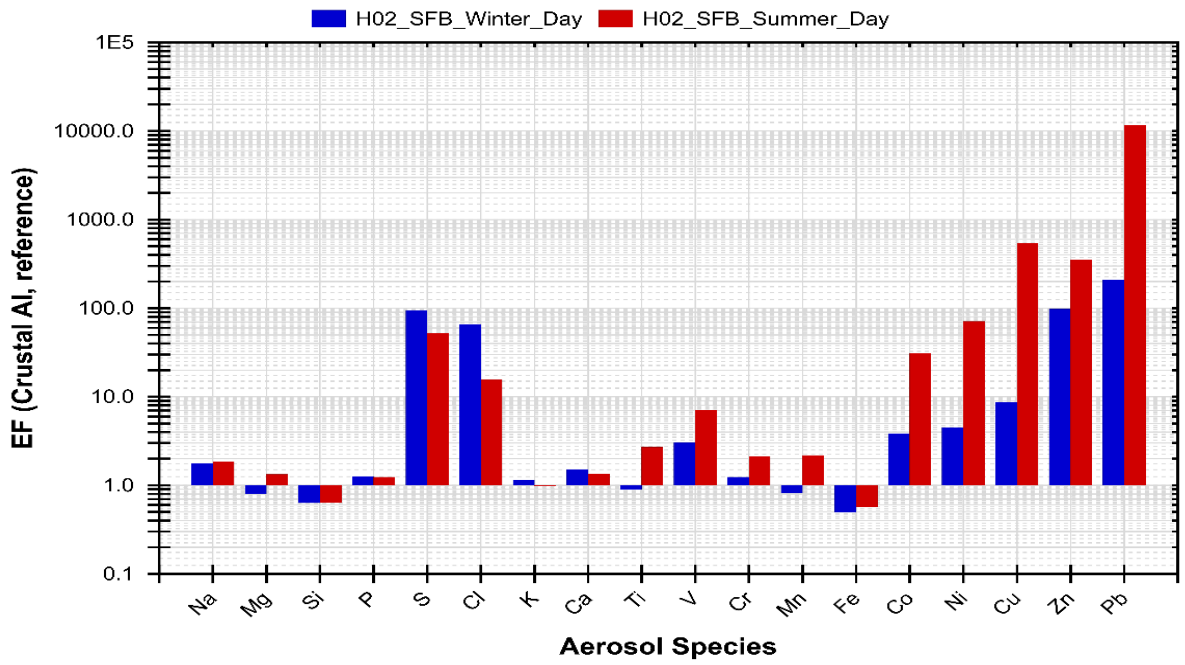

a.)

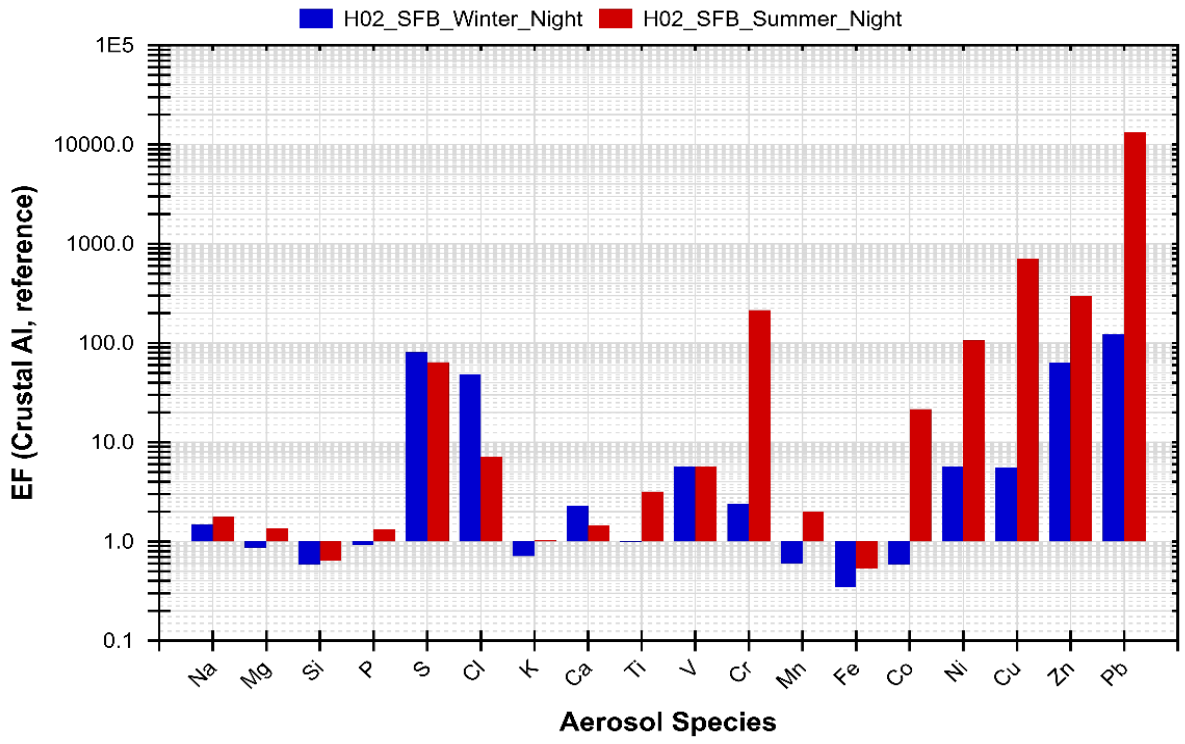

b.)

Figure 4-27. Median crustal enrichment factors (Al as reference element) for SFB during a.) daytime and b.) nigh-time for the respirable particulate fraction in KwaZamokuhle during winter and summer 2017.

CHAPTER 5 SUMMARY AND CONCLUSIONS

This chapter summarises the main findings of the study based all the parameters measured. The objectives of the study are addressed based on the findings and conclusions are drawn..

5.1 Particulate matter characterisation

The mean PM_4 mass concentration in the NSFB household was lower (40% in winter and 20% in summer respectively) than that measured in the SFB household. PM_4 mass concentrations were twice as high for the NSFB household and three times as high for the SFB household in winter compared to summer. In the household that did not practice any solid-fuel burning (NSFB), indoor PM_4 concentrations were observed to exceed the NAAQS $PM_{2.5}$ limit for more than 50% of the days sampled in winter. The daily summer indoor PM_4 concentrations in both dwellings were within the prescribed $PM_{2.5}$ guidelines for the majority (± 75%) of the days sampled. Contrary to what was expected, only 5 days out of the 28 days sampled in November 2017 had concentrations that were considered to be detrimental to health. While clear bimodal daily peaks in PM occurred in both NSFB and SFB houses in both winter and summer, the time exposed to higher PM concentration for NSFB house was shorter than that in the SFB house.

During the winter period, outdoor concentrations around the SFB household were a factor of two and three times higher than the $PM_{2.5}$ NAAQS at instruments SFB-S and SFB-E, respectively. Concentrations at the instrument SFB-N with the highest PM_4 values recorded means of 321 (± 214) (range: 940–80 µg m^{-3}) and 177 (± 206) (range: 927–21 µg m^{-3}) µg m^{-3} at both the SFB and the NSFB household, respectively. Although a bimodal diurnal PM_4 concentration pattern was shown to be typical outdoors, the pattern in the summer was found to be more variable – an additional peak was identified at around midday from at least two directions. This indicates a complex mix of impacting sources at the houses.

5.2 I/O relationship

For the SFB house, the indoor PM_4 concentration is about two and four times higher than the outdoor PM_4 concentration in summer and winter respectively. This is expected as burning of solid fuel indoors causes the PM_4 concentration to increase relative to the outdoor environment. In contrast, for the NSFB house, the indoor PM_4 concentration is two orders of magnitude higher

than the outdoor environment in the summer but not in the winter. During the winter, the influence of the majority (around 75%) of households in the broader KwaZamokuhle community makes the outdoor concentration higher than the indoor concentration for the NSFB house. In the summer, since less solid fuel is burnt, the outdoor concentration for the NSFB is lower than indoors. During the winter, the outdoor PM_4 concentration increases to a particularly high levels.: During the mornings (08h00 to 10h00) and afternoons (14h00 to 16h00) this level is about three times higher in the early evening (16h00) this level goes even higher when it increases by a factor of up to five times the outdoor level.

The maximum indoor temperature in the NSFB and SFB households was recorded in the kitchen area and at the stove. In both houses, the mean indoor temperature at all locations (bedroom, kitchen, living room and stove) were above the mean ambient temperature. The standard deviation in the temperature indicates a wider variation in the indoor temperature at the SFB than at the NSFB household. This can be explained by the fact that the indoor temperature in the SFB household depended only on burning periods while NSFB rely on electricity and so could maintain space-heating as long as they wish to. During the summer the average temperature in both houses are comparable (about 23 °C) and it is generally about 20 °C above the ambient temperature. The maximum indoor temperature is higher in the SFB house than the NSFB house and the minimum indoor temperature at SFB is lower than that of the NSFB house. The standard deviation showed that the temperature variation at SFB is twice that of the NSFB, implying that the insulation in the NSFB house regulates the indoor temperature. The variation in the indoor temperature in the SFB house is comparable to that of the ambient environment, while variation in the NSFB house is half that of the ambient environment. The use of a coal stove would better regulate the indoor temperatures in the SFB household, and would provide a constant supply of heat for a longer period of the day.

5.3 Indoor source identification

The mean winter PM_4 mass concentration in the non-solid fuel-burning household (NSFB) was 79 (±82) and 70 (±70) μg m^{-3} in the day-time and night-time, respectively. The PM_4 mass concentration in the solid fuel burning (SFB) household reach maximum loadings > 300 μg m^{-3} during both day- and night-time, with means of 149 (±99) and 103 (±99) μg m^{-3}, respectively. The mean PM_4 loading in the SFB household is ~80% and ~50% higher during the day- and night-time, respectively, when compared to the NSFB household. This also indicates that on average, during winter, the mean PM_4 loading was above the NAAQS 24-hour $PM_{2.5}$ standards for both NSFB and SFB. During summer, PM_4 mass concentration in the NSFB was < 150 μg m^{-3} during both the day- and night-time, with means of 71(±24) and 51 (±18) μg m^{-3}, respectively.

The PM_4 mass concentration in the SFB setting reach maximum loading of > 300 μg m^{-3} and < 100 μg m^{-3} during the day and night-time, with means of 72 (±73) and 65 (±25) μg m^{-3}, respectively. The mean PM_4 loading in the SFB house during the day was similar to that of the NSFB house, while the mean night-time PM_4 loadings in the SFB were ~30% higher compared to the NSFB setting. This also indicates that on average during summer, the mean PM_4 loadings were above the NAAQS 24-hour $PM_{2.5}$ standards for both the NSFB and SFB households.

The elemental composition of collected samples indicates that four source-categories are likely to impact on the indoor air quality, namely: dust (Mg, Al, Si, Fe and Ca); coal combustion (S and Cl); motor vehicle (Zn and Pb) emissions; and 'other sources' (u, Cr and CU). The 'other' category is largely linked to heavy metal elements. Dust elements (Mg, Al, Si, K) in the winter where highest in the day-time. During summer, there was no clear difference between the impact of dust during the day and night. In the SFB setting, particulate loading was higher during the day for both seasons. Day and night in both the NSFB and SFB houses, Na, Mg, Al, Si, P, S, Cl, K, Ca, V, Cr, and Fe were prominent in the winter. On the other hand, Ti, Ni, Cu, Zn, and Pb are more prevalent during summer, both in the day- and night-time. In both houses the EFs for Na, Mg, Si, P, K, Ca, Ti, Cr, Mn and Fe were close to one; these elements are thus mainly attributable to crustal dust. Elements that showed enrichment include S, Cl, V, Co, Ni, Cu, Zn, and Pb. Day-and night-time EFs were similar; however, the summer EFs were higher than winter EFs for all elements except for Si and Cl.

5.4 Limitations and Assumptions of the study

Kwazamokuhle is a densely populated area and the socio-economic aspects of the households varies significantly from one house to the next. Only two houses were selected for the purpose of this study, and a generalisation cannot be made to say that these two house types are the only types that exist throughout community. It can however be noted that a household that is well insulated seems to have lower concentrations of PM indoors and the temperature is maintained at a comfortable range (17-25 °C) in summer and winter. A household that has no insulation and practices solid-fuel burning was found to have elevated concentrations of PM indoors and the temperature dropped below 15 °C in summer and winter. The outdoor conditions are relatively similar around both houses due to solid fuel burning being practiced by the greater community. Another limitation of the study is that there are no standards for indoor monitoring of indoor pollutions therefore the ambient standards have been inferred on the indoor environment. Draft standards have been presented by the Department of Environmental affairs but have not yet been passed in law. The PM_4 size fraction does not appear in the

ambient standard but has been compared with the PM_{10} and $PM_{2.5}$ standards in this document as it also has implications for human health.

REFERENCES

Adgate, J. L., Ramachandran, G., Pratt, G. C., Waller, L. A. and Sexton, K. 2002. Spatial and temporal variability in outdoor, indoor, and personal $PM_{2.5}$ exposures. *Atmospheric environment*, 36:3255–3265.

Alastair, G. and Mhlanga, R. 2013. Powering the future: Renewable energy roll-out in South Africa. Greenpeace. AGAMA Energy (Pty) Ltd, South Africa. p 24.

Alewu, B. and Nosiri, C., 2011. Pesticides and human health. In *Pesticides in the Modern World-Effects of Pesticides Exposure*. IntechOpen.

Aluko, O. and Noll, K.E., 2006. Deposition and suspension of large, airborne particles. *Aerosol Science and Technology*, *40*(7), pp.503–513.

Amponsah-Dacosta, F., 2015. Cost-effective strategies for dust control in an opencast coal mine (Doctoral dissertation).

Anderson, J.O., Thundiyil, J.G. and Stolbach, A. 2012. Clearing the air: a review of the effects of particulate matter air pollution on human health. *Journal of medical toxicology*, 8(2):166–175.

Anderson, M.J., Miller, S.L. and Milford J.B. 2001 Source apportionment of exposure to toxic volatile organic compounds using positive matrix factorization. Journal of Exposure Analysis and Environmental Epidemiology 11, 295-307.

Andreae, M., Annegarn, H., Barrie, L., Feichter, J., Hegg, D., Jayaraman, A., Leaitch, R., Murphy, D., Nganga, J. and Pitari, G., 2001. Aerosols, their direct and indirect effects. *IPCC, Climate Change*, pp.295–306.

Annegarn, H.J., Grant, M.R., Kneen, M.S. and Scorgie, Y. 1998: Direct source apportionment of particulate pollution within a township, Draft final programme, Low smoke coal programme, Department of Minerals and Energy, South Africa.

Arkouli, M., Ulke, A.G., Endlicher, W., Baumbach, G., Schultz, E., Vogt, U., Müller, M., Dawidowski, L., Faggi, A., Wolf-Benning, U. and Scheffknecht, G., 2010. Distribution and temporal behavior of particulate matter over the urban area of Buenos Aires. *Atmospheric pollution research*, *1*(1::.1–8.

Arslan, S. and Aybek, A., 2012. Particulate matter exposure in agriculture. In *Air Pollution-A Comprehensive Perspective*. IntechOpen.

Arunrat, N., Pumijumnong, N. and Sereenonchai, S., 2018. Air-pollutant emissions from agricultural burning in Mae Chaem Basin, Chiang Mai province, Thailand. *Atmosphere*, *9*(4):145.

Atique, L., Mahmood, I. and Atique, F., 2014. Disturbances in atmospheric radiative balance due to anthropogenic activities and its implications for climate change. *System*, *6*:.2.

Balakrishnan, K., Ramaswamy, P., Sambandam, S., Thangavel, G., Ghosh, S., Johnson, P., Mukhopadhyay, K., Venugopal, V. and Thanasekaraan, V., 2011. Air pollution from household solid fuel combustion in India: an overview of exposure and health related information to inform health research priorities. *Global health ction*, *4*(1):5638.

Balmer, M. 2007. Household coal use in an urban township in South Africa. *Journal of energy in southern Africa*, 18(3):27–32.

Barnes, B., Mathee, A., Thomas, E. and Bruce, N. 2009. Household energy, indoor air pollution and child respiratory health in South Africa. *Journal of energy in southern Africa*, 20(1):4–13.

Begum, B.A., Biswas, S.K. and Hopke, P.K. 2007. Source apportionment of air particulate matter by Chemical Mass Balance (CMB) and comparison with Positive Matrix Factorization (PMF) model. *Aerosol and air quality research*; 7(4):446–468.

Begum, B.A., Kim, E., Biswas, S.K. and Hopke, P.K. 2004. Investigation of sources of atmospheric aerosol at urban and semi-urban areas in Bangladesh. *Atmospheric environment*, 38:3025–3038.

Bruce, N., Perez-Padilla, R. and Albalak, R. 2000. Indoor air pollution in developing countries: a major environmental and public health challenge. *Bulletin of the World Health Organization,* 78(9):1078–1092.

Bruce, N., Rehfuess, E., Mehta, S., Hutton, G. & Smith, K. 2002. Indoor Air Pollution. (*In* Jamison, D.T., Breman, J.G., Measham, A.R., Alleyne, G., Claeson, M., Evans, D.B., Jha, P., Mills, A. & Musgrove, P., *eds*. Disease Control Priorities in Developing Countries. New York: Oxford University Press. p. 793-815).

Calloway, C.P., Li, S., Buchanan, J.W. and Stevens, R.K. 1989. A refinement of the potassium tracer method for residential wood smoke. *Atmospheric environmen*, *23*(1): 67–69.

Chaloulakou, A., Kassomenos, P., Spyrellis, N., Demokritou, P. and Koutrakis, P., 2003. Measurements of PM_{10} and $PM_{2.5}$ particle concentrations in Athens, Greece. *Atmospheric environment*, *37*(5):649–660.

Chen, C. and Zhao, B., 2011. Review of relationship between indoor and outdoor particles: I/O ratio, infiltration factor and penetration factor. *Atmospheric environment*, *45*(2), pp.275–288.

Chen, H., Wang, H., Sun, J., Xu, Y. and Yin, Z., 2018. Anthropogenic fine particulate matter pollution will be exacerbated in eastern China due to 21st century GHG warming. *Atmospheric chemistry and physics*, *19*(1):233–243.

Chow, J.C., 1995. Measurement methods to determine compliance with ambient air quality standards for suspended particles. *Journal of the Air and Waste Management Association*, *45*(5):320–382.

Cohen, A.J., Brauer, M., Burnett, R., Anderson, H.R., Frostad, J., Estep, K., Balakrishnan, K., Brunekreef, B., Dandona, L., Dandona, R. and Feigin, V., 2017. Estimates and 25-year trends of the global burden of disease attributable to ambient air pollution: an analysis of data from the Global Burden of Diseases Study 2015. *The lancet*:389(10082):1907–1918.

Contini, D., Cesari, D., Conte, M. and Donateo, A., 2016. Application of PMF and CMB receptor models for the evaluation of the contribution of a large coal-fired power plant to PM_{10} concentrations. *Science of the total Rnvironment*, *560*:131–140.

Cosijn, C. and Tyson, P.D., 1996. Stable discontinuities in the atmosphere over South Africa (Doctoral dissertation, University of the Witwatersrand).

Davidson, C.I., Phalen, R.F. and Solomon, P.A., 2005. Airborne particulate matter and human health: a review. *Aerosol science and technology*, *39*(8):737–749.

Desai, M.A., Mehta, S., Smith, K.R. and World Health Organization, 2004. Indoor smoke from solid fuels: assessing the environmental burden of disease at national and local levels.

Dimitroulopoulou, C., Ashmore, M.R., Hill, M.T.R., Byrne, M.A. and Kinnersley, R., 2006. INDAIR: A probabilistic model of indoor air pollution in UK homes. *Atmospheric Environment*, *40*(33):6362–6379.

Dominici, F., Wang, Y., Correia, A.W., Ezzati, M., Pope III, C.A. and Dockery, D.W., 2015. Chemical composition of fine particulate matter and life expectancy: in 95 US counties between 2002 and 2007. *Epidemiology (Cambridge, Mass.)*, *26*(4):556.

Engelbrecht, J. P., Swanepoel, L., Zunckel, M., Chow, J. C., Watson, J. G. and Egami, R. T. 2000. Modelling PM 10 aerosol data from the Qalabotjha low-smoke fuels macro-scale experiment in South Africa. *Ecological modelling*, 127:235–244

Engelbrecht, J.P., Swanepoel, L., Chow, J.C., Watson, J.G. and Egami, R.T. 2001: $PM_{2.5}$ and PM_{10} concentrations from the Qalabotjha low-smoke fuels macro-scale experiment in South Africa, *Environmental monitoring and assessment*, 69(1):1–15.

Engelbrecht, J.P., Swanepoel, L., Chow J.C., Watson, J.G. and Egami R.T. 2002: The comparison of source contributions from residential coal and low-smoke fuels, using CMB modelling, in South Africa, *Environmental science and policy*, 5(2):157–167.

Etyemezian, V., H. Kuhns, J. Gillies, J. Chow, K. Hendrickson, M. McGown, and M. Pitchford., 2003. Vehicle-based road dust emission measurement (III): effect of speed, traffic volume, location, and season on PM_{10} road dust emissions in the Treasure Valley, ID.*Atmospheric environment* 37(32): 4583–4593.

Feris, L.A., 2010. The role of good environmental governance in the sustainable development of South Africa. *Potchefstroom electronic law journal/Potchefstroomse elektroniese regsblad*, *13*(1):72–99.

Francioli, A., 2018. *Investigating energy usage among low income households and implications for fire risk* (Masters dissertation, Stellenbosch: Stellenbosch University).

Freiman, M.T. and Piketh, S.J., 2003. Air transport into and out of the industrial Highveld region of South Africa. *Journal of applied meteorology*, *42*(7):994–1002.

Freiman, M.T. and Tyson P.D., 2000. The thermodynamic structure of the atmosphere over South Africa: Implications for water vapour transport. *Water SA*, *26*(2):153–158.

Friedl, A., Holm, D., John, J., Kornelius, G., Pauw, C.J., Oosthuizen, R. and van Niekerk, A.S., 2008. Air pollution in dense, low-income settlements in South Africa. P*roceedings: National Association for Clean Air (NACA)*.

Friedlander, S.K., 1970. The characterization of aerosols distributed with respect to size and chemical composition. *Journal of aerosol science*, *1*(4):295–307.

Fritz, B.K., Hoffmann, W.C., Lan, Y., Thompson, S.J. and Huang, Y., 2008. Low-level atmospheric temperature inversions and atmospheric stability: characteristics and impacts on agricultural applications. *Agricultural engineering international: CIGR journal*.

Fung, K.Y., Luginaah, I.N. and Gorey, K.M., 2007. Impact of air pollution on hospital admissions in Southwestern Ontario, Canada: Generating hypotheses in sentinel high-exposure places. *Environmental health*, *6*(1):18.

Garstang, M., Tyson, P.D., Swap, R., Edwards, M., Kållberg, P. and Lindesay, J.A., 1996. Horizontal and vertical transport of air over southern Africa. *Journal of Ggophysical research: atmospheres*, *101*(D19):23721–23736.

Gatebe, C. K., Tyson, P. D., Annegarn, H., Piketh, S. and Helas, G. 1999. A seasonal air transport climatology for Kenya. *Journal of feophysical research,* 104(D12):4237–14244.

Giri, D., Murthy, V.K. and Adhikary, P.R. 2008. The Influence of Meteorological Conditions on PM 10 Concentrations in Kathmandu Valley. *International journal of rnvironmental research*, *2*(1-12):

Govender, T., Barnes, J.M. and Pieper, C.H., 2011. Contribution of water pollution from inadequate sanitation and housing quality to diarrheal disease in low-cost housing settlements of Cape Town, South Africa. *American journal of public health*, *101*(7):. e4–e9.

Grosjean, D. and Seinfeld, J.H., 1989. Parameterization of the formation potential of secondary organic aerosols. *Atmospheric environment, 3*(8):1733–1747.

Guo, H., Morawska, L., He, C., Zhang, Y.L., Ayoko, G. and Cao, M., 2010. Characterization of particle number concentrations and PM 2.5 in a school: Influence of outdoor air pollution on indoor air. *Environmental science and pollution research*, *17*(6):1268–1278.

Haller, L., Claiborn, C., Larson, T., Koenig, J., Norris, G. and Edgar, R., 1999. Airborne particulate matter size distributions in an arid urban area. *Journal of the Air and Waste Management Association*, *49*(2):161–168.

Hamanaka, R.B. and Mutlu, G.M., 2018. Particulate Matter Air Pollution: Effects on the Cardiovascular System. *Frontiers in endocrinology*, *9-15*:

Harrison, P., 1992. Urbanization: the policies and politics of informal settlement in South Africa: a historical perspective. *Africa insight*, *22*(1):14–22.

Harrison, R.M. and Yin, J., 2000. Particulate matter in the atmosphere: which particle properties are important for its effects on health? *Science of the total environment*, *249*(1-3):85–101.

Held, G., 1996. Air pollution and its impacts on South African Highveld. Environmental Scientific Association.

Hopke, P.K., Ito, K., Mar, T., Christensen, W. F., Eatough, D.J., Henry, R.C., Kim, E., Laden, F., Lall, R.,Larson, T., Liu, H., Neas, L., Pinto, J., Stölzel, M., Suh, H., Paatero, P. and Thurston, G.D. 2006 PM source apportionment and health effects: 1. Intercomparison of source apportionment results. *Journal of Exposure Science and Environmental Epidemiology;* 16, 275-286.

Hwang, I. and Hopke, P.K., 2007. Estimation of source apportionment and potential source locations of $PM_{2.5}$ at a west coastal IMPROVE site. *Atmospheric environment*, 41(3):506–518.

Ichoku, C., Remer, L.A., Kaufman, Y.J., Levy, R., Chu, D.A., Tanré, D. and Holben, B.N., 2003. MODIS observation of aerosols and estimation of aerosol radiative forcing over southern Africa during SAFARI 2000. *Journal of geophysical research: atmospheres*, 108(D13-14):

Ismail, Z. and Khembo, P., 2015. Determinants of energy poverty in South Africa. *Journal of energy in southern Africa*, *26*(3):66–78.

Javed, A.S. Wexler, G. Murtaza, H.R. Ahmad, S.M.A. Basra. 2015. Spatial, temporal and size distribution of particulate matter and its chemical constituents in Faisalabad, Pakistan *Atmósfera*, 28:99-116.

Jiang, X., Y. Liu, B. Yu and M. Jiang, 2010. Comparison of MISR aerosol optical thickness with AERONET measurements in Beijing metropolitan area. *Remote sensing environment*, 107:45–53.

Jimoda, L.A. 2012. Effects of particulate matter on human health, the ecosystem, climate and materials: A review. *Working and living environmental protection*, 9(1):27–44.

Jollife, I.T. 1986 Principal component analysis. New York: Springer.

Kampa, M. and Castanas, E. 2008. Human health effects of air pollution. *Environmental pollution*, *151*(2):362–367.

Kaonga, B. and Ebenso, E., 2011. An evaluation of atmospheric aerosols in Kanana, Klerksdorp gold mining town, in the North-West Province of South Africa. In *Air Quality Monitoring, Assessment and Management*. InTech.

Kelly, F.J. and Fussell, J.C., 2015. Air pollution and public health: emerging hazards and improved understanding of risk. E*nvironmental geochemistry and health*, 37(4), pp.631–649.

Kim, E., Larson, T.V., Hopke, P.K., Slaughter, C., Sheppard., L.E. and Claiborne, C. 2003. Source identification of $PM_{2.5}$ in an arid Northwest U.S. city by Positive Matrix Factorization. *Atmospheric research*. 66: 291–305.

Kirkinen, J., Hillebrand, K. and Savolainen, I., 2007. Climate impact of the use of peatland for energy—land use scenario. *Espoo: VTT Tiedotteita. Research Notes*, *2365*.

Kok, J.F., 2011. A scaling theory for the size distribution of emitted dust aerosols suggests climate models underestimate the size of the global dust cycle. *Proceedings of the National Academy of Sciences*, *108*(3):1016–1021.

Kuhns, H., Gillies, J., Etyemezian, V., Dubois, D., Ahonen, S., Nikolic, D. and Durham, C., 2005. Spatial variability of unpaved road dust PM_{10} emission factors near El Paso, Texas. *Journal of the Air and Waste Management Association*, *55*(1):3–12.

Künzli, N., 2012. Is air pollution of the 20th century a cause of current asthma hospitalisations?

Language. B., Piketh, S.J. and Burger, R.P., 2016. Correcting respirable photometric particulate measurements using a gravimetric sampling method. *Clean Air Journal= Tydskrif vir Skoon* Lug, 26(1), pp.10-14.

Laratta, C.R. and Van Eeden, S., 2014. Acute exacerbation of chronic obstructive pulmonary disease: cardiovascular links. *BioMed Research International*, *2014*.

Liddament, M.W. and Agence internationale de l'énergie. Air Infiltration, 1996. *A guide to energy efficient ventilation*. Coventry: Air Infiltration and Ventilation Centre.

Lodhi, A., Ghauri, B., Khan, M.R., Rahman, S. and Shafique, S., 2009. Particulate matter ($PM_{2.5}$) concentration and source apportionment in Lahore. *Journal of the Brazilian Chemical Society*, *20*(10):1811–1820.

Luhana, L., Sokhi, R., Warner, L., Mao, H., Boulter, P., McCrae, I., Wright, J. and Osborn, D., 2004. Characterisation of exhaust particulate emissions from road vehicles. FP5 Particulates Project.

Lv, Y., Wang, H., Wei, S., Zhang, L. and Zhao, Q., 2017. The Correlation between Indoor and Outdoor Particulate Matter of Different Building Types in Daqing, China. *Procedia engineering*, *205*:360–367.

Lydia, A.O. 2010. Characteristics of particulate matter over the South African industrialized Highveld. University of Witwatersrand, Johannesburg. (Master's thesis).

Maher, B.A. Prospero, J.M., Mackie, D., Gaiero, D., Hesse, P.P. and Balkanski, Y. 2010. Global connections between aeolian dust, climate and ocean biogeochemistry at the present day and at the last glacial maximum. *Earth-science reviews*, 99:61–97.

Makonese, T., Masekameni, D.M., Annegarn, H.J. and Forbes, P.B., 2017. Emission factors of domestic coal-burning braziers. *South African journal of science*, *113*(3-4):1–11.

Manahan, S., 2017. Environmental chemistry. *CRC press*.

Maricq, M.M., Chase, R.E., Xu, N. and Laing, P.M., 2002. The effects of the catalytic converter and fuel sulfur level on motor vehicle particulate matter emissions: Light duty diesel vehicles. *Environmental science and technology*, *36*(2):283–289.

Masekoameng, E. 2014. South African policy developments for improvement of ambient air quality: Air emissions licensing and pollution offsets. Presented at a CSIR conference. 14 Feb., Pretoria.

Matooane, M., John, J., Oosthuizen, R. and Binedell, M. 2004. Vulnerability of South African communities to air pollution. Presented at the 8th World Congress on Environmental Health, Durban, South Africa. ISBN: 0-9584663-7-8.

Mdluli, T., Piketh, S.J. and Igbafe A., 2005: Assessment of indoor respirable particulate matter (PM7) in township houses with coal-fired stoves at Kwaguqua (Witbank). *Journal of the National Electricity Regulator*.

Medina, M., 2010. Solid wastes, poverty and the environment in developing country cities: Challenges and opportunities (No. 2010, 23). Working paper//World Institute for Development Economics Research.

Milner, J.T., Dimitroulopoulou, C. and ApSimon, H.M., 2005. Indoor concentrations in buildings from sources outdoors. *ADMLC Annual Report*, *2005*.

Mkoma, S. L. and Mjemah, I. C. 2011. Influence of Meteorology on Ambient Air Quality in Morogoro, Tanzania. *International journal of environmental sciences*, 1(6):1107–1115.

Moja, S.J. and Mnisi, J.S., 2013. Seasonal variations in airborne heavy metals in Vanderbijlpark, South Africa. *Journal of environmental chemistry and ecotoxicology*, *5*(9):227–233.

Morawska, L., He, C., Hitchins, J., Gilbert, D. and Parappukkaran, S. 2001. The relationship between indoor and outdoor airborne particles in the residential environment. *Atmospheric eEnvironment*, 35(20):3463–3473.

Motsoene, K.A., 2014. Urbanization and poverty in Maseru: a comparative study of Sekamaneng, Motimposo and Thibella (Doctoral dissertation).

Muthige, M.S., 2014. Ambient air quality impacts of a coal-fired power station in Lephalale area (Doctoral dissertation).

Myhre, G., Shindell, D., Bréon, F.M., Collins, W., Fuglestvedt, J., Huang, J., Koch, D., Lamarque, J.F., Lee, D., Mendoza, B. and Nakajima, T., 2013. Anthropogenic and natural radiative forcing. *Climate change*, 423:658–740.

Naidoo, S., Piketh, S.J. and Curtis, C., 2014. Quantification of emissions generated from domestic burning activities from townships in Johannesburg. *Clean Air Journal= Tydskrif vir Skoon Lug*, *24*(1), pp.34-41.

Naidoo, S., Piketh, S.J. and Curtis, C. 2013. Quantification of emissions generated from domestic burning activities from townships in Johannesburg. Paper presented at the 16th IUAPPA world clean air congress, Cape Town, 3rd October.

Nguyen, H., Evans, A., Lucas, C., Smith, I. and Timbal, B., 2013. The Hadley circulation in reanalyses: Climatology, variability, and change. *Journal of climate*, *26*(10):3357–3376.

Ni, T., Han, B. and Bai, Z. 2012. Source apportionment of PM_{10} in four cities of north-eastern China. *Aerosol and air quality research*, 12: 571–582.

Nkomo, J.C. 2005a. Energy and economic development: challenges for South Africa. *Journal of energy in southern Africa*, 16):94–104.

Nkomo, J.C. 2005b. The impacts of efficient residential lighting in Matatiela, South Africa. *Journal of energy in southern Africa*, 16(3): 33–37.

Nkosi, L.F. 2015. An evaluation of the municipal solid waste management system within City of Tshwane Metropolitan Municipality, in Mamelodi East Township, Gauteng province South Africa (Masters dissertation, University of Pretoria).

Nkosi, N., Piketh, S. J., Burger, R. P. and Annegarn, H. J. 2017. Variability of domestic burning habits in the South African Highveld: A case study in the KwaDela Township. Paper presented at 2017 International Conference on the Domestic Use of Energy (DUE), Cape Town, 3 Apr 2017.

National Research Council, 2003. Air emissions from animal feeding operations: Current knowledge, future needs. *National Academies Press*.

Nuwarinda H. 2007. 'Air Pollution Study of a Highveld Township during a Basa Njengo Magogo Rollout', Unpublished Masters Dissertation. Johannesburg: University of Johannesburg.

Paatero, P., Hopke, P.K., Begum, B.A. and Biswas, S.K. 2005 A graphical diagnostic method for assessing the rotation in factor analytical models of atmospheric pollution. Atmospheric Environment 39, 193–201.

Parker, M.J. and Raman, S., 1993. A case study of the nocturnal boundary layer over a complex terrain. *Boundary-layer meteorology*, 66(3):303–324.

Pauw, C.J., Friedl, A., Holm, D., John, J., Kornelius, G., Oosthuizen, R. and Van Niekerk, A.S., 2008. Air Pollution in Dense, Low-income Settlements in South Africa: Issue 1. *Report to the Royal Danish Embassy and the Dept. of Environmental Affairs and Tourism*, *6*.

Pernegger, L. and Godehart, S., 2007. Townships in the South African geographic landscape–physical and social legacies and challenges. *South Africa, Training for Township Renewal Initiative*.

Piketh, S.J., Annegarn, H.J. and Tyson, P.D., 1999. Lower tropospheric aerosol loadings over South Africa: The relative contribution of aeolian dust, industrial emissions, and biomass burning. *Journal of geophysical research: atmospheres*, *104*(D1):1597–1607.

Piketh, S.J. and Walton, N.M., 2004. Characteristics of atmospheric transport of air pollution for Africa. In *Air Pollution* (pp. 173–195). Springer, Berlin, Heidelberg.

Piketh, S.J. and Burger, R. 2013. Ambient air quality monitoring in Kwadela township, Mpumalanga winter 2013. Paper presented at the 16th IUAPPA world clean air congress, Cape Town, 3rd October 2013

Piketh, S.J., Wernecke, B. and Burger, R., 2016. Household air pollution in South African low-income settlements: a case study. *WIT Transactions on ecology and the environment*, 207:227–236.

Pilinis, C., Pandis, S.N. and Seinfeld, J.H., 1995. Sensitivity of direct climate forcing by atmospheric aerosols to aerosol size and composition. *Journal of geophysical research: Atmospheres*, *100*(D9):18739–18754.

Pope, C.A., Dockery, D.W. and Schwartz, J., 1995. Review of epidemiological evidence of health effects of particulate air pollution. *Inhalation toxicology*, *7*(1):1–18.

Pretorius, I., Piketh, S., Burger, R. and Neomagus, H. 2015. A perspective on South African coal fired power station emissions. *Journal of energy in southern Africa*, *26*(3):27–40.

Qi, M., Lin, K., Li, X., Sammis, T.W., Miller, D.R. and Wang, J. 2015. Particulate matter contributions from agricultural tilling operations in an irrigated desert region. *PloS one*, *10*(9): e0138577.

Reff, A., Eberly, S.H. and Bhave, P.V. 2007 Receptor modeling of ambient particulate matter data using positive matrix factorization: review of existing methods. *Journal of Air and Waste Management Association;* 57, 146–154.

Reidmiller, D.R., Hobbs, P.V. and Kahn, R., 2006. Aerosol optical properties and particle size distributions on the east coast of the united states derived from airborne in situ and remote sensing measurements. *Journal of the atmospheric sciences*, *63*(3):785–814.

Republic of South Africa. 1996. The Constitution of South Africa (Act 108 of 1996). Government Gazette, GN17678(NN2083).

Republic of South Africa .1998. National Environmental Management Act (Act 107 of 1998). Government Gazette, GN19519(NN1540), 2–72.

Republic of South Africa, 2005. National Environmental Management: Air Quality Act (Act no. 39 of 2004). Government Gazette, GN27318(NN163), 2–56.

Republic of South Africa. 2009. National ambient air quality standards. Government Gazette, GN32816(NN1210), 6–9.

Republic of South Africa. 2012. Highveld priority area air management plan. Government Gazette, GN35072(NN144), 3–233.

Rushton, L., 2003. Health hazards and waste management. *British Medical Bulletin*, *68*(1):183–197.

Saucy, Apolline, Martin Röösli, Nino Künzli, Ming-Yi Tsai, Chloé Sieber, Toyib Olaniyan, Roslynn Baatjies *et al*. 2018.Land Use Regression Modelling of Outdoor NO2 and $PM_{2.5}$ Concentrations in Three Low Income Areas in the Western Cape Province, South Africa. *International Journal of Environmental Research and Public Health* 15(7) (): 1452.

Schulz, M., Textor, C., Kinne, S., Balkanski, Y., Bauer, S., Berntsen, T., Berglen, T., Boucher, O., Dentener, F., Guibert, S. and Isaksen, I.S.A., 2006. Radiative forcing by aerosols as derived from the AeroCom present-day and pre-industrial simulations. *Atmospheric chemistry and physics*, *6*(12):5225–5246.

Scorgie, Y. 2012. Urban air quality management and planning in South Africa, University of Johannesburg. (Thesis – PhD).

Seinfeld, J.H. and Pandis, S.N., 2016. Atmospheric chemistry and physics: from air pollution to climate change. John Wiley and Sons

Seinfeld, J.H., 1986. Atmospheric Chemistry and Physics of Air Pollution Wiley. *New York*, *986*.

Spiegel, J. and Maystre, L.Y., 1998. Environmental pollution control and prevention. *Encyclopedia of Occupational Health and Safety. 4th ed. Geneva: International Labour Office*, *2*.

Stanek, L.W., Sacks, J.D., Dutton, S.J. and Dubois, J.J.B., 2011. Attributing health effects to apportioned components and sources of particulate matter: an evaluation of collective results. *Atmospheric environment*, 45(32):5655–5663.

Statistics South Africa. 2012. Census 2011. Census in Brief. Pretoria: Statistics South Africa.

Stelson, A.W. and Seinfeld, J.H., 1982. Relative humidity and temperature dependence of the ammonium nitrate dissociation constant. *Atmospheric environment*, 16(5):983–992.

Tai, A.P., Mickley, L.J. and Jacob, D.J., 2010. Correlations between fine particulate matter ($PM_{2.5}$) and meteorological variables in the United States: Implications for the sensitivity of $PM_{2.5}$ to climate change. *Atmospheric environment*, 44(32):3976–3984.

Terblance, P. 2009. Basic Assessment for the amendment of the air quality permit for the iron ore handling facility, Port of Saldanha. Health specialist study, prepared for: SRK Consulting. SRK project number: 399449.

Thompson, R.J. and Visser, A.T., 2001. Mine haul road fugitive dust emission and exposure characterisation. *University of Pretoria*, *20*.

Tian, Y., Liu, H., Liang, T., Xiang, X., Li, M., Juan, J., Song, J., Cao, Y., Wang, X., Chen, L. and Wei, C., 2018. Ambient air pollution and daily hospital admissions: A nationwide study in 218 Chinese cities. *Environmental pollution*, 242:1042–1049.

Traynor, G.W., Apte, M.G., Carruthers, A.R., Dillworth, J.F., Grimsrud, D.T. and Gundel, L.A., 1987. Indoor air pollution due to emissions from wood-burning stoves. *Environmental science & technology*, *21*(7):691–697.

TSI Incorporated, 2014. Operation and Service Manual, DustTrak DRX Aerosol Monitor, Revision L, P/N 6001898.

Tutic, A., Novakovic, S., Lutovac, M., Biocanin, R., Ketin, S. and Omerovic, N., 2015. The heavy metals in agrosystems and impact on health and quality of life. *Open access Macedonian Journal of medical sciences 3*(2):345.

Tyson, P.D. and Von Gogh, R.G., 1976. The use of a monostatic acoustic radar to assess the stability of the lower atmosphere over Johannesburg. *South African geographical journal*, *58*(1):57–67.

Tyson, P.D. and Preston-Whyte, R.A., 2000. *Weather and climate of southern Africa*. Oxford University Press.

Tyson, P.D., Garstang, M., Swap, R., Kallberg, P. and Edwards, M., 1996a. An air transport climatology for subtropical southern Africa. *International Journal of Climatology*, 16(3):265–291.

Tyson, P.D., Garstang, M. and Swap, R., 1996b. Large-scale recirculation of air over southern Africa. *Journal of applied meteorology*, 35(12):2218–2236.

United States Environmental Protection Agency, (US-EPA). 2014. Speciate data browser: Particulate matter (PM) speciation profiles by source category. Available at: http://cfpub.epa.gov/si/speciate/ehpa_speciate_browse.cfm. Accessed on: 12 April 2017.

United States Environmental Protection Agency. (US-EPA). 1995. Construction and Demolition Waste Landfills Draft Report. Office of Solid Waste. ICF Incorporated Contract No. 68-W3-0008, 18 May 1995.

van der Berg, B., Piketh, S., Enslin, N., Burger, R., Beukes P., Van Zyl, P. 2015. Source apportionment of ambient particulate matter in Kwadela, Mpumalanga. Poster presented at the NACA Conference 2015, Bloemfontein, South Africa,1-2 October.

van Wyk, E., Van Tonder, G.J. and Vermeulen, D., 2011. Characteristics of local groundwater recharge cycles in South African semi-arid hard rock terrains–rainwater input. *Water SA*: 37(2).

Voiland, A., 2010. Aerosols: Tiny Particles, Big Impact: Feature Articles.

Walton, N.M., 2006. Characterisation of Cape Town brown haze (Masters dissertation).

Wang, Q., Maezono, T., Apaer, P., Chen, Q., Gui, L., Itoh, K., Kurokawa, H., Sekiguchi, K., Sugiyama, K., Niida, H. and Itoh, S., 2012. Characterization of suspended particulate matter emitted from waste rice husk as biomass fuel under different combustion conditions. *WIT Transactions on Ecology and the Environment*, 176:365–376.

Watson, J.G., Chow, J.C., Chen, L., Wang, X., Merrifield, T.M., Fine, P.M. and Barker, K., 2011. Measurement system evaluation for upwind/downwind sampling of fugitive dust emissions. *Aerosol and air quality research*, 11(4):331–350.

Watson, J.G., Chow, J.C., DuBois, D., Green, M., Frank, N. and Pitchford, M., 1997. Guidance for Network Design and Optimum Site Exposure for $PM_{2.5}$ and PM_{10}–Draft Report. Prepared for the US Environmental Protection Agency, Office of Air Quality Planning and Standards, Research Triangle Park, NC, by the Desert Research Institute, Reno, NV.

Watson, J.G., Thurston, G., Frank, N., Lodge Jr, J.P., Wiener, R.W., McElroy, F.F., Kleinman, M.T., Mueller, P.K., Schmidt, A.C., Lipfert, F.W. and Thompson, R.J., 1995. Measurement Methods to Determine Compliance with Ambient Air Quality Standards for Suspended Particles. *Journal of the Air and Waste Management Association*, 45(9):666–684.

Weil, J.C. and Brower, R.P., 1984. An updated Gaussian plume model for tall stacks. *Journal of the Air Pollution Control Association*, 34(8):818–827.

Wernecke, B., Piketh, S.J. and Burger, R.P., 2015. Indoor and outdoor particulate matter concentrations on the Mpumalanga highveld-a case study. *Clean air journal/Tydskrif vir skoon lug*, 25(2):12–16.

Wicking-Baird, M.C., De Villiers, M.G. and Dutkiewicz, R.K., 1997. Cape Town brown haze study. University of Cape Town.

Wilkinson, P., 1998. Housing policy in South Africa. *Habitat International*, 22(3), pp.215-229.

Winkler, H., 2005. Renewable energy policy in South Africa: policy options for renewable electricity. *Energy policy*, 33(1):27–38.

Wolff, G.T., Korsog, P.E., Kelly,N.A. and Fermam ,M.A. 1985 Relationships between fine

particulate species, gaseous pollutants and meteorological parameters in [Detroit

Atmospheric Environment 19, 1341–1349.

World Health Organization, 2007. Chronic respiratory diseases. Available at: http://www.who.int/respiratory/en/. Accessed on: 05 May 2017.

World Health Organization, 2010. World health statistics 2010. Available at: http://www.who.int/mediacentre/factsheets/fs290/en/index.html.

Worobeic, A., Potgieter-Vermaak, S.S., Berghmans, P., Winkler, H., Burger, R. and van Grieken, R. 2011. Air particulate emissions in developing countries: A case study in South Africa, *Analytical letters*, 44:1907–1924

Wright, C.Y., Oosthuizen, R., John, J., Garland, R.M., Albers, P. and Pauw, C. 2011. Air quality and human health among a low income community in the Highveld Priority Area. *Clean air journal*, 20(1):12–20.

Wu, W., Jin, Y. and Carlsten, C., 2018. Inflammatory health effects of indoor and outdoor particulate matter. *Journal of allergy and clinical immunology*, 141(3):833–844.

Yatkin, S. and Bayram, A., 2008. Determination of major natural and anthropogenic source profiles for particulate matter and trace elements in Izmir, Turkey. *Chemosphere*, 71(4):685–696.

Yocom, J.E., 1982. Indoor-outdoor air quality relationships: a critical review. *Journal of the air pollution control association*, 32:500–520.

Zeng, S. and Zhang, Y., 2017. The effect of meteorological elements on continuing heavy air pollution: A case study in the Chengdu area during the 2014 spring festival. *Atmosphere*, 8(4):71.

Zhou, Q., Huang, G.H. and Chan, C.W., 2004. Development of an intelligent decision support system for air pollution control at coal-fired power plants. *Expert Systems with Applications*, 26(3):335–356.

Zunckel, M., Cairncross, E.C., Marx, E., Singh, V. and Reddy, V., 2004. A dynamic air pollution prediction system for Cape Town, South Africa. WIT *Transactions on ecology and the environment*, 74-76.

Zunckel, M., Robertson, L., Tyson, P.D. and Rodhe, H., 2000. Modelled transport and deposition of sulphur over Southern Africa. *Atmospheric environment*, 34(17):2797–2808.